

Modeling and Scheduling of a Controllable Electrolyser in an Industrial Grid

Master Thesis

R. F. P. Bentvelsen

Intelligent Electrical Power Grids



Modeling and Scheduling of a Controllable Electrolyser in an Industrial Grid

Master Thesis

by

R. F. P. Bentvelsen

to obtain the degree of Master of Science
at the Delft University of Technology,
to be defended publicly on Monday July 1, 2019 at 3:30 PM.

Student number:	4109392	
Project duration:	December 4, 2017 – July 1, 2019	
Thesis committee:	Prof. dr. ir. P. Palensky ,	TU Delft, chair
	Dr. Ir. M. Cvetkovic ,	TU Delft, supervisor
	Dr. Ir. G.R. Chandra Mouli ,	TU Delft
	Ir. D. Gusain ,	TU Delft

An electronic version of this thesis is available at <http://repository.tudelft.nl/>.

Preface

It has been a long ride since I initially started as a student here on the Delft University of Technology, doing my bachelor in Electrical Engineering. My study continued with the master Sustainable Energy Technology in which I specialised in Electrical Sustainable Energy in the 2nd year. At the end of 2017 I was ready to start my thesis and after some exploration in the wide variety of available research topics, I came across an interesting topic at the Intelligent Electrical Power Grids (IEPG) research group at the faculty of EEMCS. A month later I was ready to start working on the modeling and control of a smart energy system, or more specifically the integration of a large-scale electrolyser within an industrial grid.

Like many students, I was met with numerous challenges and difficulties during my thesis work. I wouldn't have overcome these without the help of Digvijay Gusain whose insight, feedback and tips made sure I kept on track and gave a clear direction in which my thesis had to be going. I'm more than grateful for having Digvijay as my daily supervisor. I want to thank my supervisor Milos Cvetkovic as well for the helpful brainstorm sessions that gave me new insights and inspiration to further improve my thesis. His enthusiasm made sure I left our meetings with newfound energy.

Furthermore, I want to thank my friends that made my student life in Delft more than worthwhile. The many get-togethers, festivities and hangouts made it a truly lively experience. Finally, I want to thank my family for giving me the opportunity to make the most out of my time as a student and their support during the ups and downs I had during my thesis work.

*R. F. P. Bentvelsen
Delft, June 2019*

Abstract

Natural gas has been a significant source of energy for the Netherlands for a long time, but due to developments such as climate change awareness and increased seismic activity in the Groningen area, the Dutch Government has decided to shift away from natural gas and look for alternatives. Hydrogen gas is such a contender, as it can partly use the existing natural gas pipeline infrastructure, is feasible for long-term energy storage and emits no greenhouse gasses. By utilizing green electricity from renewable energy sources, water electrolysis can be applied to produce hydrogen gas.

In this thesis, the integration of a large-scale electrolyser within an industrial grid is proposed. The industrial grid consists of a 15-bus medium voltage grid with numerous industrious loads, two wind farms and a power exchange with the transmission grid. A 10 MW Proton-Exchange Membrane electrolyser is coupled with a 18 MW wind farm with the aim to produce green hydrogen in a cost-effective manner, while also providing power scheduling and balancing. Load demand depends on the available wind power over the long-term, while also mitigating fluctuations due to intermittent renewable power production. The economic feasibility of the large-scale electrolyser is analysed as well.

OpenModelica is used to model the industrial grid with PSAT components, based on a CIGRE benchmark system for renewable technologies. A mathematical model is implemented to simulate the electrochemical process of water electrolysis, and a rule-based controller is designed and implemented with a smart control strategy to control the load demand of the electrolyser. The power demand is determined by various input data such as wind forecast, intraday market prices and real-time wind power.

The results showcases an effective integration of a large-scale electrolyser that can adapt to changing wind power patterns to provide a stable power flow to the industrial grid. The economic analysis shows a cost price of hydrogen to be in the range of €50.99-90.65/MWh, which is still significant higher compared to natural gas prices.

List of Figures

1.1	The growing energy demand during the past century. Taken from [1].	1
1.2	Rising trend of CO ₂ in parts per million (ppm) since 1958. Taken from [2].	2
1.3	Prediction of peak oil production and consumption. Taken from [3].	3
1.4	Trends in LCoE for Onshore Wind, Solar PV, Offshore Wind and Concentrated Solar Power. Taken from [4].	4
1.5	Trend in installed solar PV capacity. Taken from [4].	4
1.6	Sankey diagram of the Netherlands in 2014, showing total energy supply and demand. Taken from [5].	5
1.7	Pathways for the Port of Rotterdam to reduce CO ₂ emissions, with a large role for electrolysis in all four options. Taken from [6].	6
1.8	Conventional power grid, with an unidirectional and top-down approach. Taken from [7].	6
1.9	Future power grid, with large-scale RES like hydro and offshore wind and energy storage. Taken from [7].	7
1.10	Top: Seasonal variation of solar irradiance on the northern latitudes. Bottom: Seasonal variation of onshore windspeed (blue), offshore windspeed (purple) and sinusoidal approximation (green). Taken from [8].	8
2.1	Comparison of some large-scale storage methods in capacity and duration. Taken from [9].	15
2.2	Hydrogen pipeline network of the Netherlands and part of Germany. Taken from [10].	15
2.3	Different methods for transport of hydrogen. By pipeline (a), by compressed H ₂ via road (b) and liquefied H ₂ by road (c). Taken from [11].	16
2.4	Hydrogen production and storage, combined with wind turbines.	18
2.5	Simple model of both an alkaline electrolyser cell and a PEM electrolyser cell. Taken from [12].	19
2.6	Polarization curve of an electrolyser cell at 25C and 80C, showing the effects of the different overpotentials. Taken from [13].	21
2.7	Planned load and actual load of the Dutch Transmission Grid.	23
2.8	The "duck chart" that shows the high ramp up and down of electricity demand due to intermittent renewable sources. Taken from [14].	23
2.9	Electricity production in Germany in week 32, 2018. Data is obtained from the German TSOs. Taken from [15].	24
2.10	Demand and supply of electricity on the market, with bids for different energy sources. Taken from [16].	25
2.11	Demand and supply of electricity on the market, with negative market prices due to oversupply and low demand. Taken from [16].	25
2.12	Simple residential microgrid with a wind turbine, PV array and battery storage.	27
2.13	Different types of networks: A) centralized, B) decentralized, c) distributed. Taken from [17].	28
2.14	Overview of a smart grid and domains of operation and application. Taken from [18].	29
2.15	Methods for demand side management of the electrical grid. Taken from [19].	31
2.16	Timescale for different price-based and incentive-based DSM measures. Taken from [19].	32
3.1	Methodology steps taken to obtain the research objectives.	33
3.2	SMIB example in OpenModelica with OpenIPSL components.	34
3.3	Location of the weather station (Hoek van Holland) and the port area (Maasvlakte).	36
3.4	Wind pattern used for the January case.	38
3.5	Intraday market prices used for the January case.	38
3.6	Wind pattern used for the April case.	39
3.7	Intraday market prices used for the April case.	39
3.8	Wind pattern used for the July case.	39
3.9	Intraday market prices used for the July case.	39

3.10	Wind pattern used for the October case.	40
3.11	Intraday market prices used for the October case.	40
4.1	System overview of the modelled system	41
4.2	The CIGRE MV power system network for testing the integration of renewable DERs [20]	42
4.3	The steps taken in the electrolyser to calculate the hydrogen and oxygen mass flow.	45
4.4	OpenModelica model of the 10MW electrolyser	48
4.5	Operation diagram of the controller system	49
4.6	Algorithm flowchart for scaling factor y_1 (h)	51
4.7	Algorithm flowchart for scaling factor y_2 (t)	53
4.8	Wind power curve of the wind turbine model.	54
4.9	The complete and overarching system model in OpenModelica.	55
5.1	The relation between power and voltage within an electrolyser cell.	57
5.2	The relation between power and current within an electrolyser cell.	57
5.3	The relation between power and efficiency within an electrolyser cell.	58
5.4	The relation between power and hydrogen/oxygen production within an electrolyser cell.	58
5.5	The relation between the temperature and voltage within an electrolyser cell.	59
5.6	The relation between the temperature and current within an electrolyser cell.	59
5.7	The relation between temperature and efficiency within an electrolyser cell.	59
5.8	The relation between temperature and hydrogen/oxygen production within an electrolyser cell.	59
5.9	Power curves of the wind turbines, electrolyser and exchange with the industrial grid for the January case.	60
5.10	Comparison of the VI curve of the OpenModelica model with the VI curve of the experimental setup of [21].	60
5.11	Comparison of experimental results of large-scale electrolysers with the modeled electrolyser.	61
5.12	Power curves of the wind turbines, electrolyser and exchange with the industrial grid for the January case.	62
5.13	Voltage of the electrolyser bus for the January case.	63
5.14	Power curves of the wind turbines, electrolyser and exchange with the industrial grid for the April case.	63
5.15	Voltage of the electrolyser bus for the April case.	64
5.16	Power curves of the wind turbines, electrolyser and exchange with the industrial grid for the July case.	64
5.17	Voltage of the electrolyser bus for the July case.	65
5.18	Power curves of the wind turbines, electrolyser and exchange with the industrial grid for the October case.	65
5.19	Voltage of the electrolyser bus for the October case.	66
5.20	Power exchange curves of the 21MW wind park without electrolyser, and 18MW wind park with electrolyser.	66
C.1	Power curves of the wind turbines, electrolyser and exchange with the industrial grid for the February case	79
C.2	Power curves of the wind turbines, electrolyser and exchange with the industrial grid for the March case	80
C.3	Power curves of the wind turbines, electrolyser and exchange with the industrial grid for the May case	80
C.4	Power curves of the wind turbines, electrolyser and exchange with the industrial grid for the June case	81
C.5	Power curves of the wind turbines, electrolyser and exchange with the industrial grid for the Augustus case	81
C.6	Power curves of the wind turbines, electrolyser and exchange with the industrial grid for the September case	82
C.7	Power curves of the wind turbines, electrolyser and exchange with the industrial grid for the November case	82
C.8	Power curves of the wind turbines, electrolyser and exchange with the industrial grid for the December case	83

List of Tables

2.1	Properties of Hydrogen. Taken from [11].	14
2.2	Common smart grid elements with their symbol, constraints and free variables.	30
3.1	Range of values used for the different cost factors of the economic analysis	37
4.1	Generator data of the PSAT 4th order generator model	43
4.2	AVR data of the PSAT type II AVR model	43
4.3	Governor data of the PSAT type II governor model	43
4.4	Line data of the CIGRE MV network	44
4.5	Load data of the CIGRE MV network	44
4.6	Characteristics of hydrogen and oxygen at 353K	47
4.7	Simulation setup of the OpenModelica model	56
5.1	Yearly production, costs and benefits associated with hydrogen production.	68
5.2	Production and economic results for the first day of each month, obtained from the OpenModelica model	69

Contents

Abstract	v
List of Figures	vii
List of Tables	ix
1 Introduction	1
1.1 Background	1
1.1.1 Climate Change	2
1.1.2 Depletion of Fossil Fuels	3
1.1.3 Price-competitiveness of renewables	3
1.1.4 The Dutch Energy Case	4
1.1.5 Hydrogen	5
1.1.6 The Electrical Grid	6
1.2 Problem definition	7
1.3 Previous Work	9
1.4 Research Objectives & Approach	9
1.4.1 Model of an Electrolyser in OpenModelica	10
1.4.2 Model for an Industrial Microgrid in OpenModelica	10
1.4.3 Smart control strategy for control, optimization and scheduling of the electrolyser	11
1.4.4 Economic analysis of hydrogen production cost price	11
1.5 Outline	11
2 Literature survey	13
2.1 Hydrogen - energy source, carrier and storage	13
2.1.1 Hydrogen usage	13
2.1.2 Hydrogen as energy carrier	14
2.1.3 Hydrogen as storage	14
2.1.4 Hydrogen transport	15
2.1.5 Economic prospect of hydrogen	16
2.2 Electrolysers	17
2.2.1 Progress on Electrolysers	17
2.2.2 The Alkaline Electrolyser	17
2.2.3 The Proton Exchange Membrane Electrolyser	17
2.2.4 Electrochemical Properties	18
2.2.5 Losses of the Electrolyser	20
2.2.6 Mass flow rates	22
2.3 Electrical Power Balancing	22
2.3.1 Power balancing and grid stability	22
2.3.2 Distribution operators	24
2.3.3 Energy producers and market	24
2.4 Smart grids	26
2.4.1 Microgrids	26
2.4.2 Intelligent grids	27
2.4.3 Domains of the Smart Grid	28
2.4.4 Smart Grid elements	28
2.5 Demand side management and optimization	30
2.5.1 Demand side management	30

3	Methodology	33
3.1	Method overview	33
3.2	Software tools	34
3.2.1	OpenModelica	34
3.2.2	Pandapower	35
3.2.3	Matlab	35
3.3	Selection of input data	35
3.3.1	Wind data	35
3.3.2	Intraday market data	35
3.4	Economic analysis	36
3.5	Simulation cases	38
4	Modeling in OpenModelica	41
4.1	Overview	41
4.2	Modeling of systems	42
4.2.1	Model of Industrial Medium-Voltage Microgrid	42
4.3	Model of 10MW PEM electrolyser	45
4.3.1	Cell potentials	45
4.3.2	Hydrogen and Oxygen mass flow	46
4.3.3	Overview of electrolyser model	47
4.4	Model of controllable load	47
4.5	Model of control system	49
4.5.1	Controller parameters	49
4.5.2	Control algorithm	50
4.6	Model of the wind turbine	52
4.7	System modeling	55
4.8	Simulation setup	56
5	Results and discussion	57
5.1	Technical evaluation	57
5.1.1	Electrolyser performance	57
5.1.2	Simulation cases	62
5.2	Economic evaluation	67
6	Conclusions	71
6.1	Novelties	72
6.2	Recommendations & Future work	72
A	KNMI wind data	75
B	EPEX intraday market prices	77
C	Other results	79
D	OpenModelica code: Controller	85
E	OpenModelica code: Electrolyser	89
	Bibliography	99

Introduction

This chapter will provide a brief introduction on the current and future energy supply, transmission and distribution systems. The main drivers and barriers of the energy transition are identified, and the topic of this thesis will be introduced in section 1.1. A problem definition will be given in section 1.2, previous work on the topic will be summarized in section 1.3 and the research objectives and approach will be discussed in section 1.4.

1.1. Background

The energy landscape is being ruled by mostly conventional sources of energy (oil, gas and coal) that provide the worldwide energy demand. The energy demand has sharply risen in the past century due to growing economies, increasing human populations and the advancement of technology, as seen in figure 1.1. This has resulted in an ever increasing complex energy infrastructure for the exploitation, transport, refining and distribution of energy that is deeply integrated within the human societies.

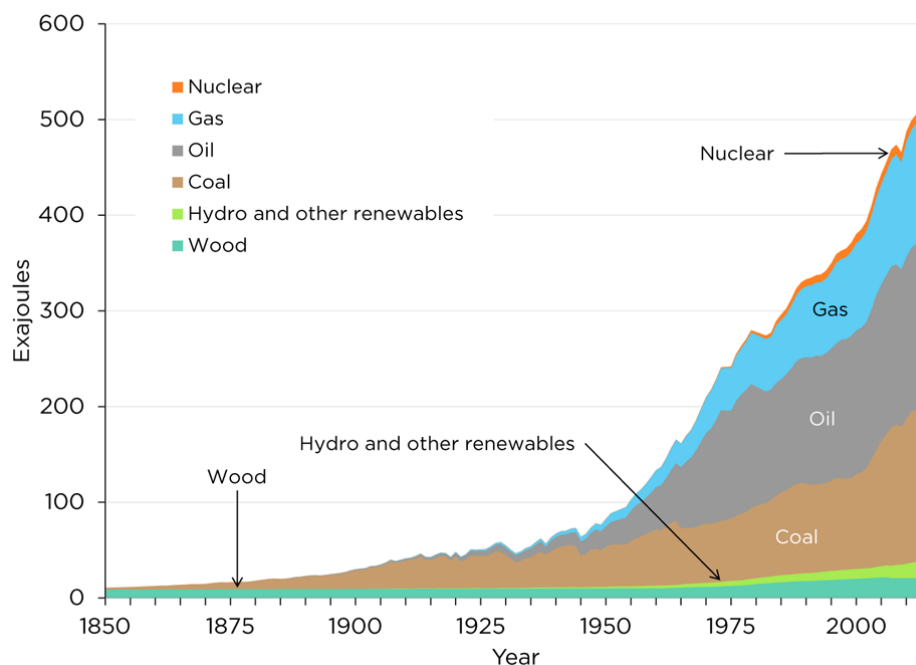


Figure 1.1: The growing energy demand during the past century. Taken from [1].

From the products we use, the cars we drive and the buildings we live in, all of this would not be possible without oil, gas and coal. Yet recently there has been a focus on pushing away from these conventional energy

sources and transition towards renewable energies like solar, wind and biomass for a number of reasons.

1.1.1. Climate Change

The first and foremost reason is the increasing awareness in climate change and the resulting global warming. It was already in 1896 that the Noble Prize winning scientist Svante Arrhenius published his models of global warming caused by increasing CO² emissions, of which the Industrial Revolution was mainly responsible for [22] [23]. In 1938 the British engineer Guy Callendar used records from 147 weather stations around the world to show that there was a clear correlation between rising temperatures and increasing CO² concentrations. This "Callendar effect" was met with skepticism by meteorologists since by then scientists could hardly believe that humanity could influence the complex climate system [24]. But in the next few decades more papers were published that showed an increasing CO² concentration in both the atmosphere [25], as well as the oceans [26], and a corresponding increase in worldwide average temperatures [27]. Measurements made since 1958 at the Mauna Loa Observatory show that CO² has been steadily increasing in the past decades, as seen in figure 1.2.

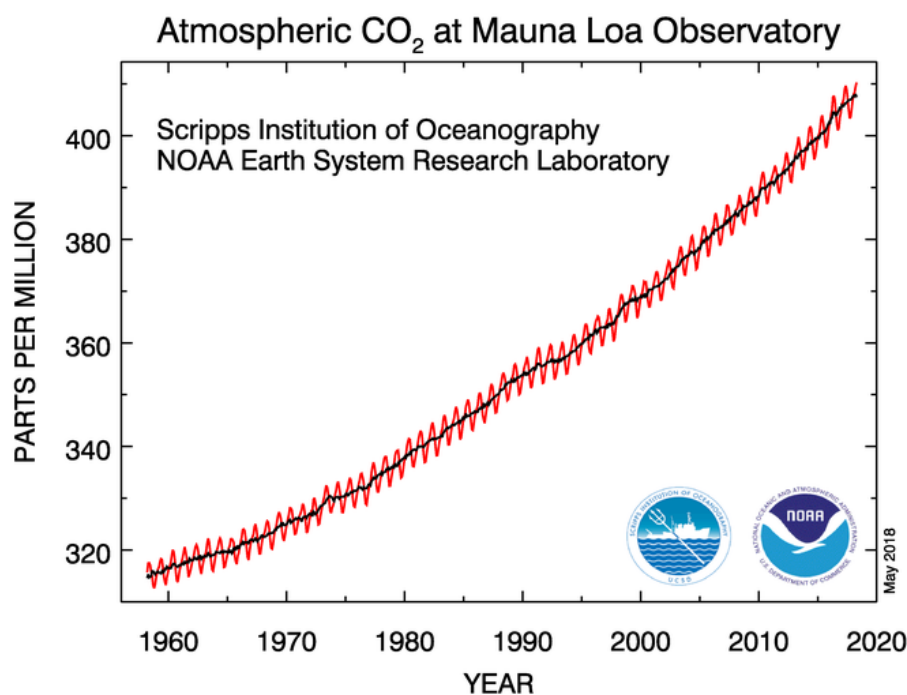


Figure 1.2: Rising trend of CO₂ in parts per million (ppm) since 1958. Taken from [2].

Eventually the Intergovernmental Panel on Climate Change (IPCC) was formed in 1988 by the United Nations (UN) to closely monitor scientific progress on climate change, and to formulate realistic strategies to mitigate further global warming and tackle the consequences. Every several years an Assessment Report is provided by the IPCC that describes the current scientific knowledge on climate change [28]. The IPCC Second Assessment Report was used as a foundation of the Kyoto Protocol that was adopted in 1997. Developed countries pledged to reduce their greenhouse gas emissions by an average of 5% compared to 1990 levels in the period of 2008 to 2012 [29]. After a couple of failed climate summits there was finally an international agreement on cutting greenhouse gas emissions, reversing climate change and limiting the global warming by a maximum of 2 degrees compared to pre-Industrial levels. This Paris Agreement was formed in 2015 and nearly all countries have pledged to take part in it. This agreement has been the main driver for many countries to enact policies that aim to reduce their carbon footprint, of which the energy transition towards renewable energy holds a significant factor[30].

1.1.2. Depletion of Fossil Fuels

Another reason for the current energy transition is the realization that the oil, gas and coal reserves are finite. The first prediction of when the peak of oil production was reached before terminal depletion would occur was done in the sixties by geologist M. King Hubbert [3], as seen in figure 1.3. The term "peak oil" was coined and widely varying predictions have been made over the years when the oil production would hit this peak. One prediction made in 2009 is that crude oil will be depleted by 2040, natural gas by 2042 and coal by 2112, but these numbers are based on proven reserves only [31].

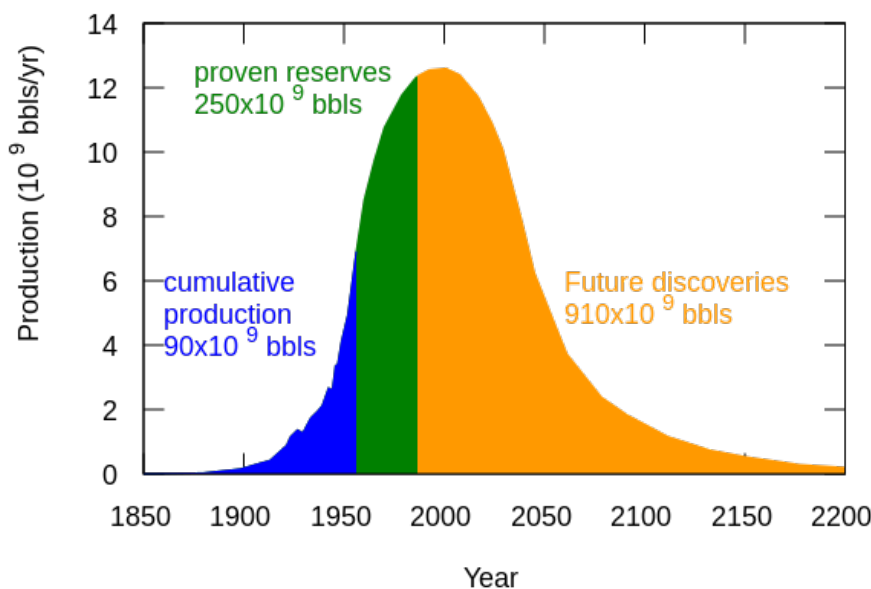


Figure 1.3: Prediction of peak oil production and consumption. Taken from [3].

Yet long before fossil fuels will reach depletion, their prices will presumably rise significantly as fossil fuels will become scarcer which will have a major impact on economies. Furthermore, fossil fuel reserves will increasingly be more concentrated in OPEC countries and Russia, which will give these countries the opportunity to use their monopoly to manipulate the oil and gas prices. Economic developments in populated countries like China, India and Brazil have vastly increased the worldwide energy demand as well. Not only will this drive up the competition on the energy market, but it will result in a faster depletion of current oil and gas reserves as well [32]. It is expected that the energy demand will continue to rise by around 0.4%-0.7% per year according to the EIA [33].

1.1.3. Price-competitiveness of renewables

Another important reason that has set the energy transitions into motion is the price development of renewable energy sources. The Levelized Cost of Electricity (LCoE) for renewables has sharply decreased in the past decade which have made them competitive with other forms of electricity generation, as seen in figure 1.4. This price development has been driven by technological improvements, competitive procurement and a large base of experienced project developers [4].

Renewable power technologies have accounted for around 70% of the added electricity power generation in 2017, and the total installed capacity of these power technologies have increased exponentially in the past years [34]. The majority of renewable power technologies consists of solar photo-voltaic(PV) energy, closely followed by wind energy. Figure 1.5 shows the significant rise in total worldwide installed capacity of solar PV in recent years. Wind energy has experienced a similar growth. Current auctions show that this growth is expected to accelerate in the next years, especially since China is ramping up its investments in renewable generation. The current price-competitiveness of renewables with fossil fuels is also expected to increase, up to the point that subsidies and feed-in tariffs are not needed anymore to make renewables competitive.

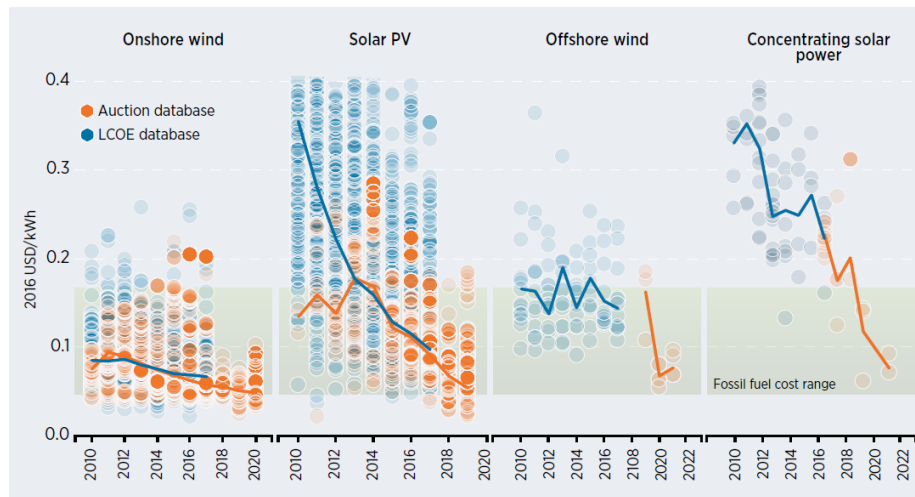


Figure 1.4: Trends in LCoE for Onshore Wind, Solar PV, Offshore Wind and Concentrated Solar Power. Taken from [4].

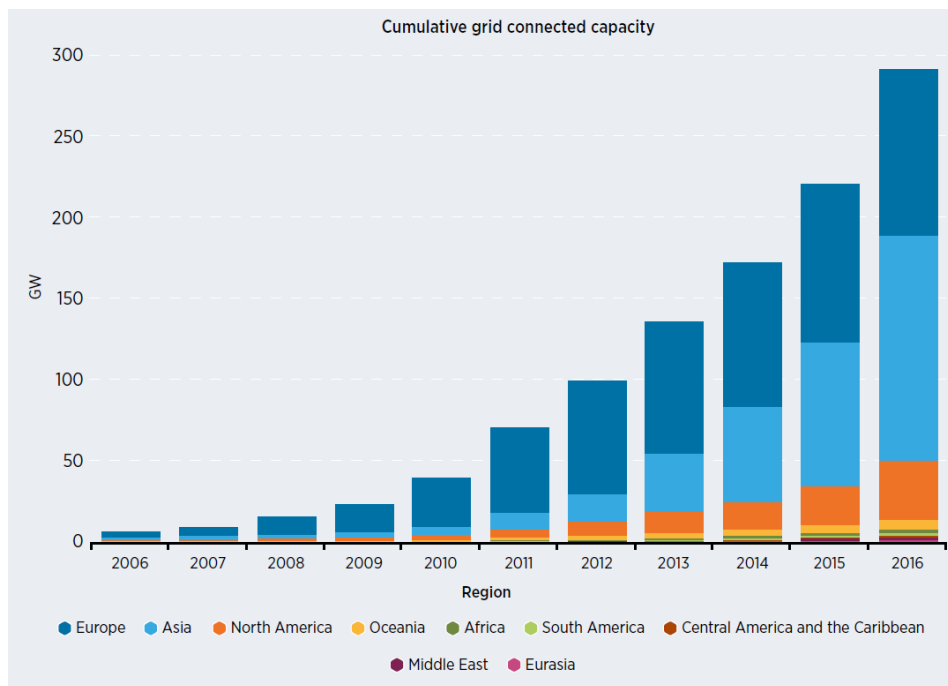


Figure 1.5: Trend in installed solar PV capacity. Taken from [4].

1.1.4. The Dutch Energy Case

Natural gas has been a significant source of energy for the Netherlands as it sits upon the largest gas reserves in the European Union (EU). The Sankey energy diagram of figure 1.6 shows that in the Netherlands a large portion of energy is supplied by natural gas. The Netherlands was the world's 15th largest producer of natural gas in 2014 and a main supplier of gas for EU countries, with the bulk of the exported gas being exported to Germany [35]. However, the extraction of natural gas has resulted in increased seismic activity in the Groningen area at where the natural gas reserves reside, which forced the Dutch Government to significantly reduce its annual production of gas. Natural gas production has dropped from more than 50 billion cube meters per annum (bcma) in 2010, to 24 bcma in 2017. The production cap for 2018 has been set to 21.6 bcma and is expected to be reduced even further in the future [36] [37]. The Dutch Government announced in March 2018

that it had decided to end all gas production in the Groningen area. The production will be reduced to zero by at least 2030, large consumers of natural gas will be forced to switch to alternatives and gas demand will be provided by imports [38]. Furthermore, the Dutch Government had already announced in 2016 that it aims towards total independence of natural gas in 2050 [39].

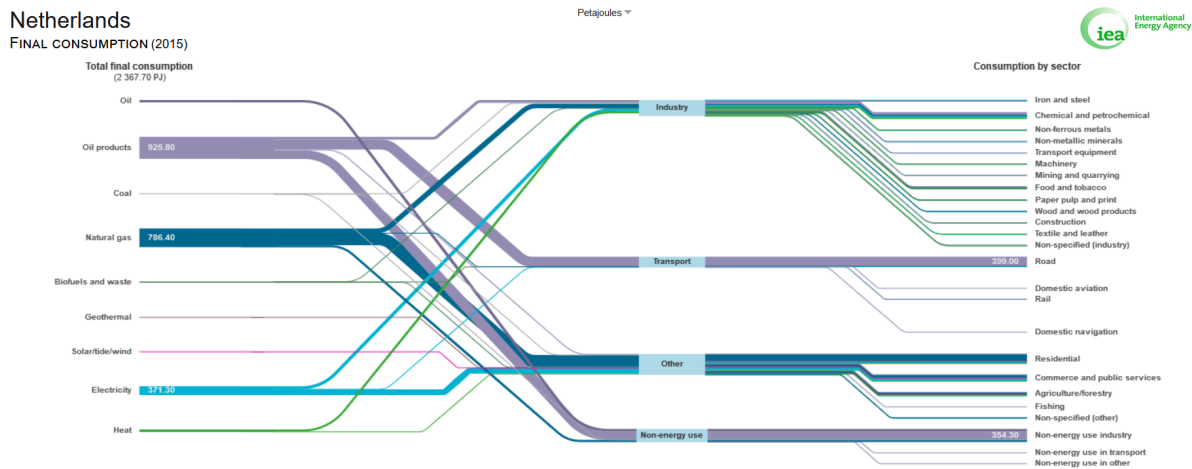


Figure 1.6: Sankey diagram of the Netherlands in 2014, showing total energy supply and demand. Taken from [5].

1.1.5. Hydrogen

A decrease in natural gas usage has the consequence that it must be substituted by other sources of energy that can supply the energy demand in the Netherlands. A possible contender is hydrogen, or more specifically dihydrogen gas (H_2), which is formed and used in many chemical processes or can be produced by electrolysis. The advantages of H_2 are that the burning of this fuel does not create greenhouse gasses, that it has a high enthalpy and that it can be transported using the pipeline network of natural gas. But the fuel also has its disadvantages and challenges; mainly its low density makes it hard to store hydrogen and it can embrittle metals and ceramics which can cause fractures in pipelines [40] [41]. Yet despite these concerns, hydrogen is still a potential substitute for natural gas. A lot of research on hydrogen in the past decades has been focused on integrating hydrogen within a sustainable energy ecosystem. Hydrogen is not only a potent fuel and energy carrier, but has also peaked interest by scientists as a means to store excess energy. A few implementations that has seen wider interest in the last years are power-to-gas applications, hydrogen cars and fuel cells.

The chemical and oil industry uses large quantities of hydrogen as well for many chemical processes, such as the production of ammonia or the refinery of crude oil. The conventional path to obtain hydrogen is by steam reforming, in which methane gas and steam is reformed into hydrogen and carbon-dioxide [42]. Around 95% of hydrogen gas is produced by steam reforming, however this is an emission intensive process and is very dependable on the availability of natural gas. The chemical and oil industry are therefore looking at alternative methods for clean hydrogen production such as water electrolysis.

The Port of Rotterdam is such an area with a very intensive chemical and oil industry, but also transport and energy industry. These industries produce a lot of CO_2 emissions and together, the industries in the Port of Rotterdam are responsible for around 20% of the total CO_2 emissions in the Netherlands [6]. The Port of Rotterdam has committed itself to pursue the goals set with the Paris Climate Accord and are taking measures to drastically reduce the port its CO_2 emissions. Figure 1.7 depicts different pathways the Port of Rotterdam has laid out to achieve this goal, and while the technologies and measures differ for each pathway, small-scale or large-scale water electrolysis is considered for all four pathways. Hydrogen production will therefore play a large role in the sustainability goals of the port area.

The introduction of hydrogen results in an ever more complex energy ecosystem that has also seen a large-scale diffusion of new renewable energy technologies. Photovoltaic (PV) panels and wind turbines have been

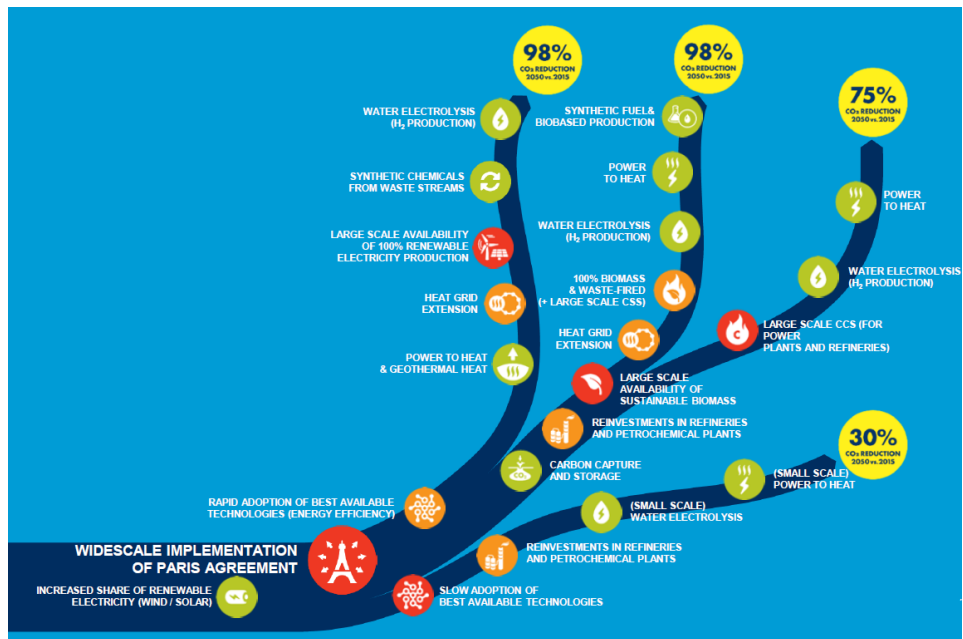


Figure 1.7: Pathways for the Port of Rotterdam to reduce CO₂ emissions, with a large role for electrolysis in all four options. Taken from [6].

widely integrated in the electric grid and their share in the electrical energy mix is still growing [43]. The first plug-in electric vehicles (PEVs) have appeared on the road and many car manufacturers are introducing new PEV models in the next years [44] [45] [46]. Furthermore, battery storages are introduced on increasingly larger scales to cope with electric supply fluctuations due to PV and wind power [47]. Still, some sort of control and optimization is needed to coordinate the distributed energy resources (DERs) and renewable energy sources (RES) within an electrical grid.

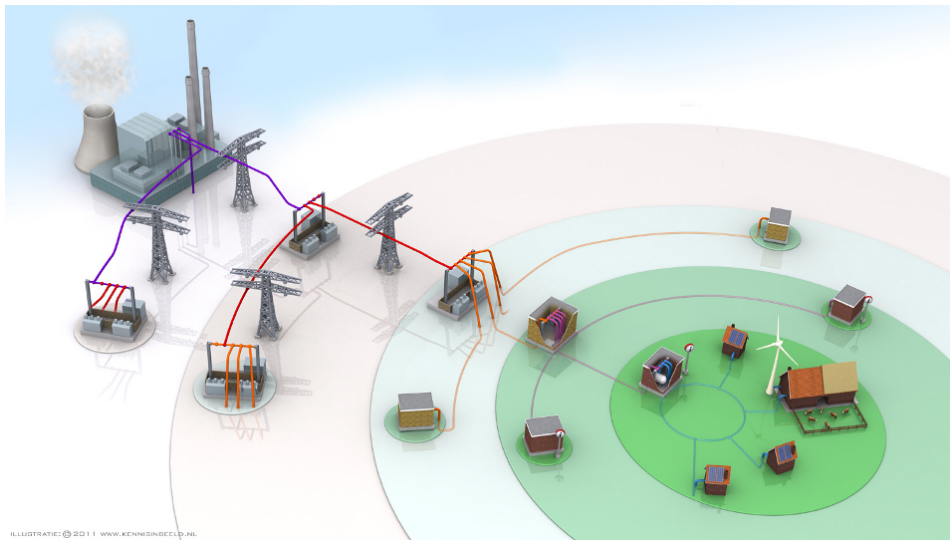


Figure 1.8: Conventional power grid, with a unidirectional and top-down approach. Taken from [7].

1.1.6. The Electrical Grid

Until now, transmission of high-voltage (HV) electrical energy was done on a high-regional, usually national level at which a net operator (TenneT in the Netherlands) is responsible for the transport, and active balancing of electricity supply and demand. The medium voltage (MV) and low voltage (LV) electrical grids on

regional level are operated by local distribution net operators (Enexis, Stedin, Liander in the Netherlands) that connect the grid to households and companies. Electricity is mainly generated by coal plants, gas plants and hydro power, which is then transported by the grid to the loads. This unidirectional and top-down approach of energy generation, transport and usage as seen in figure 1.8 made it possible to control the supply, demand and stability of the grid. But the introduction of DERs, RES, PEVs, and changing supply patterns have made the electrical grid much more challenging to control and operate.

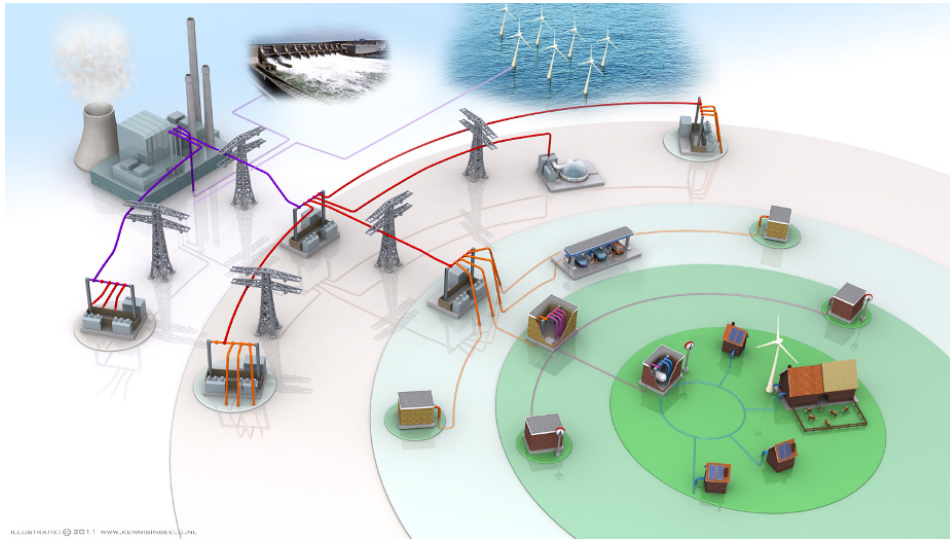


Figure 1.9: Future power grid, with large-scale RES like hydro and offshore wind and energy storage. Taken from [7].

To reduce the complexity of grid operation, the grid is divided in smaller regions known as smart grids or microgrids. A microgrid can cover for example a neighborhood or industrial zone and provides the management and control of energy, to ensure the availability and stability of electricity. The management is done by data acquisition from smart meters or smart appliances within a microgrid and a supervisory control ensures the demand and supply is matched. Excess energy is stored in energy storage systems for future use in periods of shortage. Microgrids are used in both autonomous operation (off-grid) and while being connected to the main electrical grid (grid-connected) for power exchange as shown in figure 1.9. Economic opportunities arise if the smart grid can exchange electricity with the main grid, since the price of electricity fluctuates on an hourly basis on the intraday electricity market [48]. The smart grid can sell its stored excess energy if prices are high or buy energy when the price is low. Therefore, a smart grid can be profitable if a smart control strategy is implemented that keeps track of the intraday market electricity prices, while providing a stable and resilient energy supply and demand as well.

1.2. Problem definition

PV panels and wind turbines have a fluctuating energy supply due to their intermittent behaviour, which becomes increasingly larger now that the integration and diffusion of renewable sources have taken off. Small variations can be absorbed by the main grid, but even this grid has its limits as it still needs to dump its excess electricity. Electricity cannot be buffered in the grid, and thus must be immediately consumed or stored in some form. But electrical storage is limited as well; it is common to use batteries like Lithium-ion or Sodium-sulfur, but their capacity is relatively small and the production of batteries is expensive [49]. Excess electricity is stored in some countries by pumping water to a hydro dam reservoir as a means of storage, but the exploitation of hydro dams is geographically limited and is not an option for flat countries like the Netherlands [50]. But even if countries have access to pumped hydro energy storage (PHES), the water reservoirs can only store energy that is just enough to supply energy for days or at most a week. The problem is that seasonal storage is not feasible with PHES, which will be needed to overcome seasonal fluctuations in solar and wind energy as is depicted in figure 1.10.

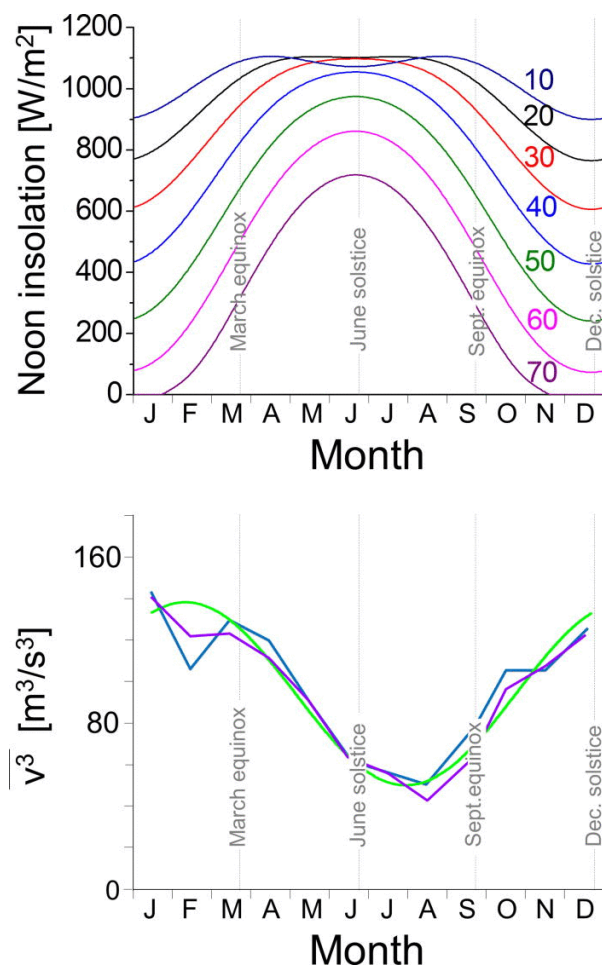


Figure 1.10: Top: Seasonal variation of solar irradiance on the northern latitudes. Bottom: Seasonal variation of onshore windspeed (blue), offshore windspeed (purple) and sinusoidal approximation (green). Taken from [8].

Hydrogen is an energy carrier that has recently peaked interest as a method to store energy as well. Aquifers, depleted oil and gas reserves, and salt caverns can be used for large scale hydrogen storage [9]. But a widespread hydrogen pipeline infrastructure that covers the transportation from and to these storage methods does not exist and the current natural gas pipeline infrastructure is not suited yet. Furthermore, appliances to convert electricity to hydrogen, and vice versa, are still uncommon. Electrolysers and fuel cells are popular research topics at universities and research centers, but these appliances are mainly modelled and studied on a small-scale within a controlled environment. Implementation and integration of the electrolyser within the electrical grid has yet to be done. There is still a gap in knowledge in how these hydrogen appliances will behave in a future distribution system. It is important to know the effect of electrolysers on the reliability and stability of a distribution grid in order to successfully implement this appliance, as well as the behaviour, effect and benefits of this appliance itself as well.

A coupling of the distribution grid and hydrogen production, and the effects on both subjects has seen limited research. Yet recently a lot of focus is being put on the hydrogen economy in which hydrogen plays an important role in the substitution of natural gas, as fuel for vehicles, resource for the industry and as a method for long-term energy storage [51]. While a majority of hydrogen gas is currently produced via steam reforming of fossil fuels, electrolysis has major potential of being the main method of hydrogen production in the future. Excess electricity produced by renewable energy sources within a distribution grid can be converted to hydrogen gas by electrolysis to replace steam reforming of hydrogen. Green hydrogen can help the industry get more sustainable, but can be used for long-term storage of renewable energy as well. A monitoring and control system is required to ensure excess power flow will be distributed among the various storage methods (battery, PHES, hydrogen) while minimizing power loss and ensuring grid stability. Current research on

smart grids focuses on power flow optimization in grids with future energy systems, yet very few research is done in combination with electrolysers. At last it is important for an electrolyser implementation to be economically feasible, and thus an economic analysis is needed that takes the production of hydrogen gas into account. The pricing and feasibility of electrolysis is currently problematic to model and is mostly an unknown research area as well.

1.3. Previous Work

The topic of smart grids is fairly new and has become popular after the introduction and diffusion of Distributed Energy Resources (DER) and Renewable Energy Sources (RES) in the electrical grid. As of now most research has focused on the generation, transmission, distribution and delivery of electricity in an isolated/islanded or urban environment [52] [53]. Lesser focus has been on other means of energy transport like cooling, heating and hydrogen in combination with microgrids, but some research has been done on this topic [54] [55]. Hydrogen has the potential of not only being an energy carrier within a microgrid, but it can be used to store energy as well. On top of that, hydrogen can be used as fuel for industrial processes [56].

Most smart grids that have been studied use a Battery Energy Storage System (BESS) to store energy [57] [58], while storage with hydrogen is an area that has not been much explored yet. One of the advantages that hydrogen storage has over BESS is the potential of storage over longer periods. This is especially beneficial for PV power which peaks in the summer period while energy demand is low. Excess hydrogen that is produced in the summer period can be used in the winter period when energy demand is usually higher [59]. Besides bridging the gap between energy supply and demand, hydrogen can be exchanged with a potential pipeline network. Hydrogen can then be bought and sold in a fluctuating exchange market for economic profit, similar to the exchange of electricity with the main grid. While the last case has been extensively studied with cost-optimization algorithms [60] [61], this is something that has yet to be done with a hydrogen grid. Economic profitability of hydrogen and electrolysers can be an important driver for the diffusion of this technology and some research has been done on this topic [62].

An Optimal Power Flow (OPF) can be achieved with optimization and scheduling, which aims to minimize the power distribution losses and minimize the cost of power supply from Distributed Generation (DGs) and the main grid. Especially smart grids have unequal loads and uneven conductor spacing on the distribution lines, causing the grid to be unbalanced and resulting into power losses [63]. Storage options within the smart grid can help maintain energy balance and improve power management in the smart grid [64]. OPF is however not easy to achieve since it requires the solving of nonlinear solutions at the injection nodes which require heavy computation. Especially transients on small periods are hard to cope with since they require immediate action, but computation times cannot keep up with that. OPF solutions are calculated for fixed time points, but dynamic loads like electric cars and electrolysers and dynamic sources like solar panels and wind turbines require continuous computation of OPF solutions [65].

1.4. Research Objectives & Approach

Many industries depend on fuel like natural gas for the operation of their factories. Since the Netherlands is trying to reduce its dependence on natural gas based energy generation, alternatives like renewable energy sources, and to some extent hydrogen gas, can play a crucial role in decarbonisation. A smart approach for electricity consumption is needed as well with the introduction of DER, RES and PEVs, and can be provided by microgrids. This provides an interesting opportunity to combine the microgrid and hydrogen in a future-proof industrial energy ecosystem. An important aspect of this ecosystem is its economic feasibility and this can be achieved by the trading of electricity and hydrogen with their respective energy markets. A smart control strategy is therefore needed to make the trade of energy profitable.

The objective of this thesis will therefore be **the modeling, scheduling and control of a hydrogen producing electrolyser in an industrial microgrid**. The approach to obtain this objective will be as follow. The electrolyser will be designed and modelled in OpenModelica, an open-source object oriented modelling software. The industrial microgrid, which will consist of an electrical grid and the electrolyser, will be modelled and simulated in OpenModelica as well. A flowchart diagram will describe the control strategy and scheduling operation of the microgrid, while also taking constraints of the grid components into account and ensuring power stability. This diagram shall form the basis of the smart control strategy that will be integrated into the

OpenModelica model. Different case studies will be applied to the industrial microgrid once all components are completed and integrated. The several objectives and requirements of the total model are described below in more detail.

1.4.1. Model of an Electrolyser in OpenModelica

The electrolyser model should be subjected to the following objectives and requirements:

- **High ramp up and ramp down of hydrogen production**
The electrolyser should be able to quickly respond to power flow fluctuations within the distributed grid. This flexibility is needed to cope with the intermittent energy sources and (small) power transients within the grid.
- **Modular by $m \times n$ cells**
A single electrolyser cell is only sufficient to convert a few Watts of electrical power. Larger electrolyser systems are possible, if these cells are modular and can be connected in both series and parallel.
- **Temperature and/or pressure dependent**
The thermodynamic properties of the electrolyser is influenced by the temperature and/or pressure in which it is operating. These properties should be taken into account to ensure a realistic behaviour of the electrolyser cell.
- **The electrolyser should be based on a feasible and proven technology**
There are different types of electrolyser cells, some are already widely used in industries while others are still in an experimental phase. A dissection of different, available electrolyser types shall be made and one of the available technologies shall be used that has already been proven to be a feasible.
- **Output hydrogen and other residual products**
Hydrogen gas produced by the electrolyser will be transported to a hydrogen pipeline infrastructure. This hydrogen grid will be modelled as an infinite sink and thus the produced hydrogen can always be fed into the pipeline.
- **The power demand of the electrolyser is controllable**
The amount of power the electrolyser demands should be controllable within its operating range. This will give flexibility in the operation of the electrolyser and will allow the component to react on external factors.

1.4.2. Model for an Industrial Microgrid in OpenModelica

The industrial microgrid should be subjected to the following objectives and requirements:

- **A 15-bus system with distributed generators and loads**
The industrial microgrid will consist of several buses from which their power flow, voltage level and phasor angle can be determined. The busses will be connected to several distributed generators with varying characteristics. The n-bus system is connected to several loads as well, each with an unique load demand profile. Loads can be factories, charger stations, electric gas boilers and electric heat pumps.
- **Integration of intermittent renewable energy sources**
Renewable energy sources like solar PV and wind energy can be integrated in the industrial microgrid. These intermittent sources will have an unique, uncontrollable supply profile taken from actual data for the Port of Rotterdam area. The energy supply will be injected into the microgrid.
- **Connection to the main transmission grid**
A connection is made with the industrial microgrid and the main transmission grid. Power exchange is possible between these two grids during power deficits or power surplus. The grid is assumed to be integrated with the intraday electricity market as well. The transmission grid is assumed to have infinite supply and demand.

1.4.3. Smart control strategy for control, optimization and scheduling of the electrolyser

The control algorithm should be subjected to the following objectives and requirements:

- **Provide a flowchart of control and operation of the algorithm**
A flowchart will be provided that visualizes the decision-making process of the control and scheduling algorithm. This flowchart will be the guideline upon which the algorithm will be based.
- **The algorithm will ensure scheduled power supply and demand is respected**
The different loads will at all times be provided with enough power to meet their demand. The algorithm has to control the power flows and energy balance of the bus on which the electrolyser is connected to ensure this demand is met.
- **Include buying/selling of electricity with the intraday electricity market**
The exchange of electricity and hydrogen with their respective grids has a cost component. Fluctuating market prices of both energy carriers should be considered when exchange is needed with the electrical main grid or hydrogen pipeline grid. The algorithm should include this cost function and aim to optimize it.
- **Decision-making and operation of the algorithm is continuously**
The algorithm should operate continuously to ensure that the microgrid and electrolyser is controlled at all times. However to avoid stalling the simulation too much, a balance shall be made between the resolution and the computation time of the algorithm.
- **A forecast of the energy output of wind energy is provided**
The intermittent wind power sources provide a fluctuating energy supply. The algorithm will use forecasts of weather conditions to predict the incoming energy supply and adapt its decision-making.
- **The algorithm can ensure load curtailment of the electrolyser**
The algorithm has a control that will curtail the power demand of the electrolyser during emergent situations to protect the microgrid from instabilities.

1.4.4. Economic analysis of hydrogen production cost price

The economic analysis should be subjected to the following objectives and requirements:

- **The investments and maintenance costs of the electrolyser**
The expected capital costs of a large-scale electrolyser is a major part of the hydrogen cost price. Furthermore, the electrolyser requires maintenance over its life time with its involved costs.
- **Levelized cost of electricity from renewable energy sources**
The electrolyser is supplied by renewable electricity from energy sources that have their own levelized cost of electricity (LCoE). This LCoE is integrated in the hydrogen cost price.
- **Cost and benefit analysis of buying from the intraday market**
The intraday electricity market is a spot to buy or sell electricity on a per hour basis after the day ahead market is closed. The electrolyser will often require the extra buy-in of electricity to remain at its minimum capacity or will buy electricity at favorable prices.
- **Power balancing to prevent production penalties**
Energy producers with renewable energy sources cope with unpredictable production fluctuations. The DSO penalizes the energy producers if it overestimates or cannot deliver the scheduled power production. Electrolyser can help in balancing the power exchange with the grid to avoid penalties.

1.5. Outline

This thesis is divided in several chapters that will be outlined. An overview of research subjects, literature and background relevant to the topic of the thesis is given in Chapter 2. The methodology to achieve the research objectives is given in Chapter 3. The components being modeled into an integrated system are laid out in Chapter 4. The results obtained by the model and applied method, and the discussion of the results themselves can be found in Chapter 5. At last, Chapter 6 will conclude the thesis, give an overview of novelties and some recommendations for future research.

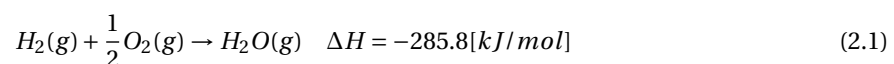
2

Literature survey

This chapter will describe the topics of research that will be used for this thesis. The potential and role of hydrogen as energy source, carrier and storage is covered in section 2.1. The working principles of the electrolyser are explained in section 2.2. Section 2.3 will discuss power system and grid stability, and the subsequent roles of the system operators, while section 2.4 presents the current research on smart grids. At last, section 2.5 will introduce the concepts of demand side management and optimization in smart grids.

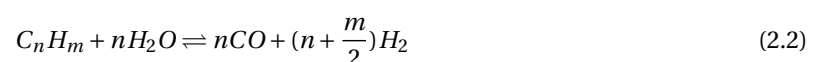
2.1. Hydrogen - energy source, carrier and storage

Hydrogen as an atom is the most abundant and lightest element in the universe, placed at the first spot in the periodic table of elements. The molecular form of the hydrogen atom, H_2 , is sometimes referred as dihydrogen but it is more commonly known as hydrogen as well. Hydrogen is a colorless, odorless and tasteless molecule, and diffuses faster than any other molecule [11]. The "discovery" of hydrogen gas was done by Henry Cavendish in around 1766-1781, although by then Cavendish described the hydrogen gas as "inflammable air". Hydrogen gas is highly flammable as it needs only a small ignition energy of 0.02mJ for it to ignite if within flammability limits and at stoichiometry ratio with oxygen. The chemical reaction of hydrogen combustion at standard conditions (0°C and 1atm) is given in equation 2.1. This is a highly exothermic reaction, as can be seen by the negative sign of the enthalpy.



2.1.1. Hydrogen usage

Since its discovery, hydrogen has been used in many applications such as balloons, rocket boosters and airships (with the Hindenberg as infamous example), as coolant of power generators (since hydrogen has the highest specific heat and thermal conductivity of all elements) and in the petroleum and chemical industry (for upgrading of fossil fuels, and the production of ammonia). Recently hydrogen has gained much interest as a clean fuel alternative for conventional fuels like gasoline, diesel and even kerosine. A proposed energy system in which hydrogen takes an important place has been coined as the hydrogen economy. The worldwide production of hydrogen was around 57 million tons in 2004, which is roughly 170 million tons of oil equivalent (toe). Since then the growth rate of hydrogen production has been around 10% per year[66]. Hydrogen is not a fuel that occurs in nature, but is trapped within water or hydrocarbons. Some transformation processes of these compounds result in the production of hydrogen gas. A majority of hydrogen production (around 48%) is done by steam reforming of natural gas, around 30% is from steam reforming of petroleum and 18% is from reforming of coal. These production processes do result in the formation of carbon dioxide as a product as well, as seen by the general steam reforming equation.



Only a small amount of all hydrogen gas is produced with electrolysis. Current estimates are that around 4% of hydrogen is produced by this electrochemical process. Electrolysis is the reverse process of hydrogen gas combustion of equation 2.1. With electrolysis, electrical energy is used to split water into hydrogen gas and oxygen. This is a zero emission process and has been the focus of the main method of hydrogen production for a clean hydrogen economy.

Some properties of hydrogen are listed in table 2.1.

Table 2.1: Properties of Hydrogen. Taken from [11].

Properties	Value	Unit
Molecular weight	2.01594	-
Gas density at 0°C/1atm	0.08987	kg/m ³
Melting temperature	-259	°C
Boiling temperature	-253	°C
Thermal conductivity at 25°C	0.019	kJ/(ms°C)
Heat capacity of gas at 25°C	14.3	kJ/(kg°C)
Energy Density per mass	140.4	MJ/kg
Energy Density per volume	8491	MJ/m ³

2.1.2. Hydrogen as energy carrier

Hydrogen has much potential as an energy carrier. Its energy density of 140 MJ/kg is significantly higher than the energy density of methane, which is 55 MJ/kg. However, hydrogen gas is very voluminous at standard atmosphere with a density of just 0.090 kg/m³ and thus requires vast volumes for its storage. As a gas, hydrogen is compressible and this is usually done to increase its energy density per volume. Hydrogen gas has an energy density of 9.17 MJ/L at 700 Bar, yet this is still smaller than convention fuels like LNG or diesel that have energy densities in the range of 22-36 MJ/L. The major drawback of hydrogen storage for vehicles is the spacious tanks that are required to store hydrogen, even when pressurized. This is one of the main barriers for the introduction of hydrogen cars. Yet the low weight of hydrogen is a major advantage over conventional fuels, especially in the space industry. Hydrogen is often the main choice to fuel space rockets where every single kilogram counts.

2.1.3. Hydrogen as storage

One of the major challenges of the energy transition from conventional fuels to renewable energy sources is a cheap, reliable and long-term form of storage. Storage is needed to cope with the intermittency of wind and solar power, which are expected to take an increasingly share of total electricity production. Batteries are used to bridge the daily, sometimes even weekly gap between energy supply and demand. But the large discharge rate and limited capacity of batteries make them unusable to cover seasonal variations. Hydrogen is a serious contender for year-round storage to overcome the seasonal energy gap. Stored hydrogen has very low energy losses, and can thus be stored for long periods of time. Besides being stored in tanks or abandoned salt caves, hydrogen can be stored (or buffered) within pipelines as well. Yet an infrastructure for large-scale transport and storage of hydrogen is still lacking and will require heavy investments to implement [9].

There are currently many options being investigated on the storage of hydrogen, as it will play a crucial role in the success of hydrogen integration in the current energy ecosystem. It has a potential for storage in the 100 GWh range for single storage systems, greatly outperforming other large-scale storage methods like pumped hydro energy storage (PHES) and compressed air energy storage (CAES) as shown in figure 2.1. Suitable storage environments are depleted oil/gas reservoirs, aquifers and salt caverns [9]. The long-term storage of energy is also more feasible with hydrogen gas than with PHES or CAES. Hydrogen is a voluminous gas and thus requires large tanks for its storage. Compression is often applied to reduce the amount of space required for hydrogen gas. Common compression rates are 350 bar and 700 bar

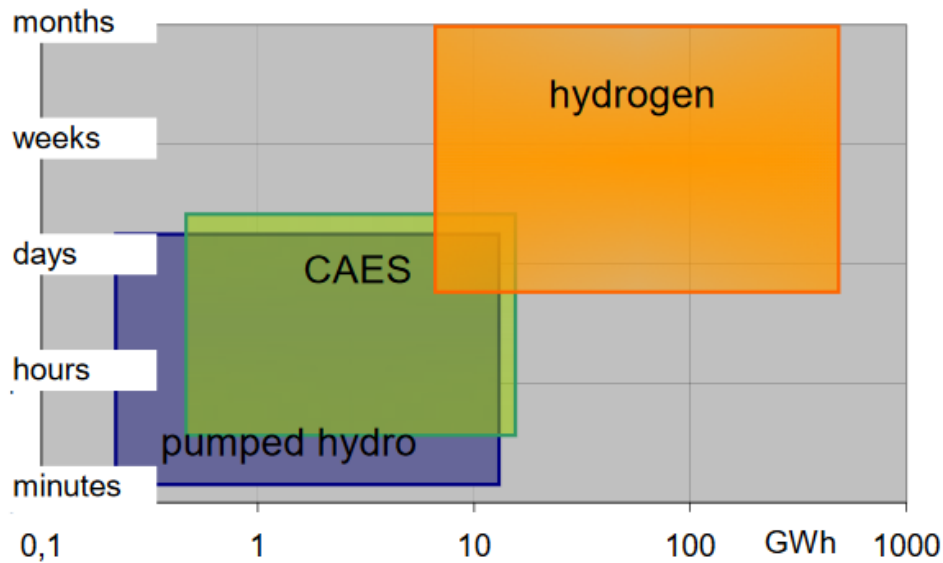


Figure 2.1: Comparison of some large-scale storage methods in capacity and duration. Taken from [9].

2.1.4. Hydrogen transport

A potential contender for hydrogen transport is by using the current natural gas pipeline infrastructure. Many countries that rely on natural gas have built an extensive pipeline network for the transport of natural gas. The Netherlands, for example, has a network that covers the whole country and has most of its buildings connected to the gas grid. Small transition steps can be made by mixing natural gas with hydrogen, which is feasible by up to 20% hydrogen content. Eventually, natural gas can be phased out and be totally replaced by hydrogen. This does however still require significant modifications to current gas applications like boilers and cooking systems, but adjustments by large industrial consumers of gas as well [67]. Figure 2.2 shows a map of the current (large) pipeline network that can potentially be used for hydrogen transport in the future. The Netherlands has been self-sufficient in its natural gas use due its large gas fields in the Groningen area. Furthermore, a share of the natural gas is exported to neighbouring countries which has resulted in an intensive intra-national pipeline network.

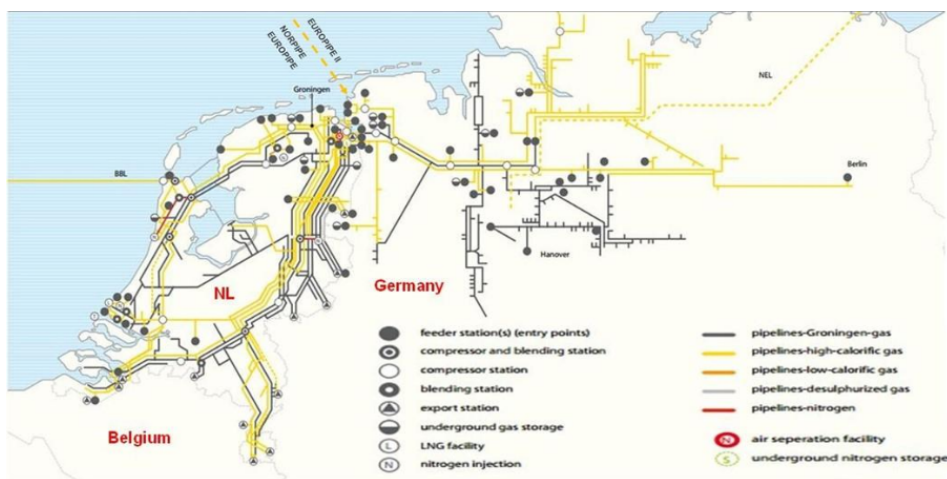


Figure 2.2: Hydrogen pipeline network of the Netherlands and part of Germany. Taken from [10].

Pipeline transport is not the only method for the transportation of hydrogen. Transport by road is considered as well, with trucks transporting highly compressed or liquidized hydrogen. The hydrogen is transported in numerous tubes that are transported by the trucks towards hydrogen stations. These stations can be po-

tentially used by drivers of hydrogen vehicles to pump hydrogen gas. Transport by road is considered in cases when a pipeline network is not sufficient or meshed enough to reach these stations. In remote regions, a pipeline to a hydrogen station would be very capital intensive and thus road transport is a cheaper alternative. It is also expected that hydrogen transport by road will play an important role in the early stages of an hydrogen economy when the hydrogen pipeline infrastructure hasn't been deployed yet. Figure 2.3 shows the different manners in which hydrogen can be transported.

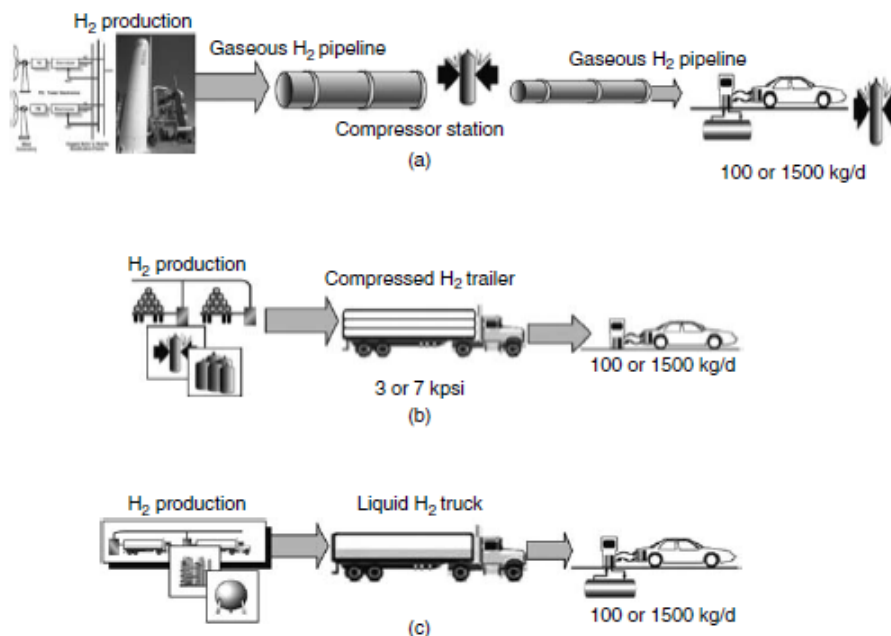


Figure 2.3: Different methods for transport of hydrogen. By pipeline (a), by compressed H₂ via road (b) and liquefied H₂ by road (c). Taken from [11].

2.1.5. Economic prospect of hydrogen

While hydrogen has many uses, eventually the cost price of hydrogen will decide if it is a worthwhile replacement for conventional options such as natural gas. A major advantage of hydrogen is that only limited investments are needed to set up the hydrogen infrastructure if gas pipelines are used for transport. However, production and consumption of hydrogen is still a problem cost-wise. Green hydrogen production by electrolysis is a technology that still needs to mature in both technology and economic feasibility. Power-to-gas also results in significant efficiency loss, thus the decision to inject the power into the grid and sell it on the electricity market is easier made and more profitable. Only if the share of renewable energy increases and periods of significant renewable power supply occurs, the decision to choose for power-to-gas instead can be made.

Demand for hydrogen is mostly in the industry, as it is an important component for many chemical processes. However, the steam reforming process to form hydrogen is often integrated within the chemical plants and extra import of hydrogen is deemed unnecessary. Many applications that use natural gas are not fitted to use hydrogen as well. Heating and cooking appliances have to be rebuilt or replaced, but consumers don't feel the necessary incentives to shift from natural to hydrogen gas. Hydrogen vehicles face the same problem: fuelling infrastructure must be built first before consumers are encouraged to buy a fuel cell vehicle and drive on hydrogen gas.

The cost price of green hydrogen production depends on a number of factors. The investment and maintenance cost of the electrolyser should be considered, as well as the levelized cost of electricity from the renewable energy source [68]. In some studies, the (prevented) social costs are considered as well, to give a better comparison of green hydrogen production with conventional production [69]. An integration of hydrogen

production with the electricity market (day-ahead or intraday) can also influence the cost price of hydrogen [70]. At last, the electrolyser can use power balancing to prevent penalties associated with the underestimation or overestimation of power production by renewable energy sources [71].

2.2. Electrolysers

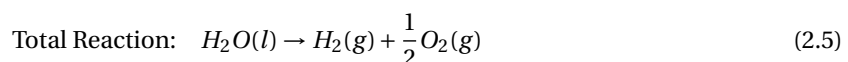
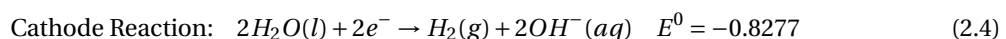
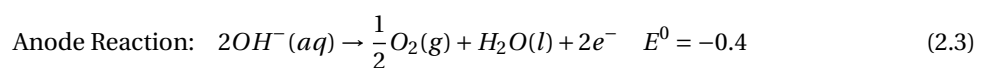
Electrolysis is the process of using electrical energy to drive a non-spontaneous chemical reaction. The electrical energy provides the difference in Gibbs free energy of the reaction plus common losses that can occur with electrolysis. A common application of electrolysis is splitting water into hydrogen gas and oxygen, of which both can be captured and used for other purposes. The electrolysis technique is being done within an apparatus called the electrolyser, and consists of two electrodes (the anode and the cathode) and an electrolyte. As of now, electrolysis is mostly done on a small scale with electrolysers operating in the kiloWatt(kW) range. These are mainly used in small-scale industries or at research institutes, but the use of hydrogen electrolysers is scarce. This is mainly due to its limited application and the high capital investment costs compared to other methods of hydrogen production, like steam reforming of fossil fuels.

2.2.1. Progress on Electrolysers

More research and development has been done on electrolysers in recent years and has resulted in the up-scaling of these energy converters. A number of projects are being considered that will build electrolyser plants ranging in the Megawatts(MW). The largest electrolyser at the moment was built in 2015 by Siemens, and is able to convert 6 MW of electricity into hydrogen gas [72]. Other projects are being considered, like a 10 MW hydrogen refinery in the Rheinland area and the European Union has provided funding for the demonstration of a >20 MW hydrogen electrolyser [73] [74]. The interest in hydrogen production by electrolysis has peaked since more focus is being put on emissionless alternatives of conventional fuels.

2.2.2. The Alkaline Electrolyser

There are two types of electrolysers that are being used most commonly. The first type is the alkaline electrolyser, a well established technology and being used since the first Apollo missions to the moon. The cell is characterized by the liquid alkaline electrolyte solution. Sodium hydroxide or potassium hydroxide solutions are mostly used, due to their low cost, high solubility and their limited corrosiveness. Nickel is a popular choice for the electrodes considering its low cost and high availability. A diaphragm is being used to separate the product gases of the alkaline cell, but is also permeable to hydroxide ions and water. The cells operate at around 40-90 °Celsius, at <30 bar and a cell voltage of in between 1.8-2.4 V. Their current density ranges at 0.2-0.4A/cm² and a cell efficiency of around 62-82% is obtained [12]. In the alkaline electrolyser cell, OH⁻ is being used as the energy carrier and its half reactions at the anode and cathode are given in equation 2.3, 2.4 and 2.5.



Some disadvantages of the alkaline electrolyser are its low current density, which is caused by the high ohmic resistances that take place within the cell. This puts a severe limit to the maximum achievable current density. Another disadvantage is the difficulties that arise with the diaphragm which is not able to prevent product gases from passing through. At last the alkaline cell is unable to operate at high pressure which would be beneficial for its efficiency and further hydrogen storage [75].

2.2.3. The Proton Exchange Membrane Electrolyser

Another type of electrolyser, the Proton Exchange Membrane(PEM) water electrolyser, is considered to be the most favorable technology for hydrogen production when coupled with renewable energy sources. Its design is simple, efficient and it can easily operate under low temperature and pressure conditions. On top of these characteristics, the PEM electrolyser has a quick ramp up and ramp down speed as well which is beneficial for working with intermittent renewable sources. Its compact design will also allow the PEM electrolyser to

be integrated with for example wind turbines, allowing direct conversion of electricity into hydrogen gas. An example of such integration is given in figure 2.4. The wind turbines have a direct connection to the electrolyser that will convert excess energy to hydrogen and consequently store the gas.

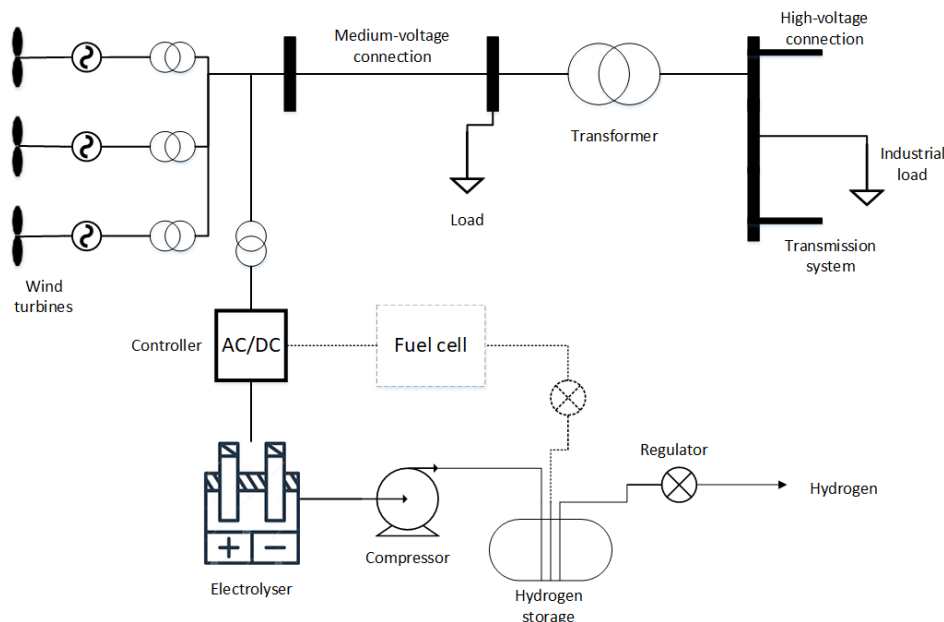


Figure 2.4: Hydrogen production and storage, combined with wind turbines.

The main characteristic of the PEM water cell is its polymer exchange membrane, usually made of Nafion. The membrane is able to withstand high pressures, easily exchanges protons but ensures low gas crossovers as well. The low gas crossover makes it possible for the cell to operate under a wide power input, increasing the flexibility of power that can be inserted. Its small thickness of around 20-300 micrometer allows for a compact design. A downside are the rare metals being used for the electrodes, with Platinum and Iridium for respectively the cathode and anode. These materials for the electrodes significantly drive up the cost of the PEM cell. The durability of the PEM cell is also less than its alkaline equivalent, especially under high operating pressures. The PEM electrolyser cells operate at around 20-100 °Celsius, at <30 bar and a cell voltage of in between 1.8-2.2 V. Their current density ranges at 0.6-2.0A/cm² which is significantly higher than the alkaline cell. The higher current density range reduces the operation costs of the PEM electrolyser cell. Its cell efficiency is around 67-82% and thus comparable to the alkaline cell [12]. In the PEM electrolyser cell, H⁺ is being used as the energy carrier and its half reactions at the anode and cathode are given in equation 2.6, 2.7 and 2.8.

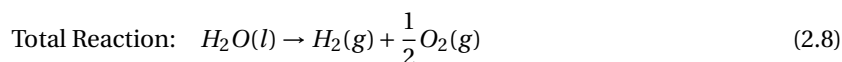
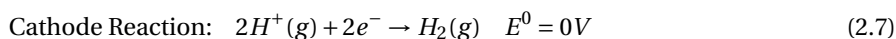
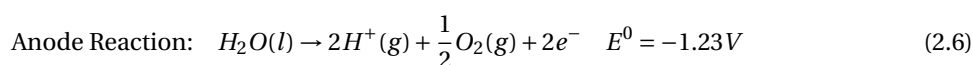


Figure 2.5 shows a simplified model of both the alkaline electrolyser cell, and a PEM electrolyser cell. While the alkaline cell has been the preferred choice as electrolyser cell for many years, the PEM cell is recently gaining much popularity due some significant advantages. Its high current density, rapid system response, compact design and dynamic operation gives this cell an edge over the alkaline cell. However, the cost and durability of the PEM cell are still at a disadvantage and a lot of current research is aimed at improving those properties [76].

2.2.4. Electrochemical Properties

The most important electrochemical property of the electrolyser cell is the electrolysis process, in which water molecules are broken down in oxygen and hydrogen atoms. Water in liquid form, or water in steam form

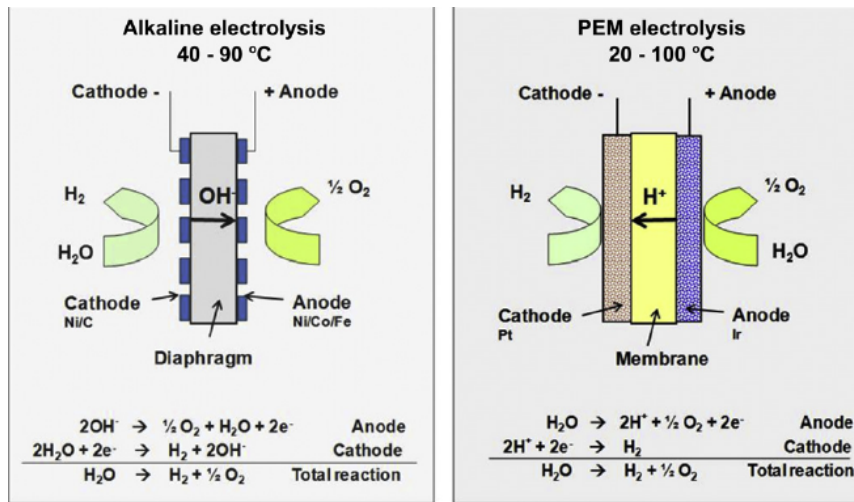
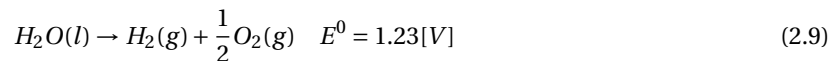


Figure 2.5: Simple model of both an alkaline electrolyser cell and a PEM electrolyser cell. Taken from [12].

can both be used as reactant for electrolysis. The steam form of water requires a lower enthalpy for its transformation to hydrogen and oxygen, and is known as the lower heating value (LHV). The enthalpy needed for water in its liquid form is known as the higher heating value (HHV) [21]. The total process of PEM electrolysis for liquid water at standard conditions ($T=298\text{K}$, $P=1\text{atm}$) is shown in equation 2.9.



With the standard cell voltage E^0 given in equation 2.10.

$$E^0 = E_{cathode}^0 - E_{anode}^0 = (0) - (-1.23) = 1.23[\text{V}] \quad (2.10)$$

The cell voltage of $E^0 = 1.23\text{V}$ states that electrolysis can only occur if this electrical potential is applied to the electrodes of the electrolyser cell under the condition that there are no heat losses. This is however not realistic and thus the total amount of energy provided must be calculated to overcome the heat losses as well. The reversible cell voltage E_{rev} is related to the Gibbs free energy by equation 2.11, which is rewritten as given in equation 2.12.

$$E_{Rev} = \frac{-\Delta G^0}{2F} \quad (2.11)$$

$$\Delta G^0 = -2FE_{Rev} = \Delta H^0 - T\Delta S^0 \quad (2.12)$$

And with F as the Faraday's constant as given by equation 2.13, where N_A is Avogadro's number and e is the charge of an electron.

$$F = N_A * e = 6.022e10^{23} * 1.602e10^{-19} = 96485[\text{C}] \quad (2.13)$$

Substituting all values in equation 2.12 results in a value for the Gibbs free energy of $\Delta G^0 = 237.2\text{kJ/mol}$. This is the amount of electrical energy that should be provided for the PEM electrolysis process. However, since the electrolysis process is endothermic, heat energy should be added as well to prevent the water from freezing. The total amount of energy can be determined by calculating the enthalpy of the reaction, which is given in equation 2.14 with T the temperature and S^0 the entropy at standard conditions.

$$\Delta H^0 = \Delta G^0 + T\Delta S^0 \quad (2.14)$$

The standard entropy can be found by adding the standard entropy of the products from equation 2.8 together, and subtracting the standard entropy of the reactants from the same equation. The result given in equation 2.15 is than:

$$\Delta S_{hydrogen}^0 + \frac{1}{2}\Delta S_{oxygen}^0 - \Delta S_{water}^0 = 130.68 + 0.5 * 205.15 - 69.95 = 163.3[J/molK] \quad (2.15)$$

Adding the values of Gibbs free energy, standard entropy and temperature (298K) together in equation 2.14 gives an enthalpy of $\Delta H^0 = 285.8$ kJ/mol. The entropy multiplied by the temperature is the amount of heat energy that should be applied to the PEM electrolysis process. The corresponding cell voltage with this enthalpy is given in equation 2.16.

$$E = \frac{\Delta H^0}{2F} = 1.48[V] \quad (2.16)$$

This is the nominal cell voltage at standard conditions that should be applied for the total reaction to occur, and results in partial electrical energy and partial heat energy to be applied. However, the Gibbs free energy and entropy are temperature and pressure dependent and so are the enthalpy and cell voltage. If changes in temperature and pressure occur, the Nernst equation given in equation 2.17 can be used to calculate the new cell voltage.

$$E_{Rev} = E + \frac{RT}{2F} \ln\left(\frac{[p_{H_2}][p_{O_2}]^{1/2}}{[p_{H_2O}]}\right) \quad (2.17)$$

In the Nernst equation, R is the gas constant (8.134 J/molK) and p are the partial pressures of the reactants and products of the electrolysis reaction.

2.2.5. Losses of the Electrolyser

The electrolysis process is never a 100% efficient reaction. There are several effects within the cell that result in losses. A higher cell voltage than the nominal cell voltage should be applied to compensate these losses. The efficiency of the electrolyser cell is then determined as in equation 2.18.

$$\text{Cell efficiency} = \frac{E_{Cell}}{E_{Total}} * 100\% \quad (2.18)$$

Effects in the cell that cause losses are due to overpotentials which have different causes. The total cell voltage that should be applied is equal to the normal cell voltage E plus the overpotential voltages ΔV . The three main overpotentials are:

- Activation Overpotential
- Ohmic Overpotential
- Concentration Overpotential

Activation Overpotential

The activation overpotential is a loss that occurs at the electrode/membrane interface, and is dominant at lower current densities. The losses are caused by the slowness of reactions at these interfaces. Extra voltage is needed to drive the reaction that transfers electrons from anode/cathode to or from the membrane. The activation overpotential is given by the Butler-Volmer(B-V) equation, and is different for the anode and the cathode. In equation 2.19 the B-V equation for both the anode and cathode are combined [77] [78].

$$E_{Act} = \frac{RT_A}{2\alpha_A F} \sinh^{-1}\left(\frac{i}{2i_{0,A}}\right) + \frac{RT_C}{2\alpha_C F} \sinh^{-1}\left(\frac{i}{2i_{0,C}}\right) \quad (2.19)$$

The subscripts A and C stand for the anode and cathode respectively. The current density of the cell is given by i while the exchange current densities of the anode and cathode are given by $i_{0,A}$ and $i_{0,C}$. The charge transfer coefficients are given by α_A and α_C .

Ohmic Overpotential

The ohmic overpotential is caused by internal ohmic resistances of the electrolyser cell. The resistances are due to the materials used for the electrodes, plates and the proton exchange membrane. Using Ohm's Law, the overpotential can be calculated for the cell. The ohmic overpotential is linear to the current flowing through the electrolyser cell, as seen in equation 2.20.

$$E_{Ohm} = R_{cell}I \quad (2.20)$$

Electricity is converted to excess heat due to the ohmic resistances, which count as losses. The ohmic overpotential becomes increasingly dominant at growing current density levels.

Concentration Overpotential

Concentration overpotential becomes a dominant factor at higher current densities. The overpotential is due to mass transport limitations, when the charge-carrying protons, hydrogen, oxygen or water molecules are not 'refreshed' quickly enough at the electrode surface and thus block the area surface. This will not form a problem at lower concentrations since there is enough space for the protons and molecules to transfer their charges, but congestion will occur with increasing concentrations as there is an increasing slowness in the mass transport. This congestion will lead to more resistance in the mass flow and will exponentially increase at higher current density levels. The concentration overpotential is hard to model and is often experimentally determined. One method to estimate the overpotential is by using the Nernst equation as seen by equation 2.21.

$$E_{Conc} = \sum \frac{RT}{zF} \ln \frac{C_1}{C_0} \quad (2.21)$$

With z the amount of electrons transferred, C_0 the reference concentration of a molecule and C_1 the concentration flowing through the electrolyser cell.

Total overpotential

The activation, ohmic and concentration overpotentials are the main causes of losses within the electrolyser cell. Each of the overpotentials is dominant at different regions depending on the current density flowing through the cell. Figure 2.6 shows an I-V curve of the cell voltage versus the current density at a temperature of 25 Celsius and 80 Celsius. It should however be noted that this polarization curve can differ depending on cell type and cell sizing, but the behaviour of the polarization is nonetheless the same.

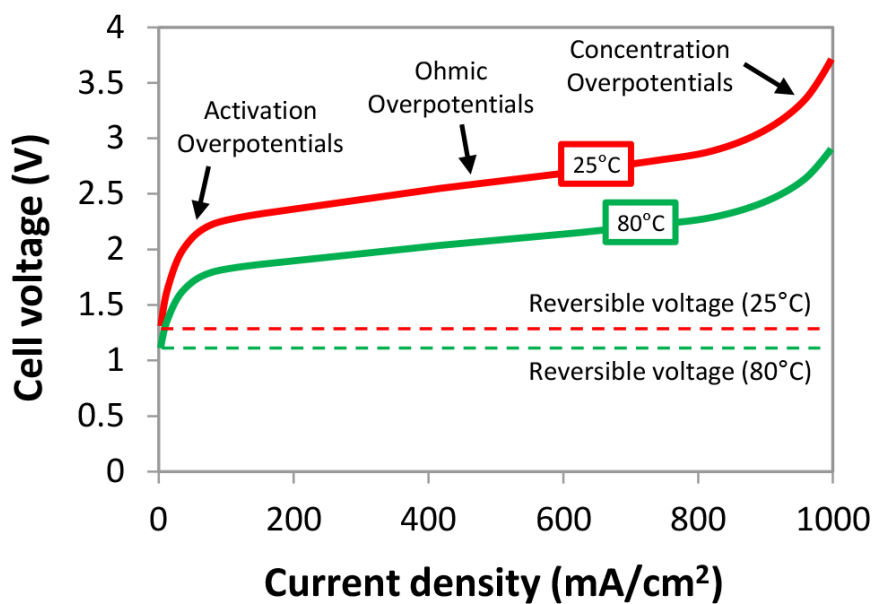


Figure 2.6: Polarization curve of an electrolyser cell at 25C and 80C, showing the effects of the different overpotentials. Taken from [13].

Now that the overpotentials are known, the total cell voltage for the electrolyser cell can be determined, as is shown by equation 2.22.

$$E_{Total} = E_{Cell} + E_{Act} + E_{Ohm} + E_{Conc} \quad (2.22)$$

And can be rewritten as equation 2.23.

$$E_{Total} = E + \frac{RT}{2F} \ln\left(\frac{[p_{H_2}][p_{O_2}]^{1/2}}{[p_{H_2O}]}\right) + \frac{RT_A}{2\alpha_A F} \sinh^{-1}\left(\frac{i}{2i_{0,A}}\right) + \frac{RT_C}{2\alpha_C F} \sinh^{-1}\left(\frac{i}{2i_{0,C}}\right) + R_{cell}I + \sum \frac{RT}{zF} \ln \frac{C_1}{C_0} \quad (2.23)$$

2.2.6. Mass flow rates

Faraday's law of electrolysis can be used to determine the amount of hydrogen mass and oxygen mass that will be produced at the outlet of an electrolyser cell. Faraday's law for hydrogen is given according to equation 2.24 and for oxygen is given in equation 2.25.

$$\dot{m}_{H_2} = \frac{M_{H_2} * I_{cell}}{zF} \quad (2.24)$$

$$\dot{m}_{O_2} = \frac{M_{O_2} * I_{cell}}{zF} \quad (2.25)$$

With \dot{m} as the mass flow of the element, M for the molar mass of the element and I_{cell} the current flowing through the cell which is determined according to equation 2.26. P_{in} in this equation is the total power input of the cell and E_{Total} is given according to equation 2.23.

$$I_{cell} = \frac{P_{in}}{E_{Total}} \quad (2.26)$$

2.3. Electrical Power Balancing

Gas and coal plants are able to provide a stable supply of electricity at all times, and can increase or decrease their output depending on the electricity demand. Renewable sources however are dependent on weather conditions for their supply of energy. The intermittent pattern of both solar and wind power, which provide a vast bulk of renewable energy, makes it difficult to match supply and demand of electricity. Both short term variations in wind and solar, as well as seasonal variations result in an energy mismatch. Electricity produced must be consumed immediately, curtailed or in some way stored, but it cannot be buffered within the transmission or distribution grid. A large influx of power by intermittent sources on the grid will result in congestion, voltage and frequency instability and even possible power outages or blackouts.

2.3.1. Power balancing and grid stability

The Transmission System Operator (TSO) is responsible for the power balancing of electricity on the transmission grid, a task that is becoming increasingly difficult and complex since the large-scale infusion of renewable power technologies. Excess energy can be sold and exchanged with neighbouring countries, but the capacity of cross-border connections is often limited and neighbouring countries are coping with intermittent power sources as well. TSOs try to make forecasts ranging from minutes ahead to days ahead to make sure an active power balance is maintained. Intermittent sources like solar PV and wind turbines are increasingly gaining a larger share in the total electrical supply, and thus weather forecasts have become more important in recent years. However, the accuracy of weather forecasts is limited and so situations may arise where expected sustainable energy cannot be delivered. Such a situation happened in the Netherlands on 30 April 2018 when it was expected to be windy and sunny, yet it instead became windless and cloudy thus causing an unexpected shortage of energy supply. TenneT, the Dutch TSO, was forced to set out an emergency alert for extra power generation to make sure the grid stability was to be maintained [79]. Eventually TenneT was forced to import hundreds of Megawatts from neighbouring countries against large sums of money, to ensure the power balance was met [80].

Figure 2.7 shows the load balancing in the Netherlands in the span of two weeks. The blue dotted line is the expected, planned load demand that is already set a few days ahead. The black solid line is the actual demand that was eventually needed. It is clearly visible that while often the planned demand matches the actual demand, often the forecasts can result in large mismatches. There is some flexibility on the generation side, since large generators like hydro dams or gas plants can quickly ramp up or ramp down their electricity production.

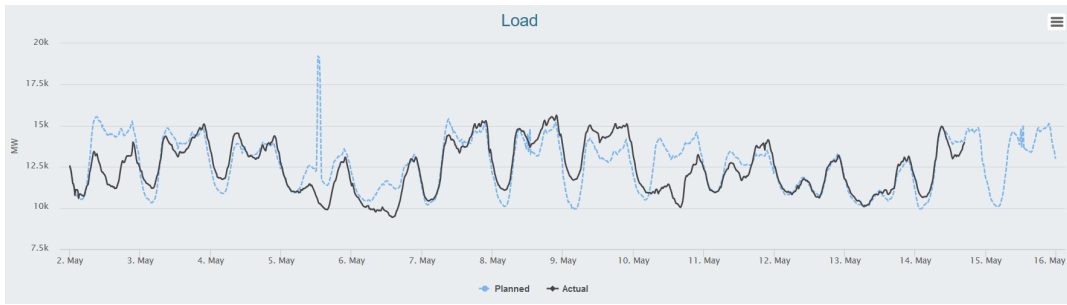


Figure 2.7: Planned load and actual load of the Dutch Transmission Grid.

However, the flexibility of these generators is limited while there is a growing demand for flexible generation. The diffusion of renewable energy sources (RES) has vastly changed the daily generation patterns and has made energy management more difficult. An example is the case of electricity demand in California as seen in the "duck chart" of figure 2.8. At sun-hours the demand for electricity sharply decreases as consumers with solar PV are able to accommodate their own energy needs. System operators might even need to turn off or curtail some of the solar power as energy supply is too high during daytime periods. But at sunset a quick ramp-up of electricity production is required since no solar energy is provided anymore and electricity demands starts to peak. Conventional plants can't cope up with the required ramp-up of 13.000MW in just three hours and thus balancing issues start to arise on the California grid. A possible solution is to "flatten" the duck by shifting supply and demand of solar electricity. This can be done by either energy storage, or with demand side management [14].

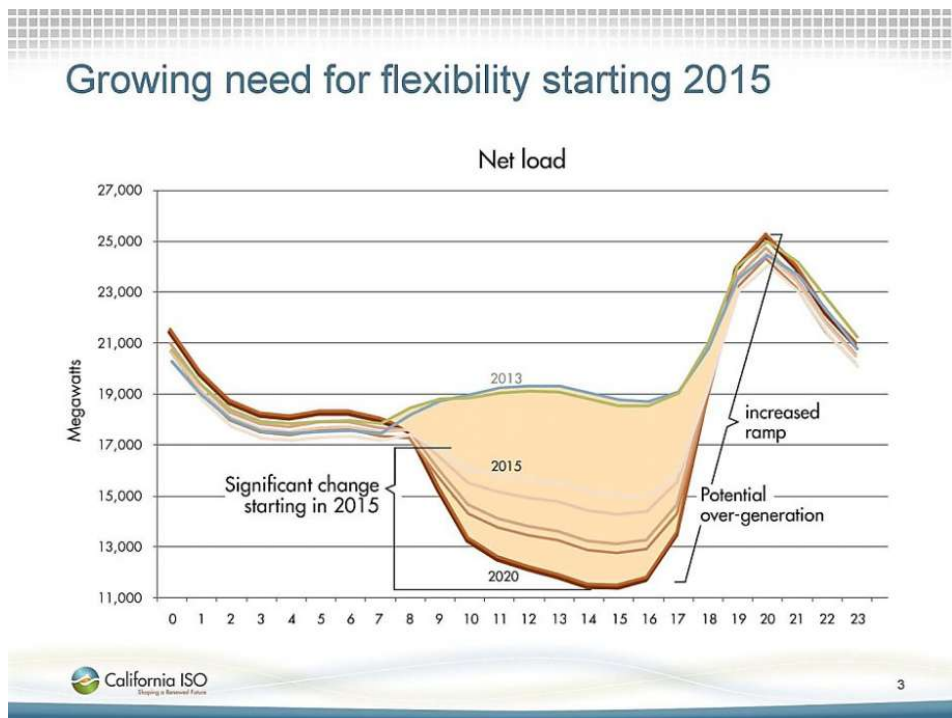


Figure 2.8: The "duck chart" that shows the high ramp up and down of electricity demand due to intermittent renewable sources. Taken from [14].

Transmission and distribution system operators are faced with a difficult task now that the energy transition has lifted off. Electricity generation and consumption is slowly shifting from a centralized, unidirectional system towards a decentralized, bidirectional system. System operators will need to adapt and adjust their electricity infrastructure to allow the integration of RES and to changing supply and load patterns. Solar en-

ergy and wind energy are no longer a niche technology but can account for a large proportion of electrical generation. Even for large economies as California and Germany this is true, as is visible from the electric energy chart for Germany of figure 2.9. Both the large fluctuations and significant share of solar and wind electricity production is clear from the graph.

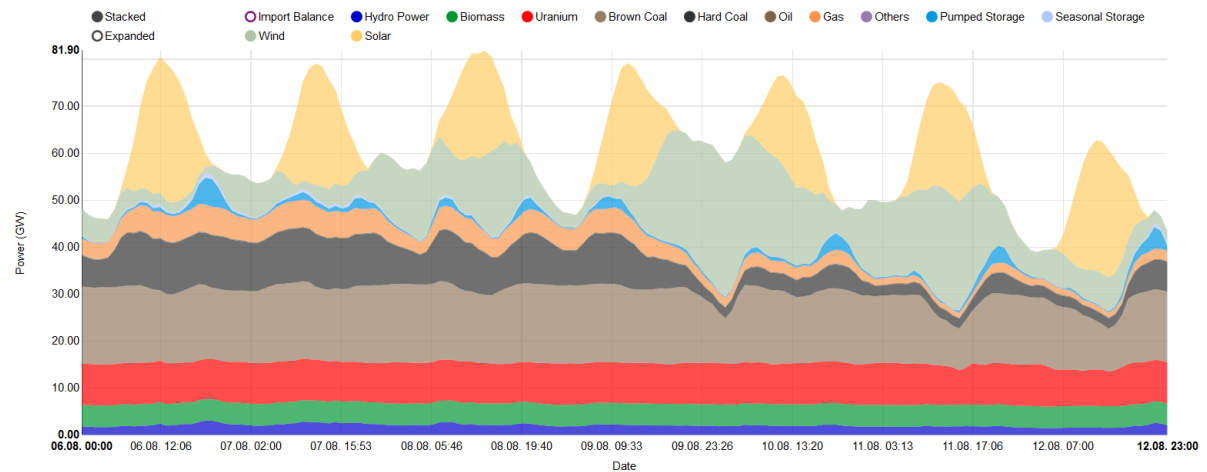


Figure 2.9: Electricity production in Germany in week 32, 2018. Data is obtained from the German TSOs. Taken from [15].

2.3.2. Distribution operators

The responsibility and role of the distribution system operator (DSO) differs from the TSO. The DSO is responsible for the maintenance, operation and development of the grid on a regional level. Consumers or producers of electricity should approach the DSO for a connection to the grid, while honoring the connection requirements set up by the system operator. An under-developed grid can lead to difficulties with integrating new renewable sources or technologies and thus the DSO has the responsibility to oversee the development of the energy infrastructure. If the rapid integration of RES is left unchecked, problems may arise such as capacity constraints of the grid or stability issues in which security of supply cannot be sustained. The DSO can be forced to forbid new connections for energy producers or consumers, which can be a major setback for the energy transition such as the installment of RES projects.

2.3.3. Energy producers and market

The electricity market was for a long time dominated by a few large energy producers, owners of large electricity plants to provide the grid of sufficient electricity. The goal of the energy producer is to provide a reliable supply of energy while maximizing profits. But the large energy producers face competition of small producers of solar and wind electricity these days. The share of renewable energy is vastly increasing, usually made possible by small co-operations (for example farmers setting up a wind park), local projects (PV farms on agricultural land) and households (solar panels on the roof). Renewable energy is often subsidized with feed-in tariffs and thus the cost price of renewable electricity is often sharper than the cost price of conventional sources such as coal, nuclear and gas. Renewable electricity is therefore often prioritized by electricity buyers on the electricity market. In most markets, renewables have priority in the power grid and renewable producers are thus the first to set up a bidding price. This is depicted in figure 2.10 which shows that meeting power supply and demand involves prioritizing renewable energy.

Energy producers are first-most obliged to help sustain the grid frequency at 50Hz, which is achieved by matching energy demand and energy supply. Shaping the electricity trading price is thus subordinate on balancing energy demand. As a result, energy producers still set up their capacity for bids on the market, even when the energy demand is low. Also, many conventional plants are inflexible in ramping up or down their production. Therefore, a plant owner prefers to keep the plant running to prevent shutdown and cold start-up costs. If there is a period of high renewable energy supply (due to lots of wind and sun) but the energy demand on the market is low, an oversupply of electricity on the market can occur. But there is still an obligation to match supply and demand to remain grid stability and thus situations can occur in which

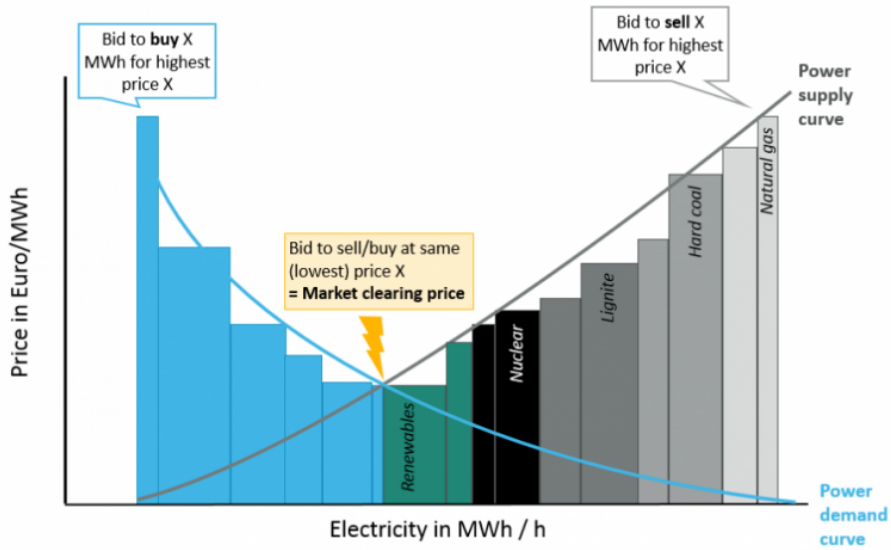


Figure 2.10: Demand and supply of electricity on the market, with bids for different energy sources. Taken from [16].

the electricity is sold for negative market prices. This is an incentive for power consumers to ramp up their demand, as is shown in figure 2.11. Oversupply of the electricity market can be mitigated by energy storage, flexible loads or exporting excess power to neighbouring countries. These solutions however are currently only available on a small scale.

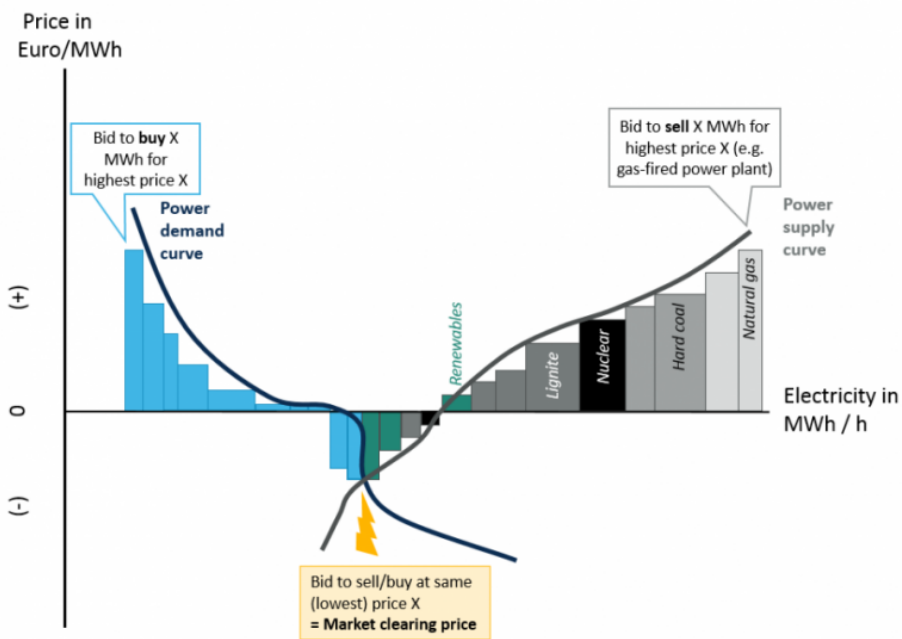


Figure 2.11: Demand and supply of electricity on the market, with negative market prices due to oversupply and low demand. Taken from [16].

The electricity market operates on three levels for power balancing, these are:

- the day-ahead electricity market
- the intraday electricity market

- the electricity balancing market

These markets all have their own function and operate in their own time frame. The day-ahead market is the main platform for trading volumes of electricity between buyers and sellers, and the majority of electricity is traded here. The energy volumes are traded a day before the power will be delivered. Sellers will determine the amount of power they can deliver at what price for different time slots, while buyers determine how much they are willing to buy for different volumes of power and place their bids. One day in advance, the prices will be settled depending on supply and demand, and power delivery will take place on the next day.

The intraday market is a continuous trading platform that cover the period between the closure of the day-ahead market and periods close to real time. The time slot in which electricity is traded usually closes 60 minutes, 30 minutes or in some markets even 15 minutes before power delivery. The market works on a first-come, first-serve principle in which the best offers will be traded first. The intraday market is important for unexpected incidents or occurrences that take place after the day-ahead market is closed. Power plants might be struck with failure, the forecast for wind or solar power might differ a lot or failures in the transmission system might occur. Especially the growth of renewable energy, is, due to its intermittent and unpredictable power production, a key factor for the importance of the intraday market.

Energy imbalances in the grid might still occur even after the intraday volumes have been traded. The electricity balancing market is therefore the final platform in which any imbalances that still occur after the markets have been closed will be settled. Balancing services that enter the market can either provide an energy balancing service or a capacity balancing service. In the energy balancing service, either extra energy can be supplied or consumed to restore balance. The capacity balancing service provides flexible loads that can be controlled to consume more power, or to temporarily curtail them. Participants of the electricity market are responsible to overcome their own imbalances and are usually represented by a 'Balance Responsible Party' (BRP). The BRP adds the balances of their members together and aims to resolve its imbalances in real time. If the BRP fails to do so, a financial settlement should be made with the TSO. The penalty applied depends on the agreements made in the bidding contracts, with differing penalties for overproduction or underestimation of power delivery. BRP's therefore have an incentive to settle their own imbalances and reduce these in the future [81].

2.4. Smart grids

An important aspect for the integration of renewable energy systems is an electrical grid infrastructure that is able to integrate these systems. The current electrical infrastructure has been mostly unchanged since the fifties and should be upgraded and modernized to deal with the changing developments in electrical supply and demand. Much focus has recently been set in coming up with solutions and methods to modernize the electrical grid.

2.4.1. Microgrids

The electrical power grid has been centralized for decades, with centralized power generators providing electricity on the national, regional and local level. Yet the ever increasing complexity of the electrical infrastructure has resulted in the decentralization of the electrical grid in so-called microgrids. In these microgrids, power production is decentralized by small generators or distributed energy resources (DERs) like diesel generators, gas turbines and fuel cells that provide electrical supply to nearby loads. This has some vast advantages over the conventional power grids, namely [82]:

- Fewer congestion problems in the lines and cables since generators are located closer to the generators.
- The DERs have higher operational flexibility and thus lesser constraints than centralized power systems.
- DERs are designated to give high priority on the support of local loads within the microgrid, ensuring better power stability.

The microgrid is a subsystem of the transmission and even the distribution grid, able to meet its own supply and demand while still being connected to the transmission/distribution grid in case power exchange is needed. The grid can be isolated or islanded during disturbances to avoid harm being done to other parts

of the electrical grid. The microgrid has made it easier for system operators to control the grid and ensure a stable and reliable power grid. Furthermore, the microgrid paves the way for a future energy system in which renewable energy sources (RES) and electrical appliances like electric cars, electric heat boilers and power-to-gas applications are integrated. An example of a simple microgrid with a wind turbine, battery and load (residential buildings) is shown in figure 2.12 [83].

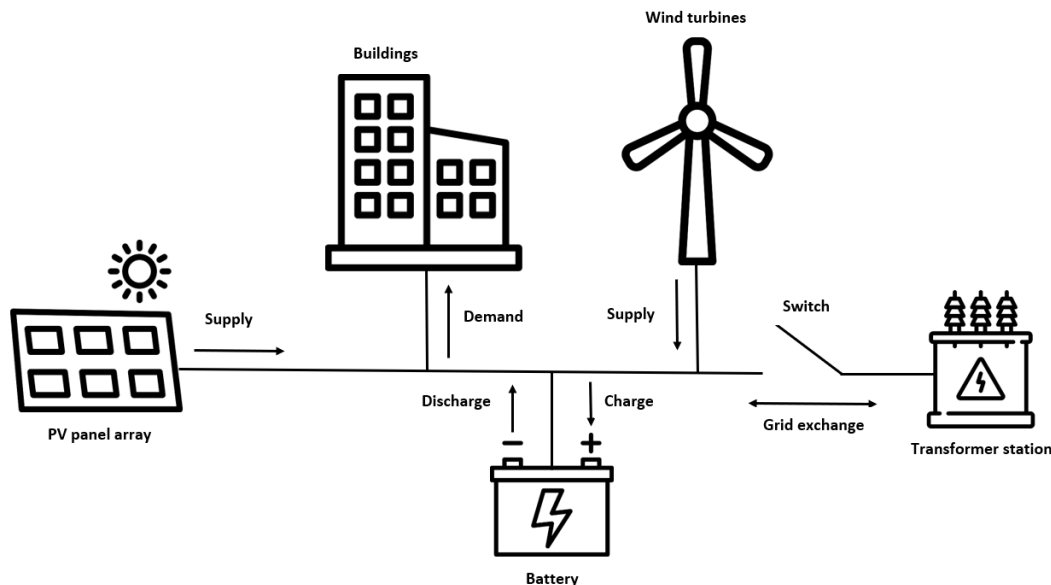


Figure 2.12: Simple residential microgrid with a wind turbine, PV array and battery storage.

2.4.2. Intelligent grids

All things considered, the microgrid is still a passive electrical grid that must be actively controlled by system operators by switching generators and substations on and off. Advancements made in information and computer technology (ICT) can be applied to the microgrid, in which informational flows are used to enhance, automate and improve the distribution of energy. This has resulted in the formation of smart grids: electrical networks that have both bidirectional power and information flows to increase the system reliability, security and efficiency of the microgrid. Simply put, the smart grid is an intelligent grid. While the conventional grid can only transmit and distribute electricity, the modern smart grid can communicate between power systems, generators and loads, and make decisions based on data. This does however require the components within the smart grid to communicate and transfer data with a central processing unit that is used for decision-making, while also being controllable [84].

The ability to communicate real-time between suppliers and consumers of electricity vastly increases the control, optimization and efficiency of electrical power usage. Storage components are increasingly integrated within the grid as well and can immediately be deployed to store excess energy or as temporary energy supply, all controlled by the smart grid. This has recently become more important with the diffusion of RES with intermittent characteristics, requiring quick adaption to fluctuating energy supply. Active monitoring and control of power flows will also help power system reliability and quality, and allow the smart grid to restore its own infrastructure after disturbances. Even more, smart grids can operate independently of the transmission or even distribution grid that have their own components for energy supply and storage [53].

Another advantage of the smart grid is that it can form a distributed network with other smart grids. Not only is the smart grid able to balance its energy supply and demand within its own network, real-time communication and energy exchange between other smart grids allows automated balancing of electricity over a wide area. The interconnection of smart grids can increase their independence of the transmission and distribution grid even more. Plus the network is more reliable since if one node (smart grid) fails, other nodes

are still able to continue their operations. Figure 2.13 depicts the difference between a centralized (traditional grid) network, decentralized (microgrid) network and a distributed (smart grid) network.

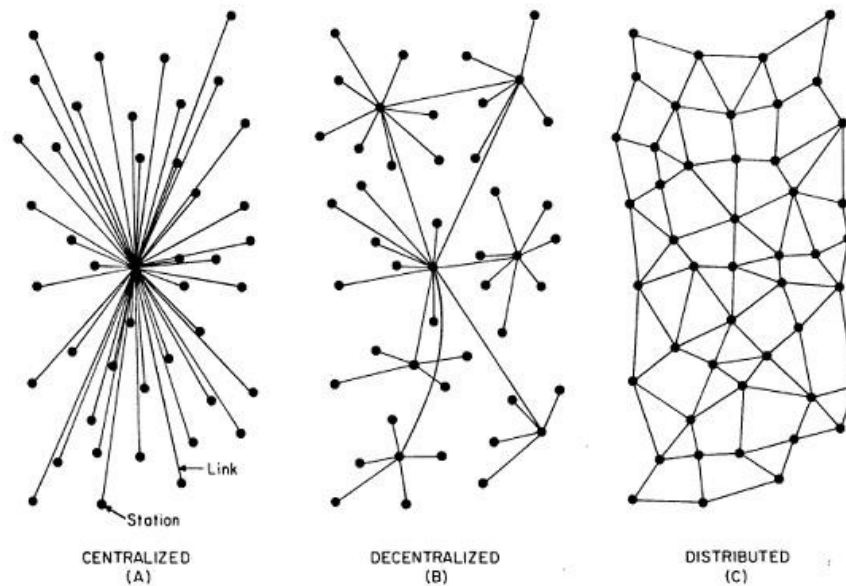


Figure 2.13: Different types of networks: A) centralized, B) decentralized, c) distributed. Taken from [17].

2.4.3. Domains of the Smart Grid

A distributed smart grid network has the potential to control the grid at local, regional and even national level. Figure 2.14 depicts four domains at which the smart grid can operate and will form synergy in the electrical energy ecosystem. The first region is the **Generation Domain** that includes power generation by centralized power plants (gas plants, nuclear plants, hydro dams), centralized generation by RES (onshore/offshore wind park, solar farms), distributed RES generation (solar panels on rooftops, single wind turbines) and cross-border power exchange with neighbouring countries. The second domain is the **Transmission and Distribution Domain**, the main infrastructure of electrical power transport. Deployment of smart substations allow the control, measuring and monitoring of both the HV, MV and LV grid networks. This is done both automatically as manually at a remote monitoring station. The third domain is the **Commercial and Industrial Domain** and combines newly introduced concepts like smart buildings, energy storage and PEV charging parks. Demand side management can be employed at this level by controlling the energy demand (especially those of industries) with cost incentives. The fourth domain is the **Residential Domain** with a large number of small loads (households) and widely varying load demand profiles. Small scale storage is often possible at this level.

The different operating domains are linked by the smart grid, which uses smart metering at all domains to obtain supply and load data. This data can be used for operation, monitoring and controlling systems like *Supervisory control and data acquisition (SCADA)* or *Wide Area Monitoring Protection and Control (WAMPAC)*. This data can be used for markets as well, with real-time buying and selling of electricity depending on the current supply and demand. Consumers, or even automated scheduling frameworks, can optimize their energy consumption by responding to the pricing of electricity. This can lead to both economic advantages (less energy costs), as well as environmental advantages (increased efficiency, less overconsumption) [85].

2.4.4. Smart Grid elements

The smart grid can be described by a number of common elements with their own characteristics and their constraints, which are used for the modelling and simulating of the total power grid. The most basic elements are the 1) power line, 2) load, 3) generator, 4) storage device and 5) point of common coupling (PCC). These elements will be discussed individually [64].

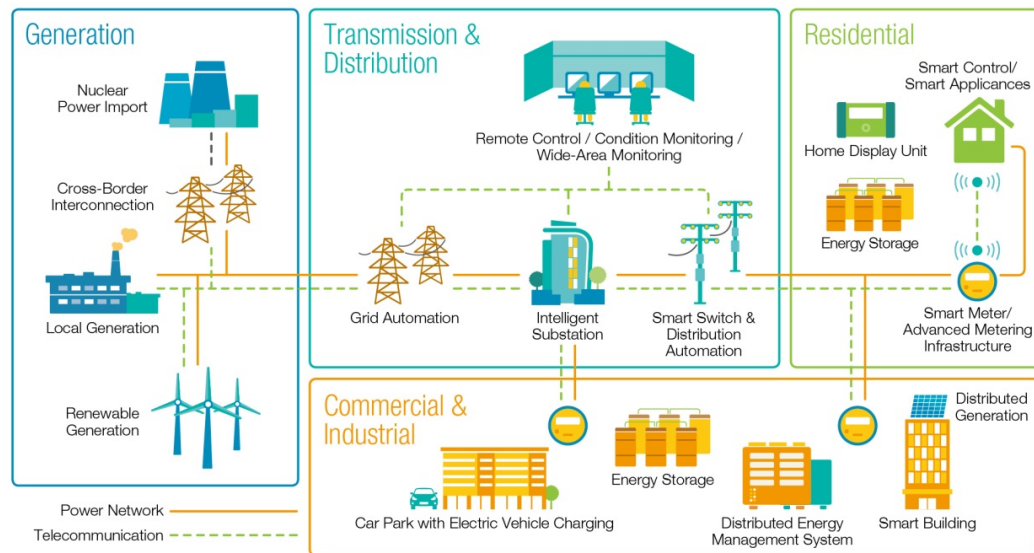


Figure 2.14: Overview of a smart grid and domains of operation and application. Taken from [18].

1) Power line

The connection between two buses i and j of the grid, in which power flows from one bus to another. Power lines can be cables or lines in the physical domain, used for the transmission and distribution of electricity from generators/storage devices to loads. The power line is constrained by its maximum power flow, which is defined by its maximum current.

2) Load

The load is connected to a bus in the grid. It draws and consumes active and reactive power from the bus. Loads can be any electrical appliance in industries, commerce and households that run on electrical power. The load voltage is restricted to a specific range while its phase angle is a free variable.

3) Generator

The generator supplies active and reactive power to the grid. Generators can be centralized like gas, coal and nuclear plants, or distributed like wind turbines, diesel generators and PV panels. The supplied voltage of the generator must be within a specific range while its phase angle is a free variable.

4) Storage device

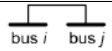



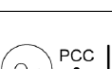
The storage device stores excess energy or lets energy be drawn by the grid during shortages. The device is essentially a buffer between energy production and consumption, in cases when supply and demand do not match. Batteries and capacitor banks are used for short-term storage, while pumped hydro, compressed air and hydrogen is used for long-term storage. The storage device has a limited capacity, with the state-of-charge (SOC) stating its capacity level. Its rated power, or charge and discharge power, also has an upper and lower limit and the device has to operate at a fixed voltage. Storage devices can also be self-discharging, losing energy in the process.

5) Point of common coupling

The point of common coupling (PCC) is always indexed as bus 1 ($i=1$), and is also known as the slack bus. Its fixed voltage and fixed phase angle (set at zero) are used as a reference for all other buses. The PCC is usually set at the connection of a microgrid with the main grid, or set at a certain generator.

The elements of the grid with their corresponding symbol, constraints and free variables are summarized in table 2.2.

Table 2.2: Common smart grid elements with their symbol, constraints and free variables.

Unit	Symbol	Constraints	Free Variables
Power line		$I_{i,j} \leq I_{i,j,max}$	-
Load		$P_i(t) = -P_{L,i}(t)$ (fixed) $Q_i(t) = -Q_{L,i}(t)$ (fixed) $V_{i,min} \leq V_i(t) \leq V_{i,max}$	$V_i(t), \delta_i(t)$
Generator		$P_i(t) = P_{g,i}(t)$ (fixed) $Q_i(t) = Q_{g,i}(t)$ (fixed) $V_{i,min} \leq V_i(t) \leq V_{i,max}$	$V_i(t), \delta_i(t)$
Storage device		$E_i(t) = \text{Stored energy}$ $V_i(t) = V_{S,i}$ (fixed) $0 \leq E_i(t) \leq E_{i,max}$ $-P_{i,ch} \leq P_i(t) \leq P_{i,dch}$	$P_i(t), Q_i(t), \delta_i(t), E_i(t)$
Point of common coupling		$\delta_i(t) = 0$ $V_l(t) = V_{in}$ (fixed) $Q_{l,min} \leq Q_l(t) \leq Q_{l,max}$ $P_{l,min} \leq P_l(t) \leq P_{l,max}$	$P_l(t), Q_l(t)$

2.5. Demand side management and optimization

Two important aspects determine the effectiveness of the smart grid. The first aspect is focused on the ability to deliver stable and reliable power, to ensure energy supply and demand is always met. The second aspect is focused on the economic aspect of the grids operation. Economic feasibility is important for the integration and diffusion of the smart grid.

2.5.1. Demand side management

Demand side management consists of measures to change the load patterns of consumers to ease the matching of supply and demand of energy. Management is done by applying measures which will result in a changing behaviour of the end-user or a flexible load. A distinction can be made by price-based incentives and event-based incentives. Price-based incentives involve the variable pricing of electricity, while event-based incentives focus on altering and controlling the amount of load. The transmission capacity of the electrical grid is designed in such a way that it can handle peak production and peak demand in an efficient and stable manner. TSOs will want to reduce the peak demand as much as possible to reduce the required transmission capacity for the whole transmission grid. There are several methods to ensure load demand is more spread out instead of it being concentrated at peak periods. The TSO will aim to increase its load factor which is defined as the ratio between the average load and its peak load in a certain time period, as determined by equation 2.27.

$$f_{load} = \frac{P_{avg}}{P_{peak}} \quad (2.27)$$

with f_{load} the load factor, P_{avg} the average load of the grid and P_{peak} the peak load of the grid.

A high load factor is preferred since it will result in less required transmission capacity and higher electrical efficiency. There are several methods to obtain, or remain, a high load factor by demand side management, of which some methods are depicted in figure 2.15. Peak clipping, load shifting and obtaining a flexible load shape are the methods most used by system operators to increase their load factor.

Demand side management can be divided in two categories as stated earlier: price-based measures and incentive-based measures. The measures operate in different time frames, with some being planned weeks or months ahead while others are planned days before economic dispatch or even on the day itself. Some popular measures are listed below [19][86][87].

Price-based measures

- **Time of use (TOU) rates**

A common financial measure is to differentiate between high and low electricity tariffs, which can result

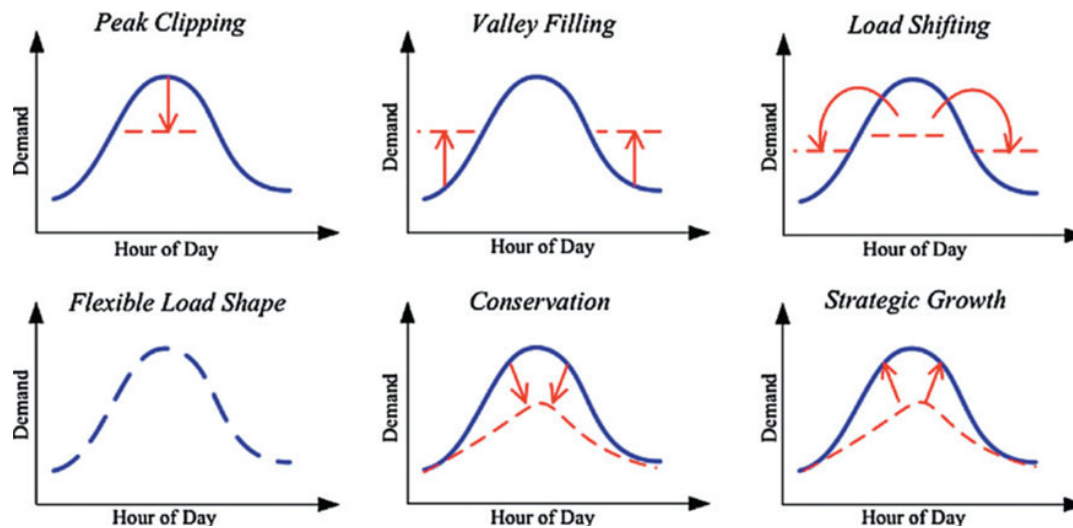


Figure 2.15: Methods for demand side management of the electrical grid. Taken from [19].

in end-users shifting their use of certain appliances towards periods of low tariff. The tariff rates are fixed and occur during specific predefined time blocks, allowing the end-user to anticipate on periods of reduced tariff. Prices are higher during peak periods and decrease during off-peak periods, with the TOU rates being set weeks or months in advance. The prices are thus not affected by day-to-day volatility of electricity costs. The result of this financial measure is load shifting.

- **Critical peak pricing**

Critical peak pricing (CPP) is similar to TOU pricing, but only occurs during high peak periods. The electricity prices at the peak periods are several times higher than normal and thus end-users are being encouraged to reduce or shift their energy demand. The peaks of energy production and thus their prices are determined on the day of economic dispatch, which can be hours or even minutes in advance. The system operator will only be limited to a specific times at which CPP can be applied to avoid over usage. CPP results in peak shaving/clipping and/or load shifting.

- **Real-time pricing**

Dynamic pricing, or real-time pricing (RTP), adds a flexibility to electricity prices that can change in short time spans depending on the energy supply and demand. Prices are continuously adjusted every hour or even more frequently. Smart systems within residential, commercial and industrial buildings can adapt and optimize their load control according to the electricity prices. Prices are determined on the day of economic dispatch or based on the day ahead.

Incentive-based measures

- **Direct load control**

An agreement is struck between the system operator and end-users that gives the operator direct control over certain loads and the right to turn on or shut these down. Dynamic loads with a quick ramp up or ramp down are preferred, since direct load control is used to apply demand side management in a small timescale. End-users are compensated for allowing the operator to control their loads. Direct load control is a method to obtain a more flexible load shape and for peak shaving.

- **Emergency demand response**

End-users are warned in advance when loads have to be reduced to ensure system reliability. This will allow the end-user to adapt its operation of loads in advance and to reduce or shut them down at specified time periods. The result of this measure is load shifting and a more flexible load shape.

- **Load curtailing**

Load curtailing is similar to emergency demand response but more urgent since the end-user will agree to curtail its loads upon request of the system operator. The curtailment must take place immediately

or shortly after the request from the system operator has been sent to the end-user, or it might face penalties. The control of the loads is fully in the hands of the end-user, which are usually medium or large consumers with interruptible programs. Peak clipping and a flexible load shape is achieved with this measure.

- **Demand side bidding**

Large consumers or small consumers that are aggregated into a single party can offer load reduction offers to the system operators on a bidding market. These offers, often combined with capacity and ancillary services, differ in time scales and magnitude. The system operator can bid on offers which suits the situation the best, while also being cost-effective.

Figure 2.16 shows the different DSM measures and in what time frame they operate. Apart from the price-based and incentive-based initiatives, energy efficiency can be considered as a form of DSM as well which is achieved by years of system planning ahead. Conservation is attained by increasing the energy efficiency.

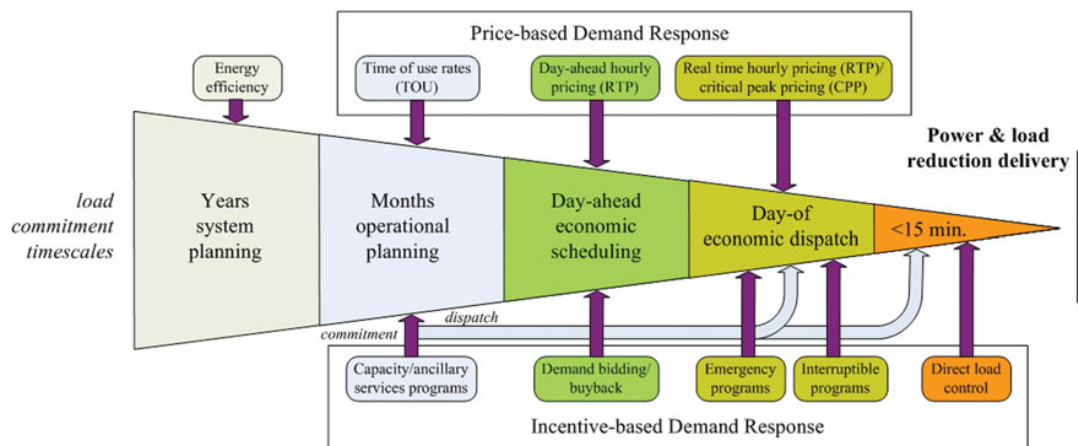


Figure 2.16: Timescale for different price-based and incentive-based DSM measures. Taken from [19].

3

Methodology

The methodology to achieve the research objectives are explained in this chapter. An overview is given over how the research is approached and which steps are taken to obtain results. A number of software packages have been used in the research process. A short description of these packages will be given. The approach taken to model the industrial grid with the electrolyser is explained, together with the constraints and boundaries the model should operate in. The choice of input data is clarified and the methodology for the economic analysis of the hydrogen production is described. At last, the cases used for the simulations will be discussed.

3.1. Method overview

The research objectives given in section 1.4 need a step-by-step approach to implement them. The approach taken for implementation is by developing a method in which decisions are made on how to achieve the objectives, which tools should be used and what constraints and boundaries should be considered. The methodology that has been developed for this research to achieve its objectives can be separated in three steps as shown in figure 3.1.

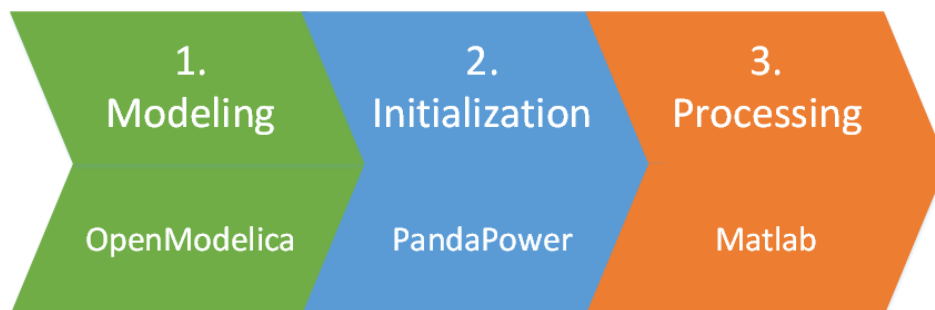


Figure 3.1: Methodology steps taken to obtain the research objectives.

To further clarify these three steps, each part is shortly described.

1. Modeling

The main bulk of the research is the modeling part in which the different components such as the industrial grid, the electrolyser but also the wind turbines and a controller to operate the electrolyser are build. The modeling also defines the sizing and design of the different components. The modeling is done in OpenModelica, a simulation tool that will be explained further on in this chapter. The model provides a framework to simulate the behaviour of the industrial grid setup, in which the user can provide its own input data to obtain results. Since the modeling is an extensive part of the research, it is described in a separate chapter. Further information can therefore be found in chapter 4.

2. Initialization

The initialization of the modeling setup is used to assign initial values for the model components, and to

assign the input data which will be processed by the model. These initial values provide a starting point for the system and the constraints the system should operate in. The input data provides the context and cases which should be processed. The model is a partial power system and its initial values are obtained via an optimal power flow calculation through Pandapower, a tool that will be explained further on in this chapter. The choice and source of input data is explained further on as well.

3. Processing

Simulating the OpenModelica model results in significant amounts of raw output data that can be used to draw conclusions about the operation of the electrolyser and the feasibility of hydrogen production amongst others. It is however cumbersome to analyze the raw data obtained from the simulation and therefore this data will need further processing. Raw data will be exported to comma-separated-values(.csv) and imported into Matlab for further processing, analysis and plotting. A description of Matlab is given in the next section.

3.2. Software tools

The three main software packages used for this research are OpenModelica, Pandapower and Matlab. All three programs are described in their own section.

3.2.1. OpenModelica

OpenModelica is an open-source modeling and simulation tool based on Modelica. Modelica itself is an "objective-oriented, declarative, multi-domain modeling language for component-oriented modeling of complex systems [88]" with models described by differential, algebraic and discrete equations. OpenModelica is therefore well-suited to build a dynamic model which integrates both the electrical, chemical and mathematical domain, as will be done in this thesis. OMEdit, the GUI of OpenModelica, is written in C++ and the integrated OpenModelica Compiler (OMC) can translate Modelica code to C code.

Models in OMEdit can both be created in a textual or in a graphical mode, and can have interconnection and interaction with other models, provided that the interconnected signals operate in the same domain. Collections of pre-built models for common components are grouped together in libraries to provide an easy method for model building. OpenIPSL[89] is such a library that provides many components used in dynamic power system modeling, with components like generators, transformers, loads etc. The models in this library will be used in this thesis to create the industrial power grid. An example of a single machine infinite bus system with OpenIPSL components in the OMEdit environment is shown in figure 3.2.

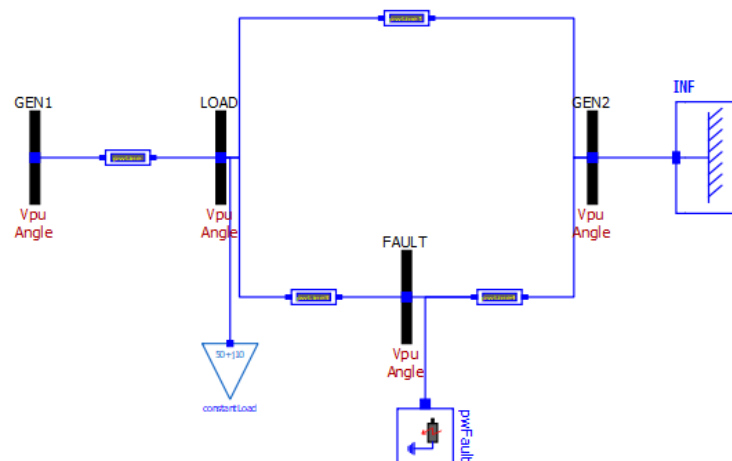


Figure 3.2: SMIB example in OpenModelica with OpenIPSL components.

The OMEdit environment also provides a plotting tool for result analysis. However, this plotting tool is limited in its use and configuration. OMEdit has an option to export results to a .csv file to provide an

opportunity to analyse and process the results in a different environment. At last, the software version used for this thesis is OpenModelica v1.13.1 (64-bit).

3.2.2. Pandapower

Pandapower is a power system analysis and electric modeling tool within Python, and combines the data analysis library pandas and the power flow solver PYPOWER[90]. The tool is suited to perform static analysis of balanced power systems, and can perform (optimal) power flow calculations, state estimations and short-circuit calculations amongst others. Dynamic power systems usually need balanced initial values for the voltage, angle, active or reactive power of electrical components such as loads, transformers and generators as a starting point to perform a dynamic simulation. The initial values are obtained in Pandapower with a power flow calculation of the desired electric grid, provided that the grid is balanced and solvable.

The Pandapower library itself also contains a number of benchmark power systems for analysis. One of these power systems is used as blueprint for the industrial grid to be build in OpenModelica and is further elaborated in chapter 4. The benchmark system is then analysed in Pandapower to obtain the initial values on which the model in OpenModelica can run. The version used for this thesis is Pandapower 1.6.0 [20].

3.2.3. Matlab

Matlab is a numerical computing and programming tool to mathematically work with matrices and arrays for data analysis, manipulation and plotting. The software is used in a wide variety of applications thanks to its wide functionalities. Matlab will process the data gained from the OpenModelica model to visualize the results and compare different simulated cases. The economic analysis of hydrogen production will be done in Matlab as well, by importing all relevant data parameters into a Matlab script to calculate the production cost. An import option for .csv files exist within the Matlab environment that enables the import of data from OpenModelica.

3.3. Selection of input data

The OpenModelica model needs two data inputs for the system to operate. The first data is the hourly wind pattern of a certain location. The second data input is the hourly electricity intraday market prices.

3.3.1. Wind data

Since the industrial grid is based in the Port of Rotterdam, more specifically the Maasvlakte area, the inserted wind data should represent the wind profile of this location. The Dutch Meteorology Institute KNMI has many weather stations spread out over the Netherlands to measure weather data such as temperature, precipitation and wind. Hourly data of these weather stations are made publicly available that can be used for all kinds of research [91]. Historical data is saved as well and thus wind profiles from specific days can be extracted. The wind data given is the average wind in meters per second during a specific hour slot, so for example the average wind speed between 00:00AM and 01:00AM on 1 January 2018 was 14.0 m/s. For this research it is assumed that there is perfect forecast knowledge of the average wind speed to be expected at least an hour in advance. Actual varying wind patterns that cause fluctuations around the average are unknown and should be compensated by the electrolyser.

The historical data from the weather station in Hoek van Holland is taken as it is the closest station post available near the Maasvlakte and the data of the wind profiles used in this research can be found in Appendix A. The location of the grid area and the weather station is shown in figure 3.3.

3.3.2. Intraday market data

The electrolyser will buy electricity from the grid if its minimum capacity cannot be fulfilled by wind energy or if market prices are opportune and the electrolyser has capacity left. The intraday electricity market is chosen to trade upon, since this market has vast volumes of wind power that are being traded at favorable prices. Intraday markets also provide the opportunity to trade electricity close to real time, from which the electrolyser can benefit from the extra flexibility if it is scheduling its own load demand. Data of electricity prices on the intraday market are therefore fed into the OpenModelica model to optimize the power exchange with the transmission grid. Many European electricity markets have the opportunity to continuously trade electricity in hourly intervals. The Netherlands has an intraday market as well, the APX Power NL market.



Figure 3.3: Location of the weather station (Hoek van Holland) and the port area (Maasvlakte).

However historical data of market prices is not available for the Dutch intraday market.

The German intraday market is provided by the EPEX Spot and does publish historical data of the electricity prices [92]. The German market is also interesting due to widespread diffusion of renewable energy sources in Germany, resulting in a dynamic power market. The influx of renewable energy supply is in some occasions larger than the power demand and the result is that electricity is sold for a negative price. However, the German intraday market is limited to the German electricity market and thus Dutch energy producers cannot trade on this market. But in recent years, the European electricity markets have become less fragmented and the European Union aims to fully integrate the electricity markets in the future [93]. Since the Dutch and German grid is already sharing many connections, it is assumed for this research that the German intraday market is already available for the Dutch electricity market. Furthermore, it is assumed that the energy producer of the electrolyser has perfect knowledge of the electricity prices up until the closing time of the market, and that supply of the intraday electricity is infinite.

The intraday prices are given in Euros per MWh for each hour slot, so for example the electricity price between 00:00AM and 01:00AM on 1 January 2018 was €0.34/MWh. Trades should have a minimum volume of 0.1 MWh and can be made until thirty minutes before delivery begins. The historical data for intraday market prices used in this research can be found in Appendix B.

3.4. Economic analysis

The economic analysis will give an estimation of the cost price of hydrogen as produced by the electrolyser. The hydrogen cost price is separated in four costs that will be analyzed. These are 1) the capital, operating and maintenance costs of the electrolyser, 2) the levelized cost of electricity from the wind turbines, 3) the cost and benefit of trading on the intraday market and 4) avoiding penalties due to overproduction and underproduction.

Capital, operating and maintenance costs

The current capital cost of large-scale electrolyser is set at around €800k/MW for a lifetime of 10 years. Due to quick developments in the production of large-scale electrolysers, it is expected to price will go down in the mid 2020's to €500k/MW [94]. These two capital costs are taken as a high-end and low-end estimate. The operating and maintenance cost of large-scale electrolysers is largely unknown, one study [68] estimates the O&M costs at around 30% of the capital costs during the lifetime of the electrolyser. This is between €150k/MW and €240k/MW on costs for the low-end and high-end capital costs respectively.

Levelized cost of electricity

The levelized cost is the electricity price of wind energy with all costs considered (capital, O&M, decommission) during its lifetime to make break-even. As was shown in figure 1.4 of chapter 1, the LCoE of onshore wind is among the sharpest of renewable energy sources and was as of 2016 at around \$8ct/kWh. Another

more recent study done by the Fraunhofer Institute gives a range of €4ct/kWh-€8ct/kWh for onshore wind energy [95]. This pricing range will be considered for the economic analysis.

Trading on the intraday market

The associated costs with buying electricity on the intraday market are integrated within the OpenModelica model. An estimate will be made of the yearly buy-in costs based on the results received from the model. At some occasions, the intraday prices will be negative and in this case the energy producer that owns the electrolyser is paid to take electricity from the grid.

Avoided penalty costs

The electrolyser can balance the power exchange with the grid according to the scheduling the energy producer has agreed upon. This makes it easier for the energy producer to predict and schedule the amount of electricity exchanged and to avoid penalties for overproduction K_H or underproduction K_L . The penalties associated with power imbalance are taken from a study [71]. The penalty of overestimation is €2/MWh, the penalty for underestimation is €5/MWh on the low-end and €10/MWh on the high-end. It is assumed that normally these penalties are integrated into the LCoE of the wind turbine. Since the penalties are being avoided, the evaded penalties are considered benefits and will be integrated in the hydrogen cost price.

Considering the above mentioned cost factors for the cost price of hydrogen, the equation to determine the cost price C_{H_2} in €/MWh is given in equation 3.1.

$$C_{H_2} = \frac{\frac{(CAP + O\&M)P_{elec,max}}{y_l} + (LCoE_{wp} * E_{y,wp}) + (C_{h,total}) - (C_{as,total})}{H_{2out,y}} \quad (3.1)$$

with CAP the capital costs of the electrolyser per megawatt in €/MW, $O\&M$ the operation and maintenance cost during its lifetime per megawatt in €/MW, $P_{elec,max}$ the rated capacity of the electrolyser in MW, y_l the lifetime of the electrolyser in years. $LCoE_{wp}$ is the levelized cost of electricity from the wind turbine in €/kWh, $E_{y,wp}$ the yearly consumption of electricity from wind power by the electrolyser in kWh. $C_{h,total}$ the total yearly buy-in costs from the intraday market in € and $C_{as,total}$ the total avoided penalties due to power balancing in €. $H_{2out,y}$ is the yearly hydrogen production of the electrolyser in MWh.

Some of these values used with the cost price calculation are given in table 3.1, the other variable parameters are determined by simulating.

Table 3.1: Range of values used for the different cost factors of the economic analysis

Parameter	Value
Capital costs (CAP)	500k-800k €/MW
Operation & maintenance costs (O&M)	150k-240k €/MW
Levelized cost of electricity (LCoE _{wp})	4-8 ct/kWh
Electrolyser lifetime (y _l)	10 years
Rated power electrolyser (P _{elec,max})	10 MW
Penalty for overproduction (K _H)	2 €/MWh
Penalty for underproduction (K _L)	5-10 €/MWh

A lot of assumptions are made for the economic analysis and many aspects are left out to determine a more realistic price. The hydrogen that is being produced by the model in this research is uncompressed hydrogen gas that is assumed to be exchanged with an infinite hydrogen pipeline grid. In reality, hydrogen is often compressed to high pressures of up to 700 Bar, depending on the method of transport or storage being used. Compression is an energy intensive process which reduces the efficiency of hydrogen production and thus lead to extra costs. Hydrogen is also converted sometimes in for example ammonia for easier storage, a chemical process that also involves extra costs. At last the energy infrastructure required for hydrogen is to be considered as a cost factor. While the natural gas infrastructure can be used to some extent to transport and store hydrogen, it is not well suited to fully use hydrogen in its current state. A complete renewed gas infrastructure (pipeline network, storage containers etc.) has to be build which requires heavy investments and drives up the hydrogen cost price.

Benefits from selling oxygen gas, a by-product of hydrolysis, is left out as well. Furthermore, the heat flow required to keep the electrolysis process at 353K is assumed to be delivered with free and infinite industrial heat, and the water feed-in required for the electrolysis is considered to be free and infinite as well. The electrolyser itself, and the wind turbines that provide electricity, are assumed to have no downtime at all and be kept at 100% operation at all times.

3.5. Simulation cases

Several simulations will be run to test the industrial grid with an integrated electrolyser. The simulations of the OpenModelica model will cover a full day (24 hours) of control, scheduling and hydrogen production. The data of a full day will be inserted for each case, from 00:00AM to 23:59PM. Twelve days spread out over one year will be picked to simulate, to give a good representation of different wind profiles and market prices that can occur over the year, and to take seasonal variation into account. The first day of each month from the year 2018 will be simulated: 1 January 2018, 1 February 2018, 1 March 2018... etc. The historical data, previously discussed in this chapter, that belong to these days will be used. This will give a total of twelve cases to be simulated, each case belonging to one of the twelve months. These twelve simulations should give a clear view and estimation of the implementation and cost of hydrogen production in the industrial grid.

Four cases spread out over the year will be picked and further analyzed in the results section. These are the winter case (1 January 2018), the spring case (1 April 2018), the summer case (1 July 2018) and the autumn case (1 October 2018). The wind profiles and the intraday market graphs of each of these cases will be presented below.

Winter Case

The winter case is represented by the January case, with the wind pattern shown in figure 3.4 and the intraday market prices shown in figure 3.5. The wind forecast initially starts high at above rated wind speed for the wind turbines and gradually drops down during the day, even to below the cut-in speed of the turbines. The market prices show a reverse relation, in which excess electricity is available in the first half of the day. Prices are even negative, which means the supply is significantly higher than the demand. The market prices start to become positive again halfway the day, but still remain relatively low for the whole case.

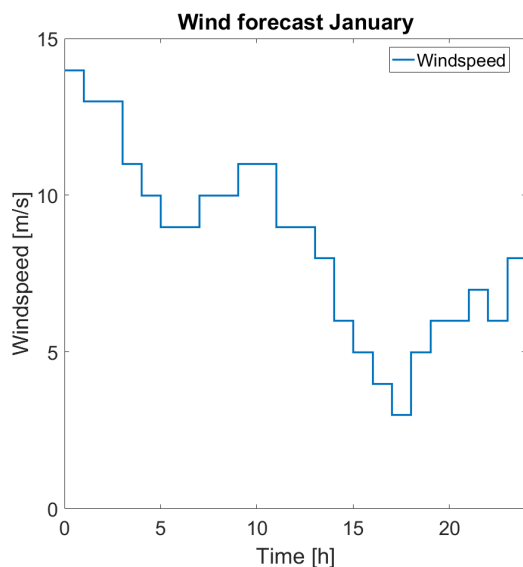


Figure 3.4: Wind pattern used for the January case.

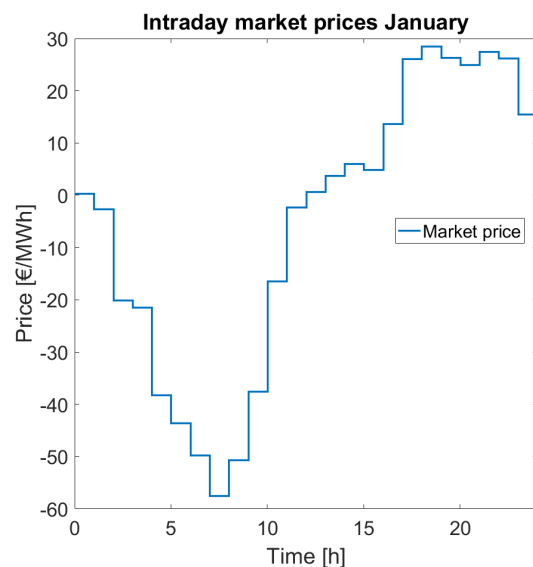


Figure 3.5: Intraday market prices used for the January case.

Spring Case

The spring case is represented by the April case, with the wind pattern shown in figure 3.6 and the intraday market prices shown in figure 3.7. The wind forecast of April shows that on average a low windspeed is to be expected. There are two peaks during the day in which the wind is somewhat higher than average, but at the

end of the day periods that are almost windless will occur. The intraday market shows average prices as well for most of the day, with suddenly a price drop for an hour in which the electricity price almost goes to zero. The price then quickly ramps up to average market prices again.

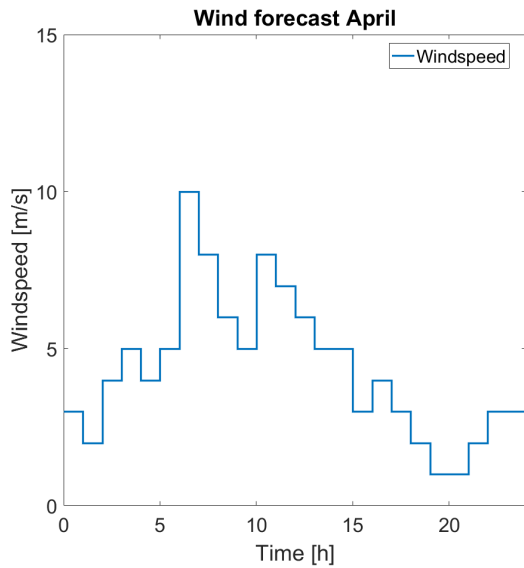


Figure 3.6: Wind pattern used for the April case.

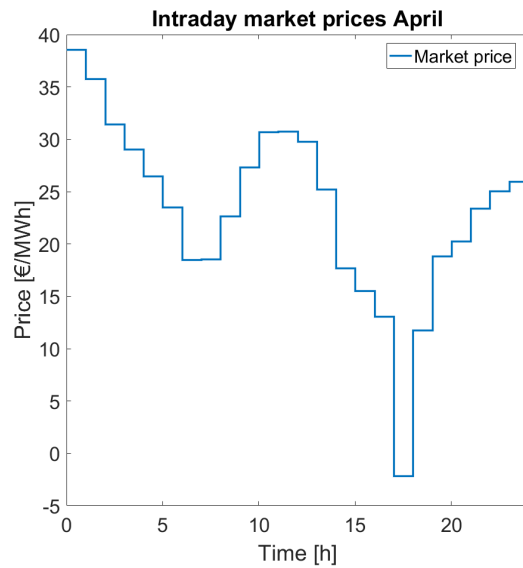


Figure 3.7: Intraday market prices used for the April case.

Summer Case

The summer case is represented by the July case, with the wind pattern shown in figure 3.8 and the intraday market prices shown in figure 3.9. The wind forecast is mostly constant during the day, with some fluctuations for a few hours during the morning and in the evening. Electricity prices are initially low and drop even further during the day to negative prices. In the afternoon, the prices quickly ramp up to high prices in which it is less feasible to buy electricity from the market.

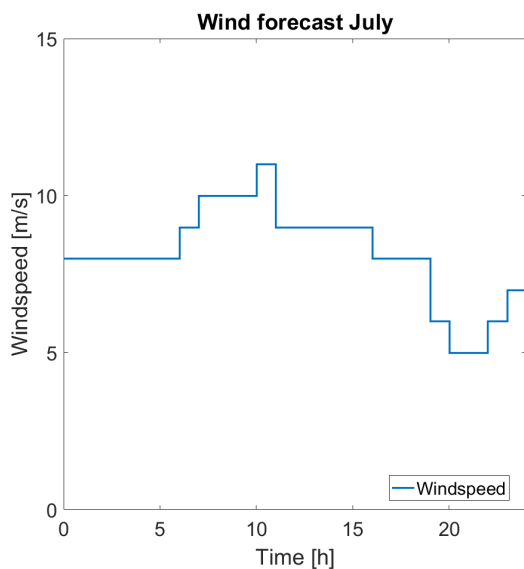


Figure 3.8: Wind pattern used for the July case.

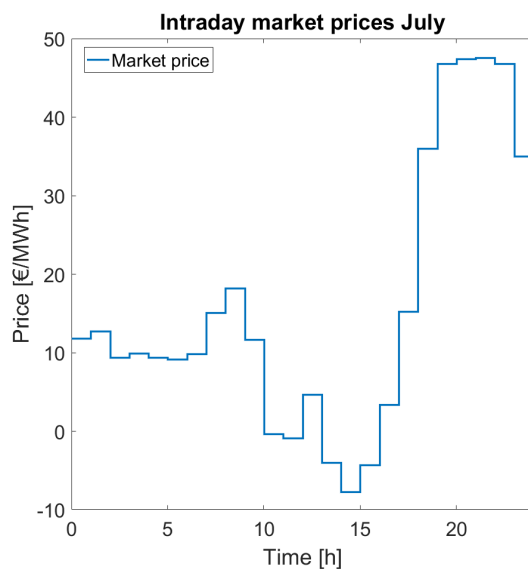


Figure 3.9: Intraday market prices used for the July case.

Autumn Case

The autumn case is represented by the October case, with the wind pattern shown in figure 3.10 and the intraday market prices shown in figure 3.11. The wind forecast shows a strong wind during the day, with a

drop in speed at start and end of the day. The market prices for electricity are relatively high for the whole case, with an even higher peak during the morning. Buying extra electricity for this case would be very expensive.

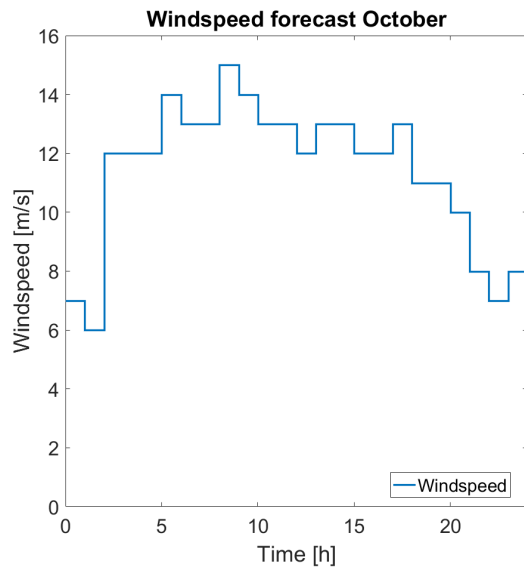


Figure 3.10: Wind pattern used for the October case.

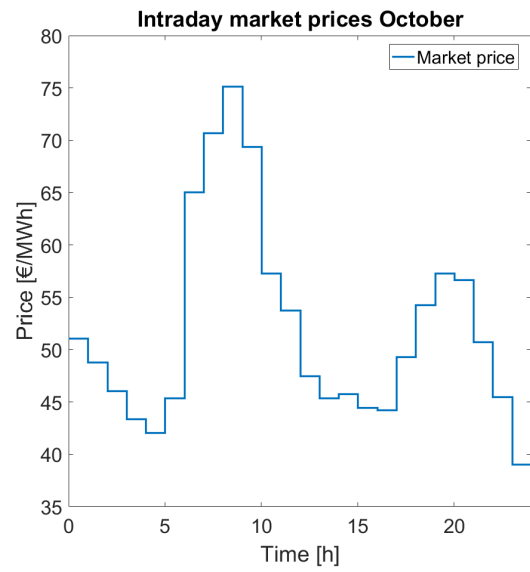


Figure 3.11: Intraday market prices used for the October case.

4

Modeling in OpenModelica

This chapter presents the modelling done for the different components of the industrial grid and electrolyser. The different components are modelled and simulated within OpenModelica, with all components connected in an overarching model. The five components are (1) the industrial medium-voltage microgrid representing the Maasvlakte; (2) a 10 MW PEM electrolyser; (3) a controllable load that represents the power consumption of the electrolyser; (4) the control system for controlling the power demand of the electrolyser, and (5) a simplified model for a wind turbine. The simulation of the components will happen simultaneously.

4.1. Overview

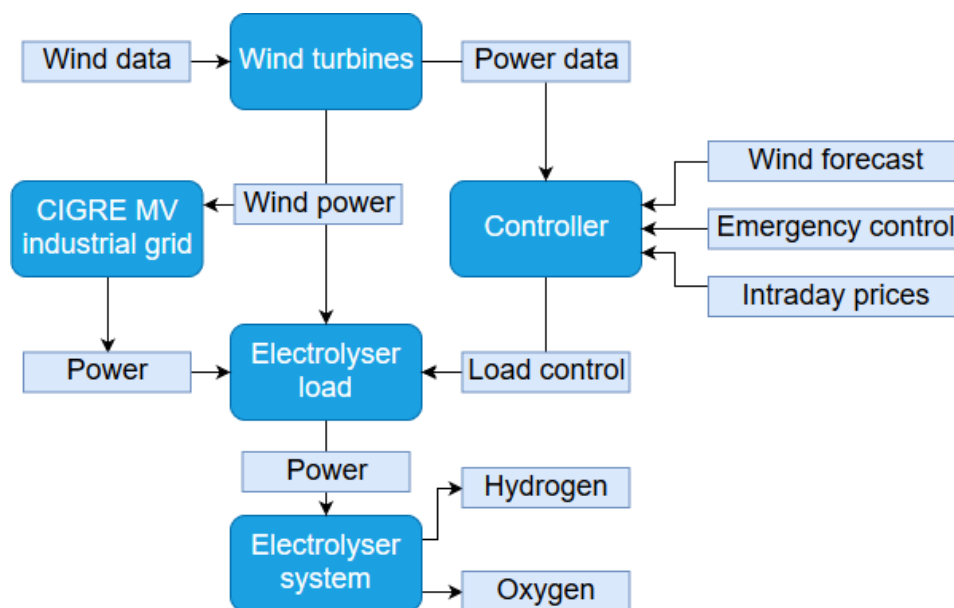


Figure 4.1: System overview of the modelled system

The proposed system consists of an medium-voltage(MV) industrial microgrid, representing the Maasvlakte electrical grid. The industrial grid is connected to the high-voltage(HV) transmission grid. Two wind parks supply the industrial microgrid with wind power. The first wind park injects its power into bus 1 and has a rated power of 21 MW. The second wind park feeds the grid at bus 12 and is rated at 18 MW. An electrolyser with a base load of 5 MW and rated load of 10 MW is connected to bus 12 as well, with a direct feed-in power supply from the second wind park. The electrolyser is modeled in two parts: one part representing a flexible and controllable load, the second part as a stack of electrolysis cells converting water into hydrogen and oxygen driven by electrical power. A controller is connected to the electrolyser load which can control the load demand of the electrolyser.

4.2. Modeling of systems

4.2.1. Model of Industrial Medium-Voltage Microgrid

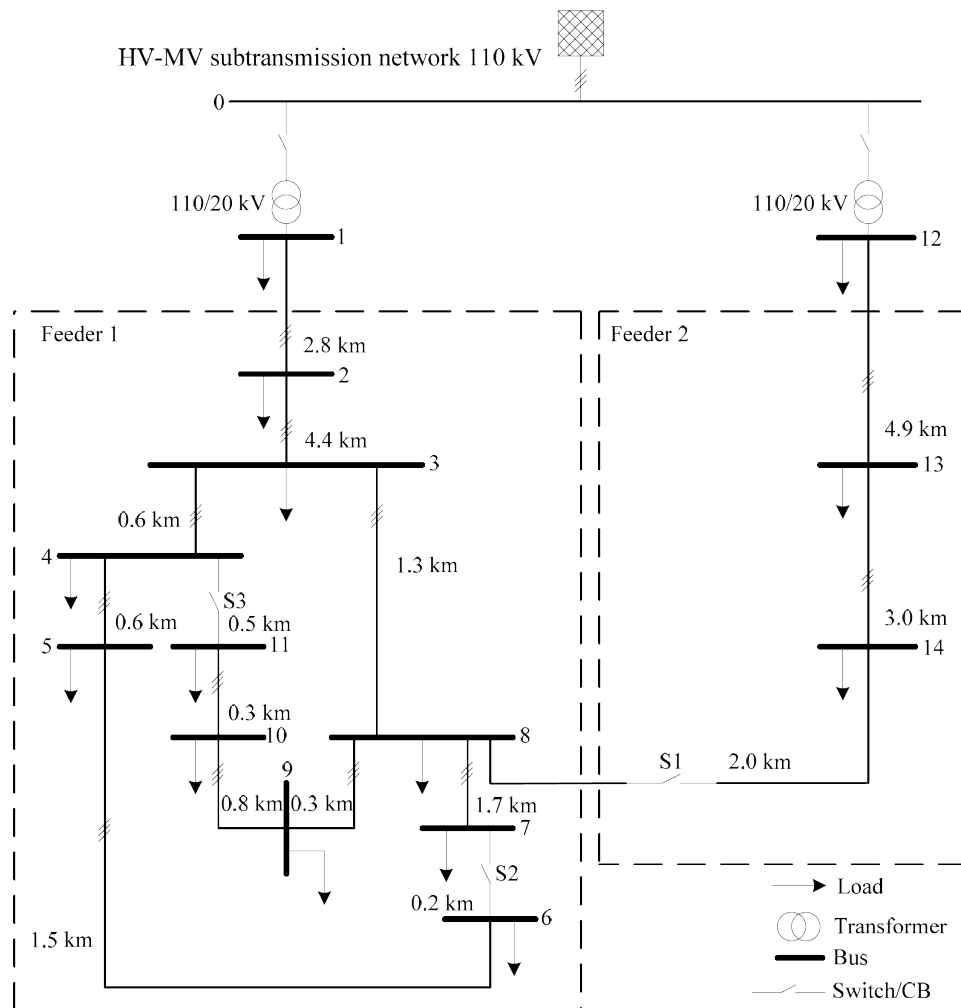


Figure 4.2: The CIGRE MV power system network for testing the integration of renewable DERs [20]

The industrial microgrid is the basis of the complete model, representing the power system grid of the Maasvlakte area at the Port of Rotterdam. The CIGRE MV network is used as benchmark system for the integration of the electrolyser system. The CIGRE networks were developed by the CIGRE Task Force to test, analyse and validate the integration of new methods and/or techniques, specifically of renewable energy sources and technologies [96]. The CIGRE power system is robust enough to integrate renewable DERs and test their effect on the stability on the system. The network operates on a base system power of 1 MVA and a frequency of 50 Hz. The network topology of the base power system is given in figure 4.2.

The base network is connected to a 110kV high-voltage external grid which exchanges active and reactive power with the CIGRE power system. Since OpenModelica has no component representing an external grid, a generator with Active Voltage Regulator(AVR) and governor is used instead. The AVR is a component of the generator that aims to automatically maintain a stable voltage level. The speed of the generator, and thus the frequency it generates, is controlled by the governor. The generator is represented by the PSAT fourth order OpenModelica model and table 4.1 shows the parameter data of the generator. The PSAT AVR type II within OpenModelica is used as model for the AVR and table 4.2 shows its parameter data. At last, the PSAT type II governor model is used and the parameter data of the governor is given in table 4.3. For simplifications, it is assumed that the generator is able to provide, or consume, infinite active and reactive power. Power demand of the industrial grid is thus always met by the exchange grid and is not affected by transmission and exchange constraints.

Table 4.1: Generator data of the PSAT 4th order generator model

Parameter	Value	Unit
V_0	1.03	p.u.
angle_0	0	deg
P_0	50	MW
Q_0	13	Mvar
xd	0.9	p.u.
xq	0.6	p.u.
xld	0.3	p.u.
xlq	0.5	p.u.
T1d0	8	s
T1q0	0.8	s
Sn	50	MVA
Vn	110	kV
ra	0	p.u.
M	12.8	kWs/kVA
D	2	-

Table 4.2: AVR data of the PSAT type II AVR model

Parameter	Value	Unit
vrmin	-5	p.u.
vrmax	5	p.u.
Ka	100	p.u./p.u.
Ta	0.5	s
Kf	0.15	p.u./p.u.
Tf	0.1	s
Ke	0	p.u./p.u.
Te	0.2	s
Tr	0.001	s
Ae	0.0006	-
Be	0.9	-
v0	1	p.u.
vref	1.03	p.u.

Table 4.3: Governor data of the PSAT type II governor model

Parameter	Value	Unit
wref	1	p.u.
R	0.2	p.u.
pmax0	1.2	p.u.
pmin0	0	p.u.
Ts	0.1	s
T3	-0.1	s
Sn	50	MVA

The 110kV from the exchange grid is transformed to 20kV and is used as base voltage for the rest of the network. The network is a 15-bus system with two 110/20kV transformers, eighteen loads spread out over the busses and five switches. The network is divided into two feeder regions, each with their own power injection. The two regions are connected to each other as well to allow power transfer. Connection between the busses are done by transmission lines of varying length, resistance R and reactance X . Susceptance of the transmission lines is neglected due to their relative short lengths. Line parameters for the CIGRE MV network

are given in table 4.4. The name of the line corresponds to the busses the line is connected to.

Table 4.4: Line data of the CIGRE MV network

Line	Length (km)	R (Ω)	X (Ω)
Line_1-2	2.82	1.41282	2.01912
Line_2-3	4.42	2.21442	3.16472
Line_3-4	0.61	0.30561	0.43676
Line_4-5	0.56	0.28056	0.40096
Line_5-6	1.54	0.77154	1.10264
Line_7-8	1.67	0.83667	1.19572
Line_8-9	0.32	0.16032	0.22912
Line_9-10	0.77	0.38577	0.55132
Line_10-11	0.33	0.16533	0.23628
Line_3-8	1.3	0.6513	0.9308
Line_12-13	4.89	2.4939	1.78974
Line_13-14	2.99	1.5249	1.09434
Line_6-7	0.24	0.12024	0.17184
Line_11-4	0.49	0.24549	0.35084
Line_14-8	2	1.02	0.732

Most busses in the grid have one or two loads connected, each with a unique power demand. The loads used in the network are the PSAT constant PQ load models in OpenModelica. The electrolyser and wind turbine will be integrated at bus 12, with the electrolyser replacing one of the base loads (load CI12) at bus 12. The active and reactive power data of the loads and the electrolyser are given in table 4.5. Industrial loads are usual heavy on power demand, but are predictable in their power curves as well since industrial processes run for fixed periods with fixed power requirements. The industrial loads in this research are assumed to always be kept at constant active and reactive power for simplifications. Dynamics in power demand only origin from the electrolyser load.

Table 4.5: Load data of the CIGRE MV network

Load	Bus	P (kW)	Q (kVar)
R1	1	14994	3044.662
R3	3	276.45	69.2849
R4	4	431.65	108.1817
R5	5	727.5	182.3287
R6	6	548.05	137.3543
R8	8	586.85	147.0785
R10	10	475.3	119.1214
R11	11	329.8	82.65567
R12	12	14994	3044.662
R14	14	208.55	52.26756
CI1	1	4845	1592.474
CI3	3	225.25	139.5974
CI7	7	76.5	47.41044
CI9	9	573.75	355.5783
CI10	10	68	42.14262
Electrolyser	12	10000	3297.359
CI13	13	34	21.07131
CI14	14	331.5	205.4452

At last it is assumed that the industrial grid will always operate in perfect conditions and will face no failures such as short-circuits, line overloads or other failure causes that might result in power failures of the grid. Its operation time during the simulations is considered to be 100%.

4.3. Model of 10MW PEM electrolyser

A mathematical model of the electrolyser is considered, in which OpenModelica provides the necessary mathematical blocks to simulate the electrochemical process taking place in the electrolyser cells. The electrolyser is first modelled as a single Proton-exchange membrane (PEM) cell. The cell is designed for an input power ranging between 0 and 3 Watt. It should however be noted that there is a difference in the maximum input power the cell can receive and its rated power. Electrolyser cells are able to sustain short periods of power consumption up to 150% of their rated power. In this design, the rated power of a single cell is set at 2 Watt and its maximum input power is set at 3 Watt (150% of the cell its nominal rated power). The electrolyser cell is operating at atmospheric pressure (1 atm) and a temperature of 80 Celsius (353.15 K), and will output both hydrogen (H₂) gas as well as oxygen (O₂) gas at 80 Celsius.

The model is expanded to a large scale electrolyser by multiplying the number of cells required to obtain the desired rated power. For simplifications, the behaviour and output of a single cell is not affected by other cells; the behaviour and output of a single cell will be simply multiplied by the number of cells. This is done due to simulation time constraints and to reduce the complexity of the model. The pressure and temperature is therefore uniform and constant within the cell stacks.

The rated power of the electrolyser is set at 10MW, with the ability to sustain 150% of its rated power (equal to 15MW) for short periods of time. The minimum base load required to maintain the operation of the electrolyser is 5MW, but it can operate below the minimum required base load for short periods. The ramp-up and ramp-down speeds of the electrolyser is set at around 500kW/s, which ensures a quick response to changing load demand. The ramping speeds are implemented by integrating a first-order function in the electrolyser that will limit the rate of change in power consumption.

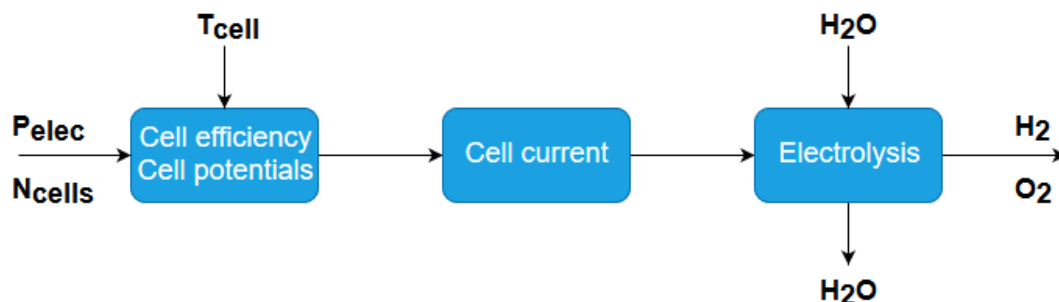


Figure 4.3: The steps taken in the electrolyser to calculate the hydrogen and oxygen mass flow.

A number of steps are taken to determine the amount of hydrogen and oxygen produced. First the cell potentials and cell efficiency are calculated. Secondly, with the potential and efficiency the cell current can be found which is inserted into the electrolysis process. At last, the electrolysis produces an hydrogen and oxygen mass flow. The complete electrolyser process is given in figure 4.3.

4.3.1. Cell potentials

The efficiency of the cell is determined by the ratio of the required reversible cell voltage (E_{Rev}) to make electrolysis happen, and the total voltage with losses included. Voltage losses occur due to activation overpotential (E_{Act}) and ohmic resistances (E_{Ohm}) within the cell. The concentration (saturation) overpotential is neglected for the electrolyser model since this potential is highly non-linear, thus significantly increasing the complexity of the OpenModelica model, while its effect on the overall cell potential is limited.

The reversible voltage is determined by the temperature of the electrolyser cell, an approximation for the reversible potential will be mathematically modelled as [97]

$$E_{Rev}(T) = 1.5148 - 1.5421 * 10^{-3} T_{cell} + 9.523 * 10^{-5} T_{cell} \ln T_{cell} + 9.84 * 10^{-8} T_{cell}^2 \quad (4.1)$$

The activation overpotential is linearized in [21], making the overpotential only depend on the input current of the cell. The overpotential is approximately given as

$$E_{Act}(I) = 0.0514I_{cell} + 0.2798 \quad (4.2)$$

The ohmic resistance is linearized in [21] as well, and is approximately given as

$$E_{Ohm}(I) = 0.09I_{cell} \quad (4.3)$$

The potentials are then combined and the cell efficiency is determined by

$$\eta_{cell} = \frac{E_{Rev}}{E_{Rev} + E_{Act} + E_{Ohm}} \quad (4.4)$$

The power injected into the electrolyser is equally divided over each cell, thus the cell power is equal to the total power injection divided by the number of cells

$$P_{cell} = \frac{P_{elec}}{N_{cells}} \quad (4.5)$$

The total current input into the cell stacks is then determined by

$$I_{cell} = \frac{P_{cell}}{E_{Rev} + E_{Act} + E_{Ohm}} \eta_{cell} \quad (4.6)$$

The cell current is dependent on the overpotentials, while at the same time both the activation and ohmic potential depend on the cell current. A zero hold order block is placed between the calculated cell current and the calculations of the overpotentials to prevent algebraic loops within the model. Since the cell potential constantly changes, the voltage level of the whole electrolyser changes as well. Flexible AC/DC conversion is required to constantly adapt to the fluctuating potential levels. It is assumed for this model that the AC/DC conversion is always optimal, 100% efficient and always results in a perfect voltage level. While this is far from realistic, this assumption leads to a significantly easier integration of voltage and power conversion while dealing with a flexible load in both power and voltage.

4.3.2. Hydrogen and Oxygen mass flow

The amount of hydrogen and oxygen produced by the electrolyser is determined by the input current I_{cell} . Faraday's Law provides a formula to determine the relationship between input current and the amount of hydrogen gas output produced

$$m = \frac{Q}{F} \frac{M}{z} \quad (4.7)$$

With m the mass of gas produced, Q the total charge inserted into the electrochemical process, F the Faraday constant, M the molar mass of the produced gas and z the number of electrons transferred. By replacing the total charge by current per second ($Q=I_{cell} \cdot t$) and dividing by hydrogen density the hydrogen output in m^3 per second is obtained

$$H_{2,prod} = \frac{M_{H2}}{\rho_{H2}} \frac{I_{cell}}{zF} \quad (4.8)$$

The same can be done for the oxygen output in m³ per second

$$O_{2,prod} = \frac{M_{O_2}}{\rho_{O_2}} \frac{I_{cell}}{zF} \quad (4.9)$$

The mass flow of water (H₂O) is not taken into consideration for the model as the availability of water is assumed to always 100% match the demand for the electrochemical process. The parameters for the previous equations are given in table 4.6.

Table 4.6: Characteristics of hydrogen and oxygen at 353K

	Hydrogen	Oxygen
Molar mass (M)	2.016*10 ⁻³	31.999*10 ⁻³
Density (ρ)	0.06953	1.104
Faraday constant (F)	96485	96485
Valency (z)	2	4

Since the cell is operating at a temperature of 80 Celsius, the hydrogen and oxygen density is different from standard values, as density is temperature dependent.

The hydrogen and oxygen mass flows are integrated to provide the total amount of substances produced over the operating time period, and is multiplied by the number of cells placed in the electrolyser stack.

$$H_{2,total} = N_{cells} \int_0^t H_{2,prod} dt \quad (4.10)$$

$$O_{2,total} = N_{cells} \int_0^t O_{2,prod} dt \quad (4.11)$$

The total produced volume of both gasses in m³ will be passed on as outputs of the model.

4.3.3. Overview of electrolyser model

The equations of the previous sections are combined and implemented in a mathematical model. The model has two inputs: electrical power and rated power. The first input $u1$ scales the electrolyser and determines the size, the cell amount and its rated power. The second input $u2$ is the continuously electrical power that is inserted into the electrochemical process to produce hydrogen and oxygen. These products are passed as output, with $y1$ for oxygen and $y2$ for hydrogen. The mathematical model as implemented in OpenModelica is shown in figure 4.4.

4.4. Model of controllable load

The controllable load is a modified standard load which can be scaled accordingly to a scaling factor. The load is used to set the power demand of the electrolyser which will be extracted from the main grid. The flexible and controllable property of the load creates the opportunity for demand side management of the electrolyser.

The PSAT LOADPQ model in OpenModelica is used as base model and is extended with an input for the control signal, and an output that will pass on the real-time amount of power consumed. The control signal will be received from the control system which will be discussed further in section 4.5. The output signal of consumed power will be send to the electrolyser system discussed in the section 4.3. The base model has an electrical pin component for connection with the industrial grid.

The active power P and reactive power Q of the load are formulated as

4.5. Model of control system

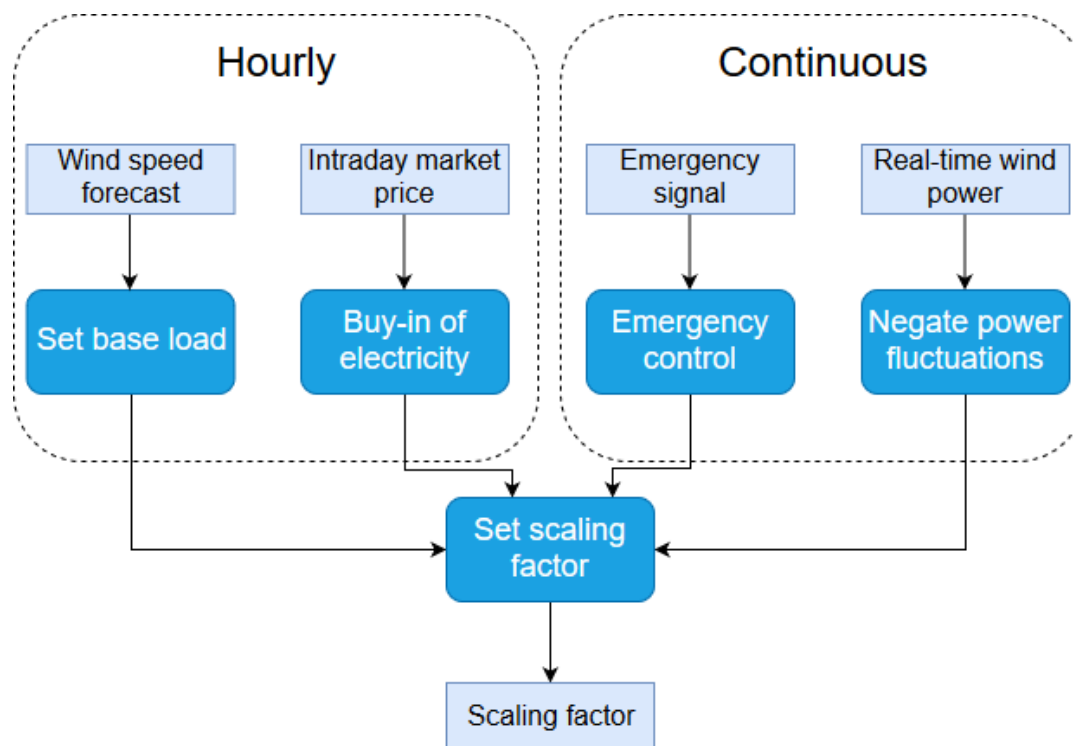


Figure 4.5: Operation diagram of the controller system

4.5.1. Controller parameters

The control system is modelled in OpenModelica and is a custom-made model that is responsible for determining the scaling factor u which will be passed upon the electrolyser load. The goal of the controller is to optimize the load demand of the electrolyser. Hourly scheduling is done by taking the weather forecast to determine the power demand in advance. A balancing service is provided by continuously adapting the power demand of the electrolyser to the real-time generated wind power. This ensures a stable power supply or demand to and from the main grid.

An emergency control is implemented as well, which is used to curtail the electrolyser load in case of emergencies. Furthermore, the controller can decide to buy extra electricity from the grid if intraday market prices are below a minimum set price and the electrolyser has remaining capacity left. Fluctuations in the scaling factor, and thus the electrolyser power demand, is affected by four conditions:

- Wind speed forecast
- Real-time wind power
- Intraday market prices
- Emergency situations

The model will receive these four conditions as input data and an algorithm will decide upon the scale factor. A diagram of this process is shown in figure 4.5. The model will be built in such a way that the wind park and electrolyser are sizeable.

- **Wind speed forecast $P_{f,h}$**

A day-ahead forecast of the wind speed is made each day and gives an estimate of the expected wind power to be produced which determines how much power will be scheduled by the wind turbines and

the electrolyser. The wind speed is given per hour and takes the expected average wind velocity of that time slot. The rated power of the wind park is taken as the power forecast if the expected wind power production exceeds the rated power of the wind turbines.

- **Real-time wind power P_{wp}**

The actual power supplied by the wind turbines will vary from the expected supply based on the day-ahead forecast. Wind power is a function of wind speed, so an intermittent wind pattern will result in an equal intermittent power supply. The wind turbines measure the real-time power produced and will send the data to the control system. By monitoring the wind power data, the control system can scale the electrolyser power demand accordingly to neutralize fluctuations. The real-time data is assumed to be sent to the controller with no lag, so that the controller can immediately respond to a change in wind power production.

- **Intraday market price C_h**

The control system can decide to ramp up the hydrogen production if electrical power is cheap on the intraday market. Hourly data of the electricity price is given and the controller decides to buy-in extra electricity if the price is under a predefined minimum and the electrolyser has available capacity. Auctions and prices go per megawatt-hour (€/MWh). The controller will also register the total price it will have spend or earned on the intraday market per day.

- **Emergency situations E_c**

The DSO can send a request for load curtailment in cases of emergency, or the operator of the electrolyser can decide to shutdown its operation for maintenance. The controller is able to curtail the electrolyser power demand in these cases by sending a stress signal that overrides all other actions. The electrolyser will only continue operation if the stress signal is lifted.

Configurable parameters

The model can be applied to a wind park and electrolyser of any size by setting the configurable parameters of the control system. The controller is then scaled accordingly to the given characteristics of the wind turbines and electrolyser. The custom parameters that can be modified in the controller are

- $P_{elec,base}$: base load of the electrolyser in MW
- $P_{elec,max}$: maximum load of the electrolyser in MW
- $P_{wp,rated}$: Rated wind power of the wind park at maximum wind velocity in MW
- v_{max} : Rated wind speed of the wind turbines in m/s
- v_{min} : Cut-in wind speed of the wind turbines in m/s
- C_{max} : Maximum buy-in price of electricity in €/MWh

4.5.2. Control algorithm

The controller takes the custom parameters and input parameters as input for decision making. The input parameters are P_{fc} for the expected power to be produced by the wind turbines based on the forecast, and P_{wp} for the actual wind power generated by the wind turbines. Furthermore, v_{fc} is the wind speed that has been forecast on which P_{fc} is based. The output parameters are a base scaling factor y_1 which is set on a per hour basis and depends on the wind forecast and the intraday market price. The variable factor y_2 is adjusted continuously and depends on the actual measured wind power. The factor c is the emergency control factor and changes depending on the emergency status. The three factors combined form scaling factor u as seen in equation 4.19.

$$u = c(y_1(h) + y_2(t)) \quad (4.19)$$

Scaling functions y_1 & y_2

The first scaling factor is updated on a per hour basis, as both the forecast of wind power $P_{fc,h}$ and the intraday market price C_h are updated per hour. The aim of this scaling factor is to set a base point of load demand that the electrolyser will use. The scaling factor y_1 is then given as in equation 4.20. It should be noted that the priority of the function that will be applied is from top to bottom. The first function will be applied if its conditions are met, otherwise the second function will be applied if those conditions are met. If that is still not the case, than the third function will be applied. The first function of equation 4.20 checks if the buy-in price on the intraday market is below a critical price threshold or if the predicted wind power production exceeds the rated power of the electrolyser. The second function checks if the minimum base load required for the electrolyser exceeds the wind power forecast. The third function is applied if the power production is in between the rated power and minimum base load of the electrolyser.

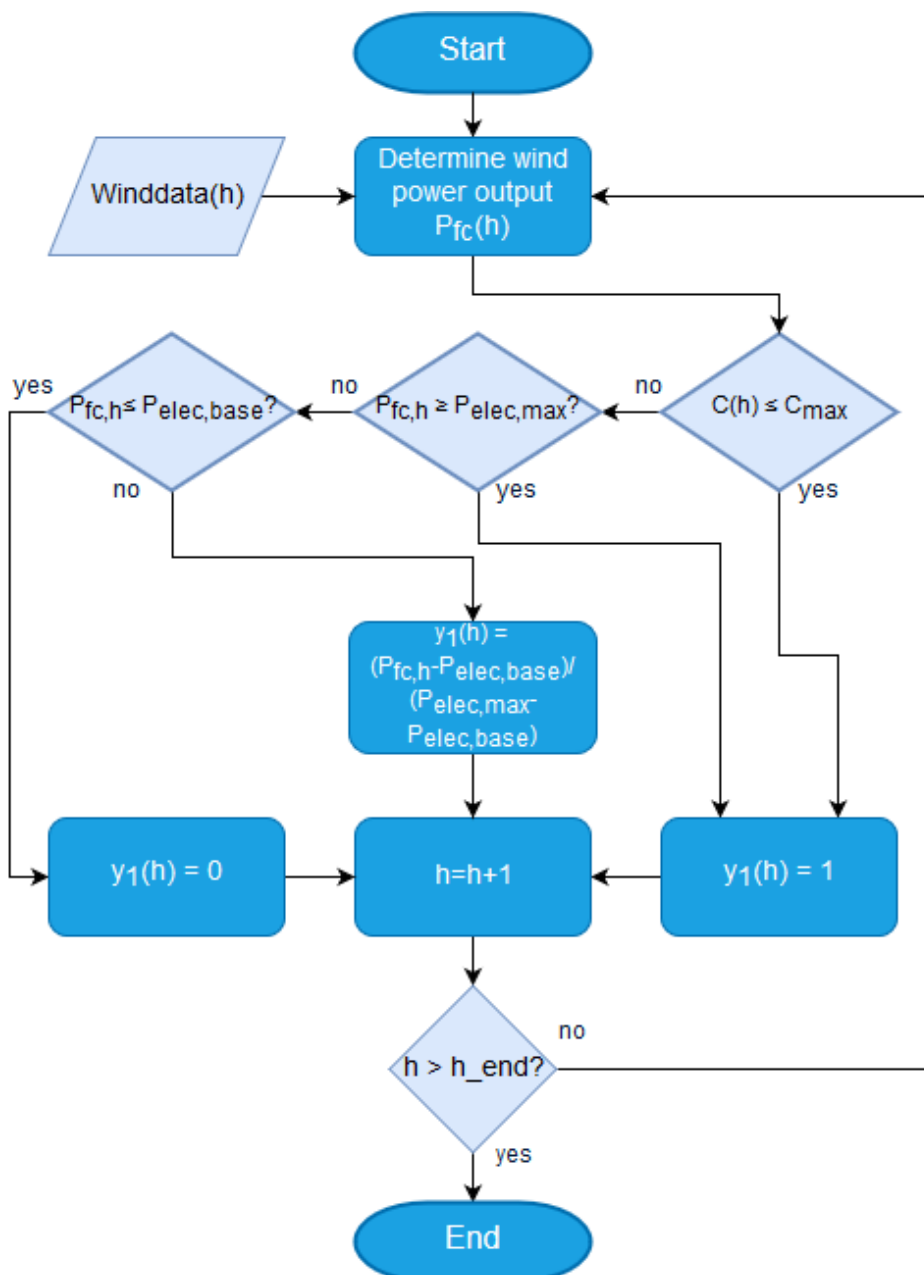


Figure 4.6: Algorithm flowchart for scaling factor $y_1(h)$

$$y_1(h) = \begin{cases} 1 & \text{if } P_{fc,h} \geq P_{elec,max} \text{ or } C_h \leq C_{max} \\ 0 & \text{if } P_{elec,base} \geq P_{fc} \\ \frac{P_{fc,h} - P_{elec,base}}{P_{elec,max} - P_{elec,base}} & \text{if } P_{elec,base} \leq P_{fc} \leq P_{elec,max} \end{cases} \quad (4.20)$$

with h standing for hour of the day (0, 1, 2, ..., 23). The algorithm flowchart for $y_1(h)$ is shown in figure 4.6.

The second scaling factor is adjusted continuously as the actual wind power fluctuates continuously as well. Depending on conditions the function of which the conditions are fulfilled will be applied. Priority is given from top to bottom, similar to the first scaling factor function. The first function is applied if the wind power prediction is equal to, or exceeds, the rated power of the wind turbines. The second function is used if there is a difference between the predicted power production and the real-time wind power production. The third equation is applied if the wind power forecast is equal to the real-time wind power production.

$$y_2(t) = \begin{cases} \frac{P_{wp} - P_{wp,rated}}{P_{elec,max} - P_{elec,base}} & \text{if } P_{fc,h} \geq P_{wp,rated} \\ \frac{P_{wp} - P_{fc,h}}{P_{elec,max} - P_{elec,base}} & \text{if } P_{fc,h} - P_{wp} \neq 0 \\ 0 & \text{if } P_{fc,h} = P_{wp} \end{cases} \quad (4.21)$$

Emergency control factor c

The emergency control works like a simple binary switch, it is either turned on or turned off. If there is no emergency situation, the control factor c will have value '1'. In case of emergency, the control factor will be set to value '0'. The emergency control is implemented within the algorithm used to determine scaling factor $y_2(t)$ since it is continuous and the corresponding flowchart can be seen in figure 4.7.

Over- and underproduction

The controller also registers the difference in wind power produced between what is expected from the forecast, and the actual power produced. Power shortage and power excess are tracked separately and passed on as outputs of the controller, with y_3 the total shortage in power production and y_4 the total excess power generated. These are needed for the economic analysis.

$$E_L = \int_0^t (P_{fc,h} - P_{wp}) dt \quad \text{for } P_{fc,h} > P_{wp} \quad (4.22)$$

$$E_H = \int_0^t (P_{wp} - P_{fc,h}) dt \quad \text{for } P_{fc,h} < P_{wp} \quad (4.23)$$

4.6. Model of the wind turbine

A custom-made model is created for the wind turbine, which will be used as the primary renewable energy source in the industrial grid. Existing wind turbine models do exist in OpenModelica but they focus mostly on the mechanical behaviour and characteristics of the turbine and therefore add much complexity to the overall model. A simplified turbine model is designed instead to reduce the complexity of the simulations, a model which directly translates the wind speed to electrical power. A downside of the simplified design is that the turbine has no mass inertia.

The relation between wind speed v and electrical wind power P_{wp} is a function of wind speed. The complete formula is given as

$$P_{wp} = \frac{1}{2} C_p A v^3 \quad (4.24)$$

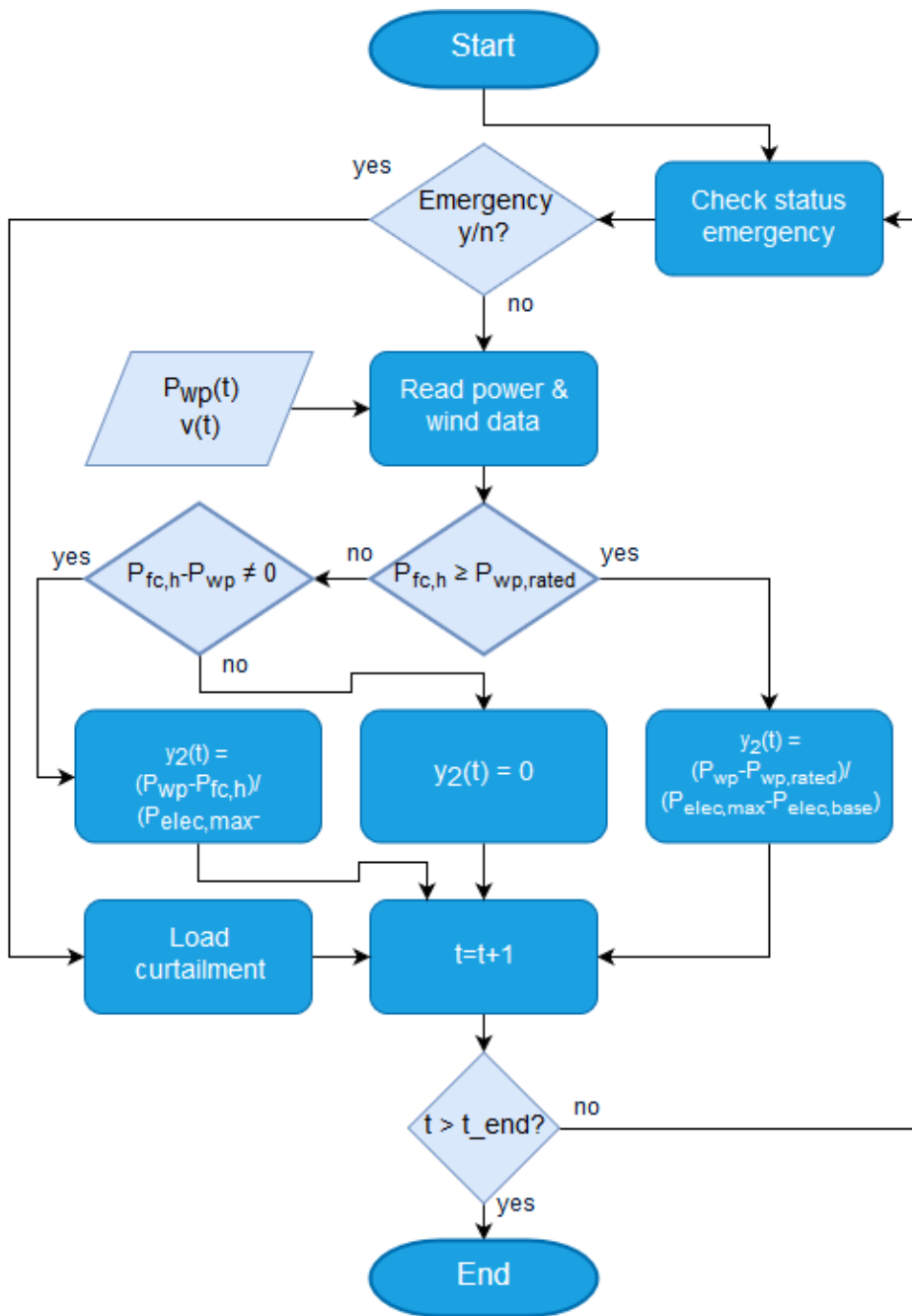


Figure 4.7: Algorithm flowchart for scaling factor $y_2(t)$

with C the coefficient factor (unique for each turbine model), ρ the air density and A the area in which the rotor blades rotate. Since all variables in the formula are constant except for the wind speed, the electrical wind power can be rewritten in which the constants are substituted to the rated power $P_{wp,rated}$ of the turbine and its maximum velocity v_{max} to reach rated power

$$P_{wp} = P_{wp,rated} \frac{v^3}{v_{max}^3} \quad \text{for } v_{min} \leq v \leq v_{max} \quad (4.25)$$

with v_{min} the cut-in wind speed at which the turbine start to operate. If the wind speeds drops below the cut-in speed, the turbine will be stopped. This will be case as well at very high wind speeds, at which the turbine will be stalled as well

$$P_{wp} = 0 \quad \text{for} \quad v < v_{min} \text{ or } v > v_{cut-off} \quad (4.26)$$

with $v_{cut-off}$ the cut-off wind speed of the turbine. In the region between v_{max} and $v_{cut-off}$ the generated wind power is equal to the rated power of the wind turbine

$$P_{wp} = P_{wp,rated} \quad \text{for} \quad v_{max} \leq v \leq v_{cut-off} \quad (4.27)$$

A base model for a generator is used in OpenModelica and modified with the aforementioned wind power equations. This results in a simplified wind turbine that takes wind as input and outputs electrical power. The wind power curve for a 18MW wind park is given in figure 4.8.

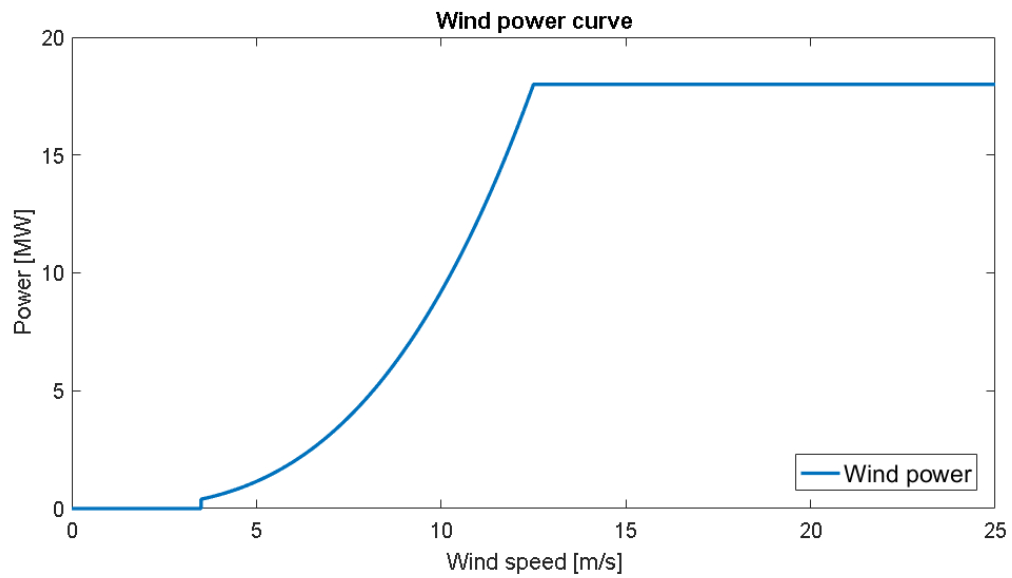


Figure 4.8: Wind power curve of the wind turbine model.

The CIGRE MV network will have a wind park of 21 MW rated power connected to bus 1 and a wind park of 18 MW rated power connected to bus 12, the same bus at which the electrolyser is placed. Since the wind park and the electrolyser are so close together, it is assumed that the power flow from the wind turbine to the electrolyser leads to no transport losses and the data flow is directly available without lag.

4.7. System modeling

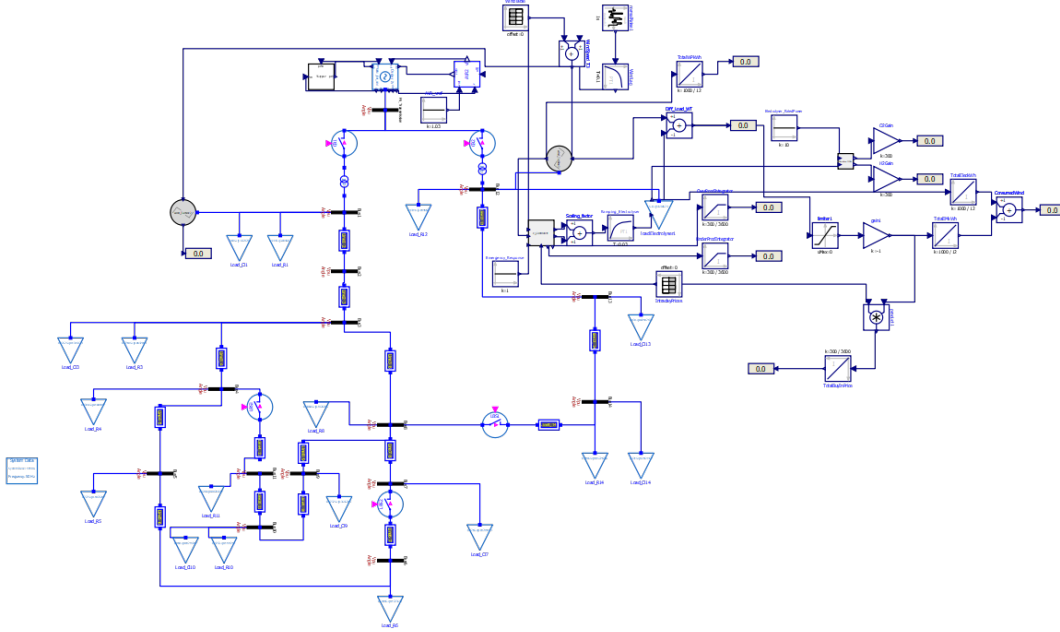


Figure 4.9: The complete and overarching system model in OpenModelica.

The components described in the previous sections are combined in an overarching model within OpenModelica. The models are interconnected with each other as was shown in the system overview of figure 4.1 at the start of this chapter. Apart from the models themselves, a few additional blocks and components are added to complete the simulation setup. Two tables from which the system takes data from: one table is filled with the wind forecast data and the other table is filled with the intraday market price data. The wind forecast data is combined with an uniform noise block ($\mu = 0$, $\sigma = 0.5$) as to simulate a continuously varying wind pattern. This wind pattern is fed into the wind turbine.

The net power exchange of the combined wind park and electrolyser setup is calculated as well, by subtracting the the electrolyser power demand from the generated wind power as given in equation 4.28.

$$P_{bus} = P_{wp} - P_{elec} \quad (4.28)$$

If the net power exchange with the industrial grid is known, the total buy-in cost of electricity from the intraday market can be calculated as well with equation 4.29. The division by 3600 in the equation is done for the conversion from MW to MWh.

$$C_h = \frac{1}{3600} \int_0^t (-P_{bus} C_h) dt \quad \text{for } P_{bus} < 0 \quad (4.29)$$

At last the total electricity generated from wind power is calculated by integrating the wind power generation and converting the generated MW to kWh.

$$E_{wp} = \frac{1000}{3600} \int_0^t (P_{wp}) dt \quad (4.30)$$

The three equations given in this section are implemented with mathematical blocks in the overarching model in OpenModelica. These implementations finish the overarching model resulting in the model as shown in figure 4.9 and this model is used for to simulate the integration of the electrolyser in the industrial grid. The blue components represent the power system part of the model, the grey components represent the mathematical system part of the model.

4.8. Simulation setup

The aim of the model is to simulate the behaviour of the industrial grid and the components described in the previous sections over a period of 24 hours. OpenModelica however is restrained in simulating for lengthy periods and simulating over a complete day is too excessive for the program. The simulation time is therefore drastically reduced to circumvent this issue. The reduction in time is done by a factor of 300, or in other words: one second of simulation time represents 300 seconds. The components and equations in the complete OpenModelica model are scaled by a factor of 300 as well to still obtain outputs that would represent the results of a single day. The downside of scaling the model is that the accuracy of the results is affected since small disturbances in the model are amplified. Possible deviations in simulation behaviour are prevented by sampling some parameters which might otherwise cause issues in the results. Sampling is applied to the wind patterns and the electrolyser, which will improve the stability of the complete model and deliver more accurate results.

OpenModelica provides a simulation setup with a number of options that involve the simulation time, the interval between time steps, the integration method for simulating and the tolerance of results. The simulation setup used for this project is shown in table 4.7.

Table 4.7: Simulation setup of the OpenModelica model

Parameter	Value	
Start time	0	s
Stop Time	288	s
Number of intervals	288	
Interval	1	s
Integration method	dassl	
Tolerance	1e-1	
Jacobian	none	
Max. integration order	5	

5

Results and discussion

The results obtained from the industrial grid and electrolyser model are shown in this chapter. The behaviour of an electrolyser cell is shown and discussed based on the influence of characteristic parameters. The simulated cases are shown as well, in which four of the twelve cases are selected to show the operation of the industrial grid integrated with an electrolyser. At last an economic analysis is made to estimate the cost price of hydrogen production and the feasibility of it.

5.1. Technical evaluation

In this section, a technical evaluation is performed for the electrolyser and the simulation cases. The results are shown and analyzed at first, then the results will be discussed at the end of each section.

5.1.1. Electrolyser performance

The behaviour of the electrolyser is studied under different circumstances by plotting key parameters of the apparatus with each other. Two external parameters, the injected electrical power and the temperature of the electrochemical process, are graphed out against four characteristic parameters: the cell voltage, cell current, cell efficiency and hydrogen/oxygen production per second.

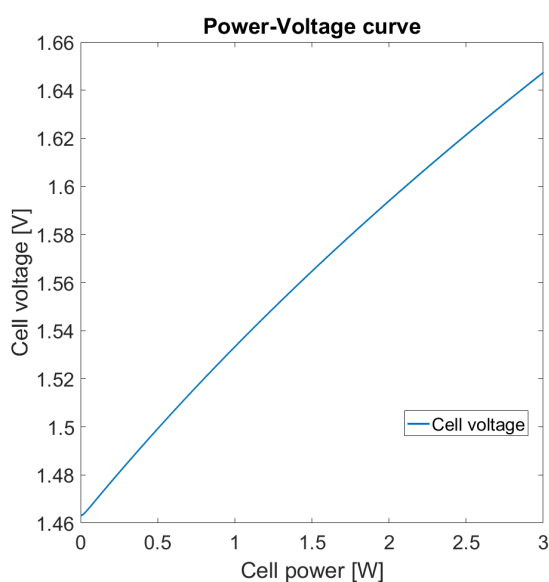


Figure 5.1: The relation between power and voltage within an electrolyser cell.

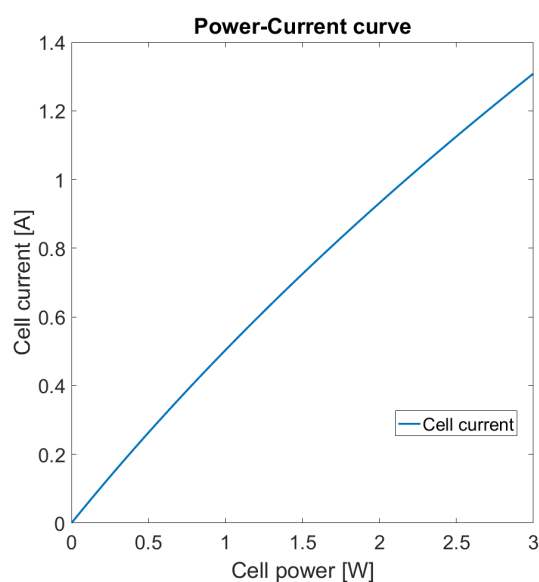


Figure 5.2: The relation between power and current within an electrolyser cell.

Power curves of the electrolyser

The first four graphs show the influence of power on the electrolyser performance. A single cell is analyzed which is subjected to power ranging from its operating range from 0 to 3 Watt. Figure 5.1 depicts the power-voltage relation with an increasing cell voltage by increasing power, going from 1.46V at 0 Watt to 1.65V at 3 Watt. The same can be said for the power-current relation shown in figure 5.2, going from zero ampere to 1.3A. The efficiency of the cell drops with increasing power injection, dropping from 81% to 72% over the range of 3 Watt as seen in figure 5.3. The production of the hydrogen and oxygen gasses increases with power, but slightly stagnates with increasing power. This is shown in figure 5.4. At maximum cell power, almost $2e^{-7}$ cubic metre hydrogen gas is produced per second.

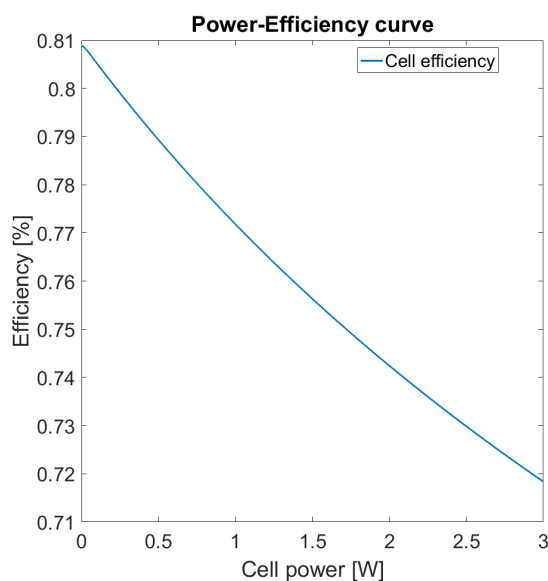


Figure 5.3: The relation between power and efficiency within an electrolyser cell.

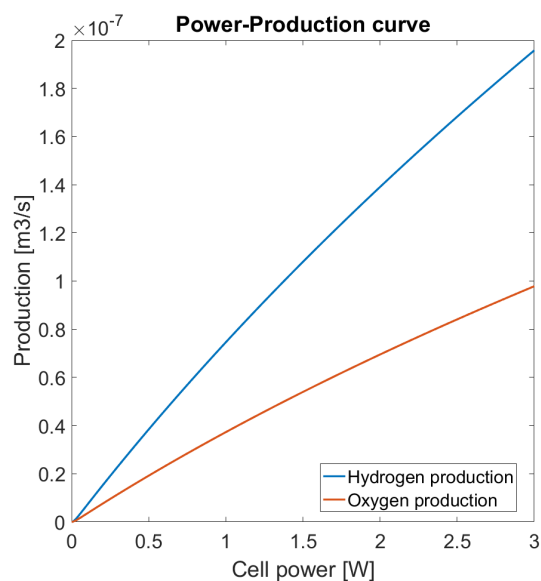


Figure 5.4: The relation between power and hydrogen/oxygen production within an electrolyser cell.

Temperature sensitivity of the electrolyser

A sensitivity analysis with varying temperature of the electrolyser cell was performed, with the temperature ranging between 273.15 and 373.15 Kelvin in which the cell power is set at a constant 2 Watt. The first graph in figure 5.5 shows the relation between temperature and cell voltage. The initial cell voltage is high at 1.66V at 273K and then linearly ramps down with increasing temperature to a voltage of 1.58V at 373K. A lower cell voltage is beneficial for a higher hydrogen production. The opposite relation can be seen in figure 5.6 between the temperature and cell current in which the current is initially low at around 0.91A and then linearly rises to 0.935A at 373K. An increasing current leads to higher hydrogen production as well. The resulting cell efficiency seen in figure 5.7 starts at 75.4% at 273K and slowly drops to 74.0% efficiency at 373K. Energy losses of the electrolyser cell are thus higher with increasing temperature. The final graph, figure 5.8, shows the hydrogen and oxygen production and clearly shows that both increase for higher temperatures. The production of hydrogen is around $1.37\text{m}^3/\text{s}$ at 273K and then proceeds to slowly ramp up to $1.41\text{m}^3/\text{s}$ at 373K, which is an increase of 2.92% hydrogen production.

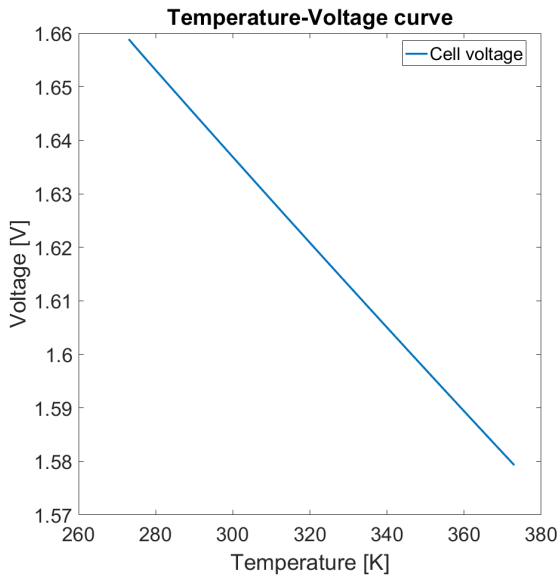


Figure 5.5: The relation between the temperature and voltage within an electrolyser cell.

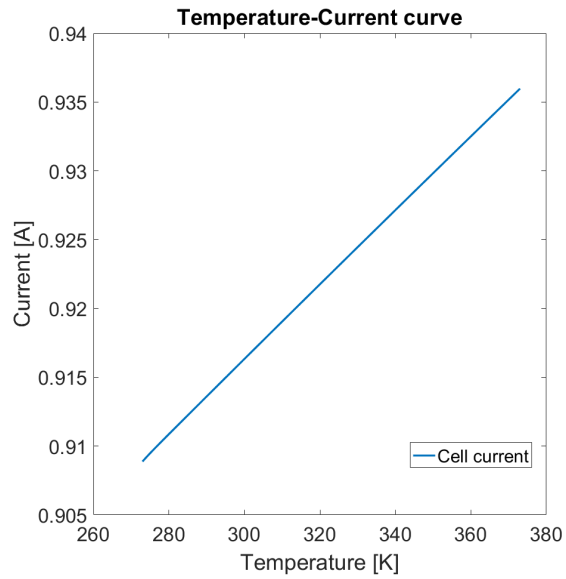


Figure 5.6: The relation between the temperature and current within an electrolyser cell.

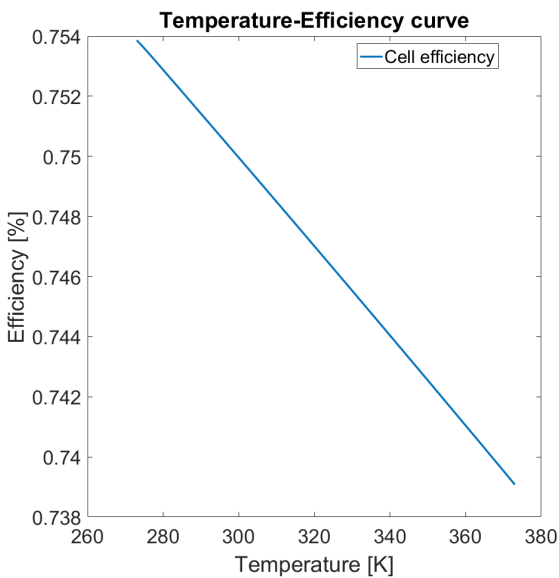


Figure 5.7: The relation between temperature and efficiency within an electrolyser cell.

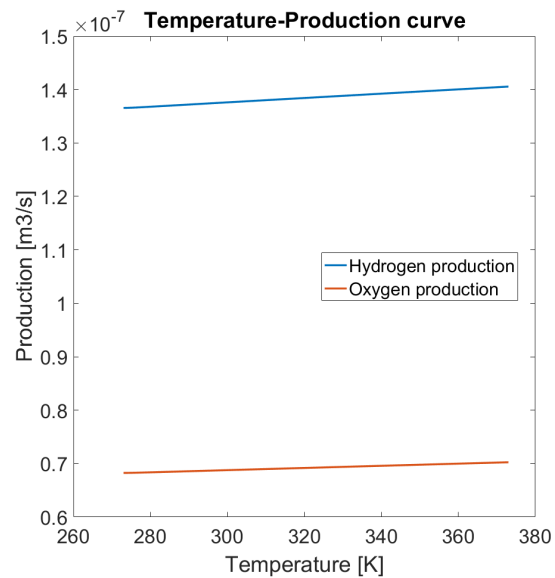


Figure 5.8: The relation between temperature and hydrogen/oxygen production within an electrolyser cell.

Ramp-up speed electrolyser

The ramp-up speed of the electrolyser model is tested by applying a step response to the load demand, in which the initial base load demand at 5 MW is ramped up to 10 MW. The resulting response is shown in figure 5.9 in which the step function is applied at 30 seconds into the simulation and the electrolyser starts to ramp up towards 10 MW. The initial ramp up speed is high, in the order of 500kW/s in the first few seconds but then starts to slow down over time. The halfway mark of 7.5 MW power demand is reached after 6.2 seconds, which corresponds to an average ramp speed of 403kW/s. The rise time to reach 95% (9.75 MW) of the maximum power demand is 27 seconds, giving an average ramp speed of 176kW/s.

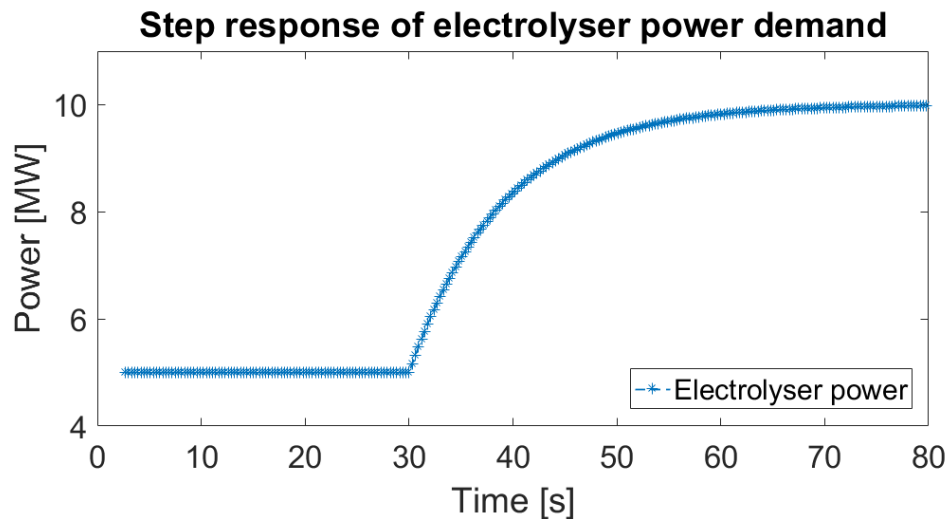


Figure 5.9: Power curves of the wind turbines, electrolyser and exchange with the industrial grid for the January case.

Model validation

The electrolyser cell model done in OpenModelica is compared to experimental results obtained from an actual PEM cell to validate the model. The experimental results are obtained from [21] and gives a VI curve in the range of 0 to 1.5 Ampere at a temperature of 298K and 1 atm. The comparison is presented in figure 5.10 and shows similar VI curves for both the model and the experimental results. The cell voltage of the model has an initial error of 2% at small currents close to 0A, with a cell voltage of 1.487V for the experimental setup compared to 1.518V for the model. The VI curves then cross each other at 0.6A and remain almost equal for the current range. The error at the high-end, at 1.3A, is 0.6% with 1.7V for the experimental setup and 1.69V for the model.

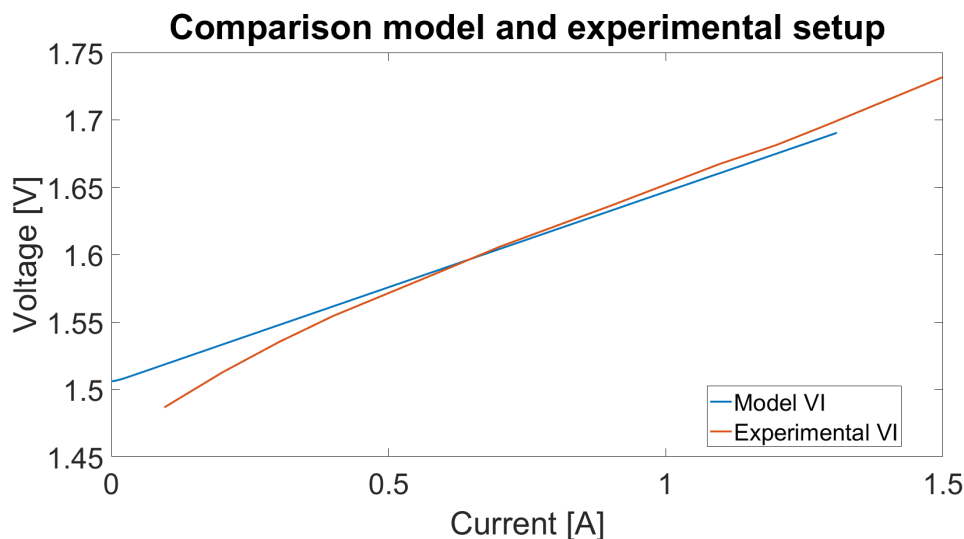


Figure 5.10: Comparison of the VI curve of the OpenModelica model with the VI curve of the experimental setup of [21].

Hydrogen production comparison

The modelled electrolyser can be compared with experimental results of large-scale electrolysers. The comparison is done by calculating the total amount of produced hydrogen gas in kilograms per day if an electrolyser is under full load during the whole period. The result is shown in figure 5.11 which shows the production in kilogram per kiloWatt. The OpenModelica model produces 0.4127 kilogram per kiloWatt of electrolyser capacity and performs better than comparable electrolysers. The best performing electrolyser that has been

commissioned is the ITM Power 3.62 MW, with a production of 0.3702 kilogram per kiloWatt. The performance of the 10 MW electrolyser is 11.5% better compared to the 3.62 MW one.

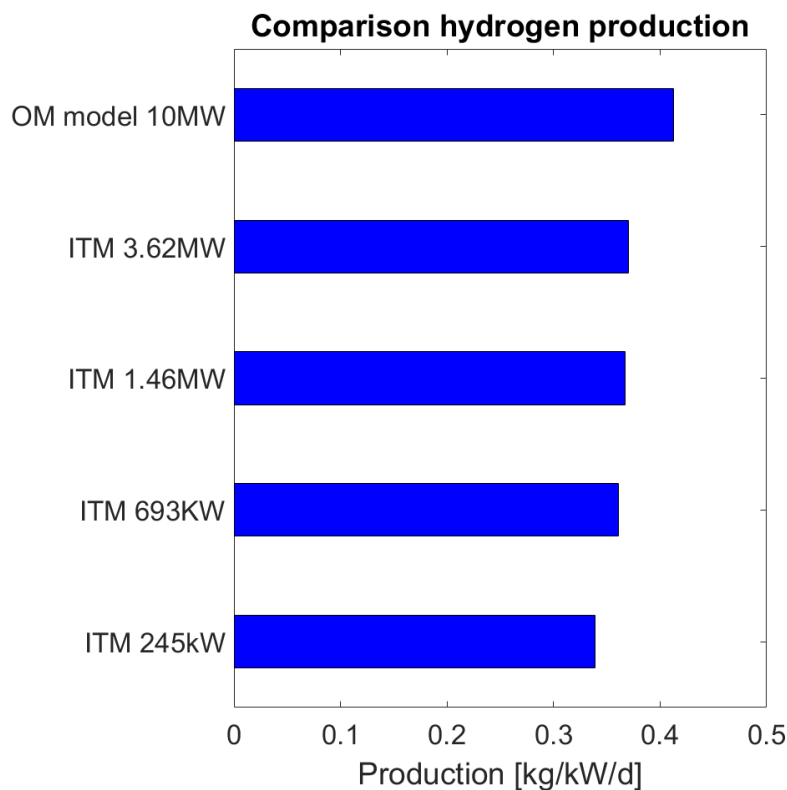


Figure 5.11: Comparison of experimental results of large-scale electrolysers with the modeled electrolyser.

Discussion of electrolyser performance

The power curves of the electrolyser cell show a predictable trend, in which an increase in power results in higher hydrogen and oxygen production. But the efficiency is affected by increasing power injection into the cell, which is caused by an increase in cell voltage that has a negative impact on the cell performance. This is mostly due to an increase in ohmic resistance in the cell at higher power which results in higher cell voltages and thus higher losses. Nevertheless it shows that the PEM cell can operate at high efficiency in a wide operating range.

The sensitivity analysis with temperature shows a linear relation with the characteristic parameters of the electrolyser cell as well. It is shown that the performance of the cells increases at higher temperatures, which has mostly to do with a decrease in the reversible cell voltage. The actual increase in hydrogen and oxygen production however is relative low at higher temperatures, thus its influence on the cell performance is quite small. It should be noted however that the PEM electrolyser does require some heating, since water electrolysis is an endothermic process. This will result in dropping temperatures in the electrolyser cell towards the freezing point of water. Frozen water stalls the electrolysis process and should thus be avoided. It is therefore preferable to operate at a higher temperature.

The cell behaviour is mostly linear which in reality is true for a specific operating range. However, at power and temperature outside the operating range the cell will mostly show a non-linear behaviour which is not integrated into this OpenModelica model. This PEM cell model is therefore only valid for a cell power range of 0-3W and a cell temperature range of 273-373K at standard atmosphere. The resulting hydrogen being produced showcases that the modelled electrolyser is comparable to existing designs. While the performance of the model is 11.5% better than real cases, it can be seen in figure 5.11 as well that the performance of electrolysers improve by increasing size.

5.1.2. Simulation cases

Four cases are selected to present the results from the simulation of the industrial grid model. The selected cases are 1 January, 1 April, 1 July and 1 October since these dates are spread out over the year and represent the seasonal variation during the year. The power curve simulation results for the remaining months are found in Appendix C. The power curves of the wind turbine, electrolyser and the grid exchange are shown for each case. The bus voltage of the bus that connects the electrolyser and wind park with the industrial grid is shown as well for these cases.

January case

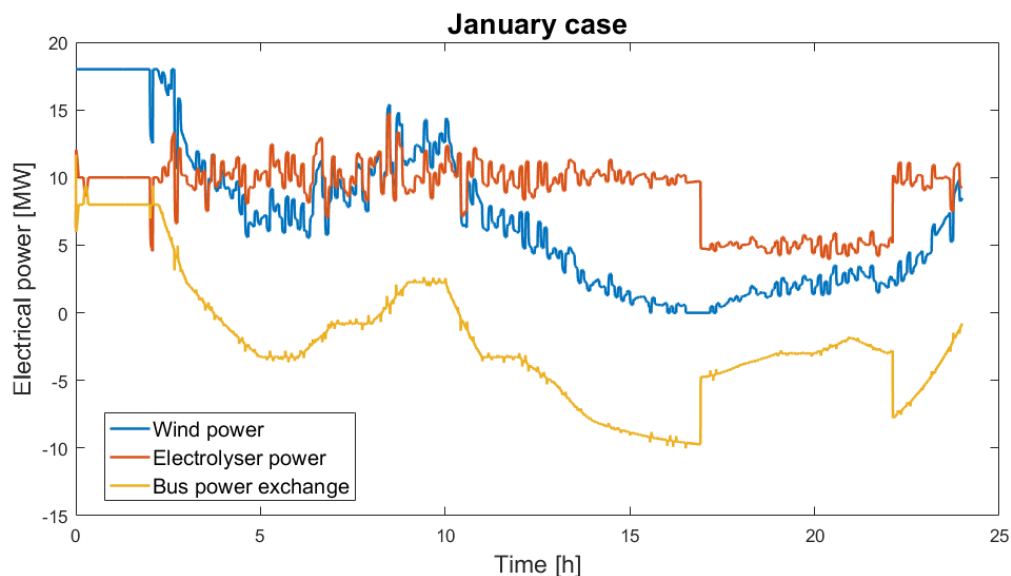


Figure 5.12: Power curves of the wind turbines, electrolyser and exchange with the industrial grid for the January case.

The January case as seen in figure 5.12 starts in the first 3 hours with rated wind power which can be clearly seen as the curve is flat at the rated power of 18 Megawatt. The wind power diminishes over the day with a lot of fluctuations and then drops below the cut-in wind speed at around Hour 17, shown with a flat curve at 0 Megawatt. The wind power then slowly grows again with fluctuations. The electrolyser power demand fluctuates in synchronization with the wind power fluctuations, while also remaining a base power demand. The graph shows the electrolyser base demand at 10 Megawatt, even while the wind power keeps dropping below 10 Megawatt. A sudden power drop to 5 Megawatt base load happens at around Hour 17, caused by the intraday market prices raising above the critical buy-in price. Eventually the market prices drop again and the electrolyser its base demand is increased again. Even while the wind power production is fluctuating, the resulting power exchange with the industrial grid is a smooth curve since fluctuations are mitigated by the electrolyser. A positive power exchange means electrical power is injected into the grid, a negative power exchange means power is extracted from the industrial grid.

Figure 5.13 shows the bus voltage from the bus that is connected with the wind park and electrolyser for the January case. The bus voltage remains mostly between 0.9 and 1.0 p.u. and the voltage curve shows a similar pattern with the bus power exchange. The bus voltage drops if power is taken from the grid (corresponding to a negative power exchange), while the voltage shows an increase if power is injected into the grid.

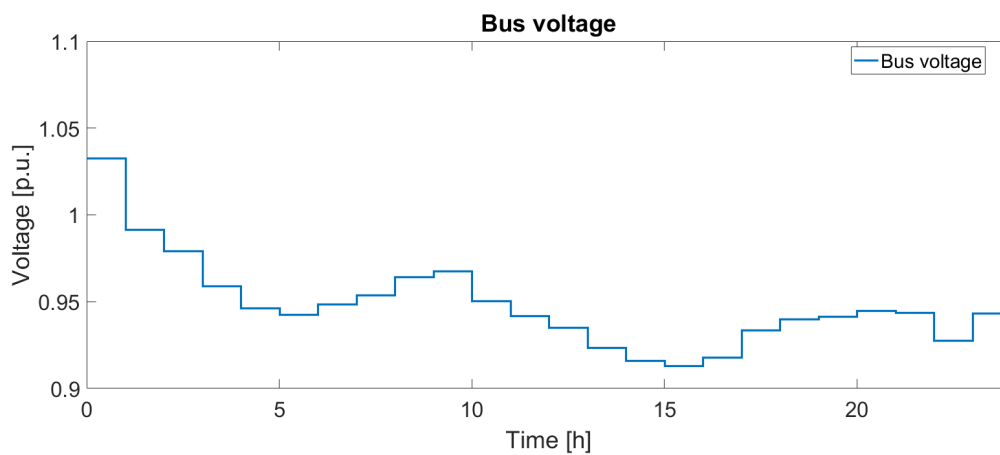


Figure 5.13: Voltage of the electrolyser bus for the January case.

April case

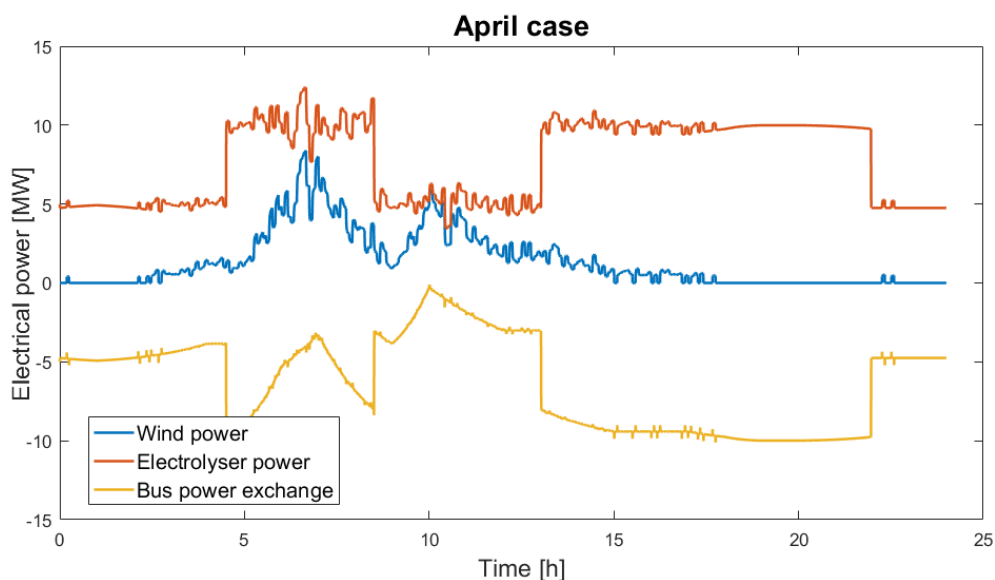


Figure 5.14: Power curves of the wind turbines, electrolyser and exchange with the industrial grid for the April case.

The power curves from the April case are shown in figure 5.14. The initial wind power is zero and proceeds to increase to a maximum of 8 Megawatt at Hour 6. The power remains relative small during the day and the turbines are shutdown due to lack of wind at around Hour 18. The electrolyser power demand is higher than the wind power generation during the whole case. Power demand of the electrolyser jumps in base load a few times due to fluctuating intraday market prices and has two periods in which it proceeds at maximum base load. Wind power fluctuations are still mitigated and thus the electrolyser is both utilizing its maximum capacity and its ability to balance the power exchange with the industrial grid. The resulting mostly negative power exchange shows there are significant jumps and drops, which correspond with the jumps in power demand from the electrolyser.

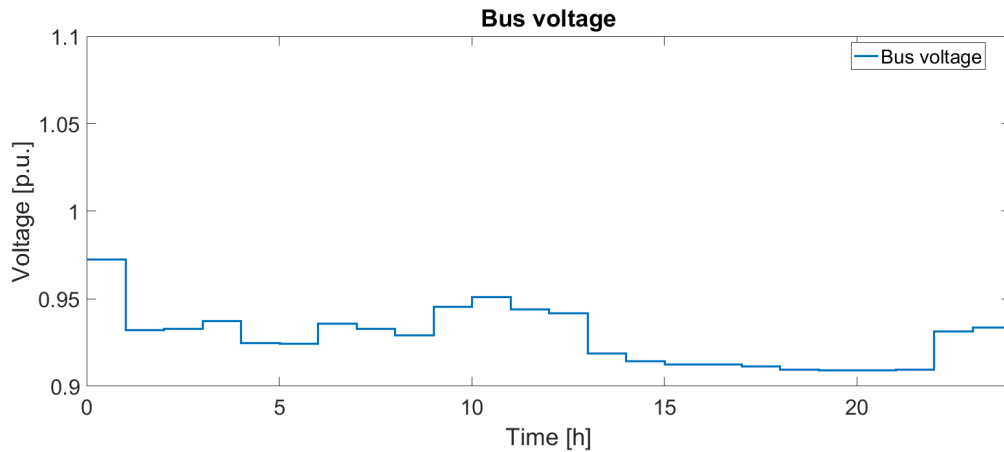


Figure 5.15: Voltage of the electrolyser bus for the April case.

Corresponding with the jumps in power exchange with the industrial grid, the bus voltage of figure 5.15 also fluctuates often. With every power jump, the voltage changes accordingly. The bus voltage remains in the range of 0.9 p.u. and 0.96 p.u. for most part of the simulation.

July case

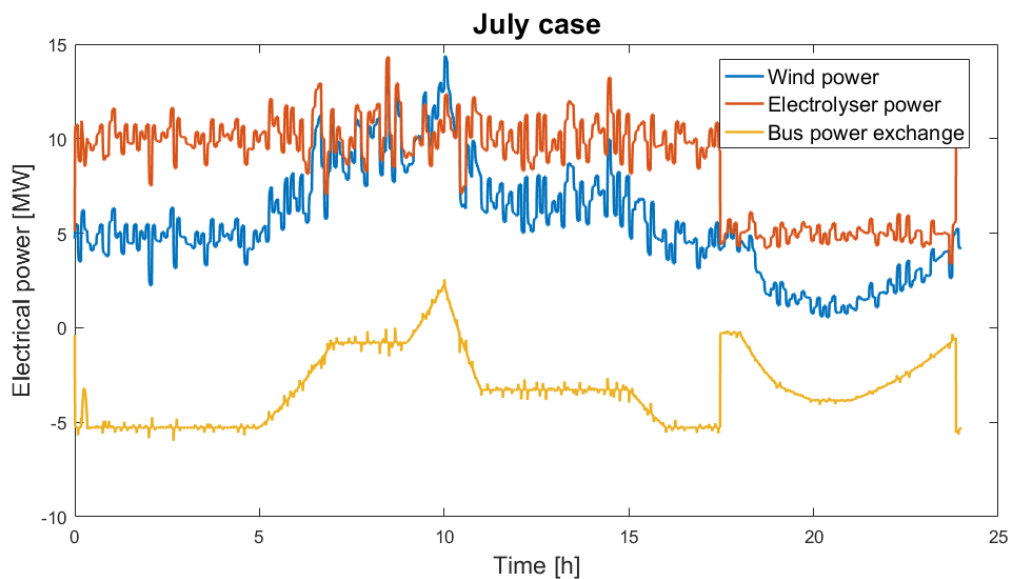


Figure 5.16: Power curves of the wind turbines, electrolyser and exchange with the industrial grid for the July case.

The July case of figure 5.16 shows an average wind power generation over the whole case and an electrolyser power demand that is slightly higher. The resulting power exchange curve smoothly goes up and down during the simulation with a sudden jump at around 6PM and again at the end of the day. At different periods, such as between Hour 11 and Hour 15, the power exchange curve is flat, even while there is a lot of wind power fluctuation in this period. The electrolyser controller is able to adequately track and react upon these fluctuations. The bus voltage jumps accordingly but remains stable at around 0.93 p.u. and 0.97 p.u. for most of the time as seen in figure 5.17.

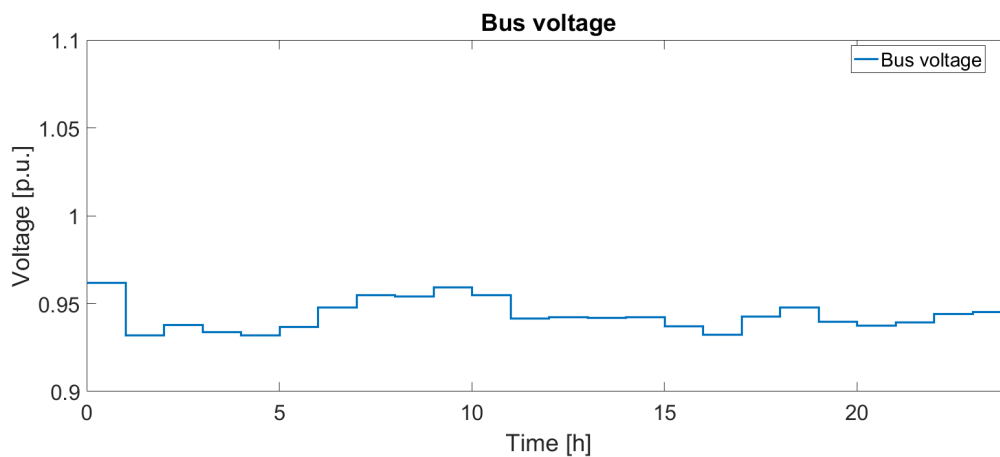


Figure 5.17: Voltage of the electrolyser bus for the July case.

October case

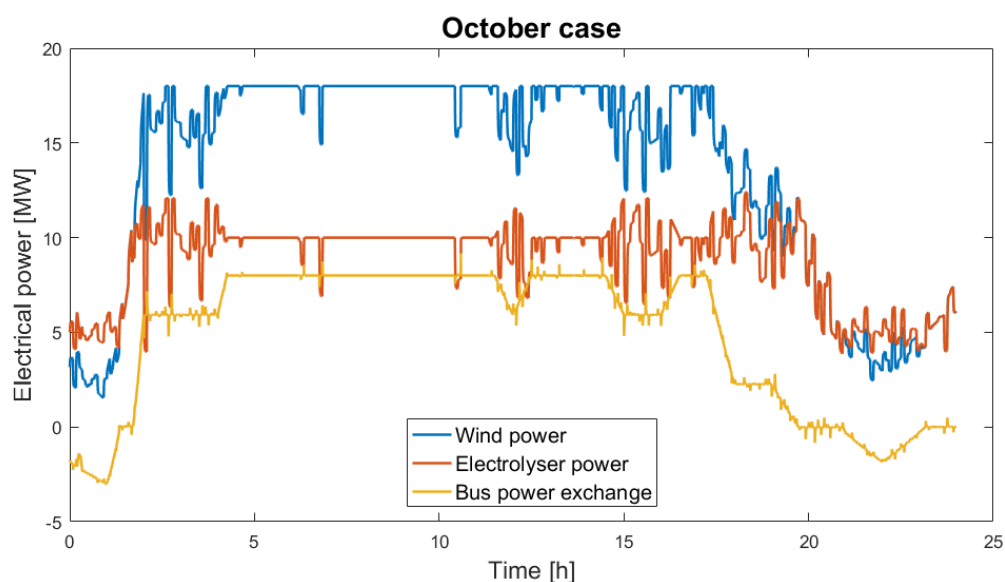


Figure 5.18: Power curves of the wind turbines, electrolyser and exchange with the industrial grid for the October case.

At last the October case of figure 5.18 shows a high ramp up of wind power production towards its maximum rated capacity of 18 MW in the first three hours of the simulation. The electrolyser is able to easily keep up with this ramp up and the power exchange curve is smoothly ramped up. While the wind power is at its rated capacity, the same is true for the electrolyser and small fluctuations in power production are still negated. The resulting power exchange curve is shown to be smooth and stable during the whole simulation case. At around 6PM, the wind power starts to drop slowly and the electrolyser controller responds by also dropping its power demand. Especially between Hour 19 and Hour 21 both power curves overlap each other and the net exchange power curve smoothly drops to lower levels. This also has its effect on the bus voltage which ranges between 0.95 p.u. and 1.0 p.u. during the October case. The bus voltage is shown in figure 5.19.

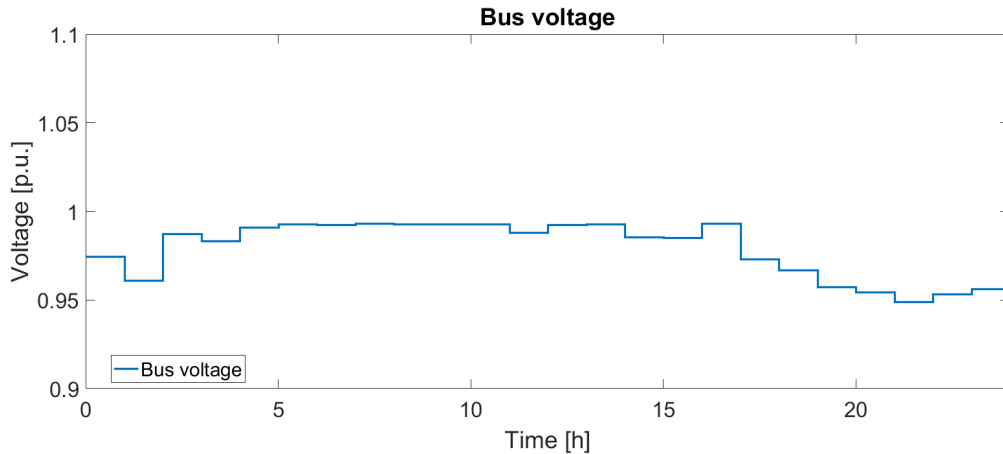


Figure 5.19: Voltage of the electrolyser bus for the October case.

Comparison with normal wind park

The model of the industrial grid has two wind parks, the 21MW wind park without further additions, and the wind park of 18 MW with electrolyser. A comparison is made between the power exchange and bus voltage of the wind park that is integrated with an electrolyser and controller, and the wind park without electrolyser and controller. The results obtained from the January case are presented.

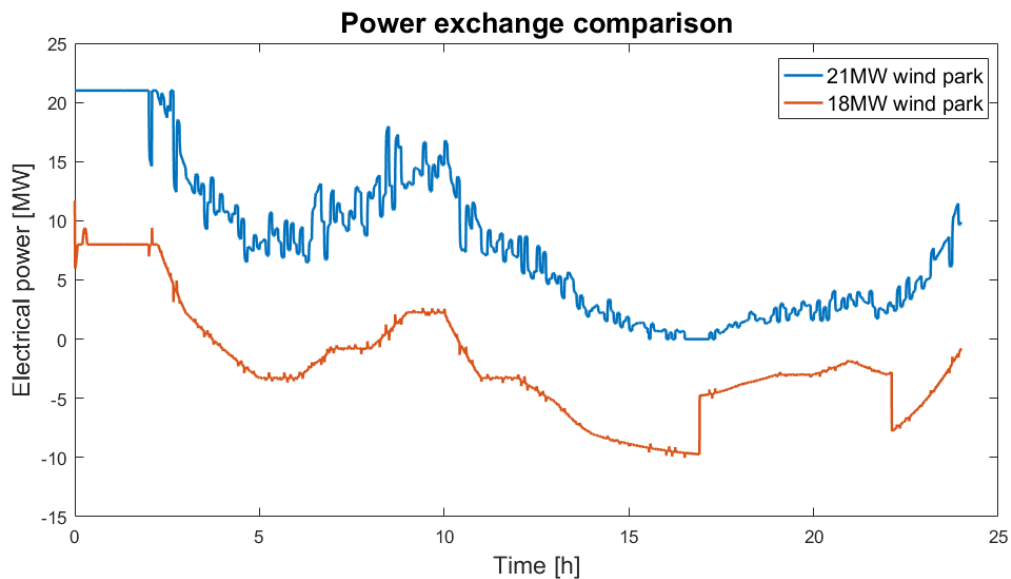


Figure 5.20: Power exchange curves of the 21MW wind park without electrolyser, and 18MW wind park with electrolyser.

Figure 5.20 depicts the power exchanges that occur from both wind parks with their respective bus. The power exchange of the 18MW wind park is not only lower due its lower rated capacity, but also due to the electrolyser that consumes a significant chunk of the power generated. It shows that the electrolyser and controller result in a much more smooth power exchange curve in comparison to a normal wind park. The normal wind park starts with a smooth power curve since it is operating at rated power, but as the power drops the power exchange becomes unstable and starts to fluctuate.

Discussion of simulation results

Four cases have been picked to showcase the operation of the electrolyser and the controller system. In all four cases with wildly different wind speed profiles and thus wind power curves, the electrolyser is able to

keep up with the ramping and fluctuations of power production by the wind turbines. The controller can easily adapt to power changes and control the electrolyser power demand. The net power exchange curves show a stable power profile which is smooth, controllable and predictable. While sudden jumps in net power exchange do happen, these are scheduled since these are caused by changing intraday market prices which are known in advance and are communicated by the energy producer to the TSO.

A right operation of the electrolyser controller depends on the accurate measurements of wind turbines and the real-time availability of these data. It is assumed for this model that this is the case, but this might be different in realistic scenario's in which measurements might lag or are inaccurate. The electrolyser also depends much of its operation time from electricity bought from the market instead of only being depend-able on wind power. While this does increase the capacity coefficient of the electrolyser, it might not always results in the production of green hydrogen since the origin of the electricity is unknown. It is questionable if hydrogen production with fossil-fuel power electricity is more sustainable than direct steam reforming to produce hydrogen.

A comparison is made between a wind park with a controllable electrolyser, and a wind park that directly injects its generated power into the grid. The power exchange from bus 12 is more smooth and predictable since the electrolyser and its controller take out most fluctuations that occur due to variations in wind power generation. At last the bus voltage curves show that the voltage remains in stable regions even during sudden power jumps, with a voltage mostly in the range of 0.9 and 1.0 p.u.

5.2. Economic evaluation

The hydrogen cost price is an indicator of the economic feasibility of the large-scale electrolyser. Equation 3.1 from chapter 3 is used to calculate the cost price with the price ranges from table 3.1 found in the same chapter. The unknown parameters of the hydrogen cost price equation are determined by the simulation of the OpenModelica model for different cases.

Table 5.2 give production and economic results obtained from the simulations. H_{2out} is the produced hydrogen in m^3 , H_{2out} is the produced oxygen in m^3 , E_{tot} is the total consumed energy by the electrolyser in kWh, E_{wp} is the consumed wind power, E_{grid} is the consumed power from the grid. C_h is the total buy-in cost of electricity in €, E_H is the amount of overestimated wind energy and E_L is the amount of underestimated wind energy. The daily results of the first day of each month is given and the average daily value is given in the last column. The yearly average of the parameters are obtained by multiplying the daily results.

The values used for the cost analysis are given in table 5.1 and this results in a cost price of €0.18-0.32/ m^3 hydrogen gas, or €50.99-90.65/MWh hydrogen gas. Compared to current natural gas prices, which is traded for €20-30/MWh, the hydrogen cost price is significant higher. And while natural gas has a widely integrated pipeline infrastructure, this is not the case for hydrogen gas. It is clear that hydrogen gas is not yet competitive enough with natural gas on the energy market.

The investment and O&M costs are a significant part of the current hydrogen cost price, but the technology and production of large-scale electrolysers are in their infancy and it is expected that growth of this technology will cut these costs. A thumb of rule is that a doubling of installed capacity results in a 20% price drop of the technology, a rule that has been validated with solar panels and wind turbines.

Electricity consumption is a major cost factor for hydrogen production, with most electricity being consumed from wind power. Yet buying electricity from the intraday market is cheaper than wind power, with an average of €3.2ct/kWh compared to €4ct/kWh for wind power in a best price scenario. A scenario with a higher critical buy-in price for electricity might be beneficial. If electricity becomes cheaper, for example by a lower LCoE for wind power, it will significantly cut the cost price of hydrogen production.

The ancillary service and benefits that has been applied in this model doesn't seem to provide much benefits at all. In a best case scenario, there is only a price cut of €0.40/MWh for hydrogen. But a more in-depth look into possible ancillary services and benefits hasn't been provided in this thesis and further research is therefore needed.

Other cost factors not integrated in this cost price analysis are losses due to hydrogen compression for transport and storage, benefits from selling oxygen gas, costs associated with an hydrogen pipeline infrastructure and heating of the electrolyser. These factors can affect the cost price of hydrogen production but require further research and a different modeling setup.

Table 5.1: Yearly production, costs and benefits associated with hydrogen production.

Parameter	Value	Unit
Yearly hydrogen production	16 702 765	m3
Total capital cost	5 - 10M	€
Total O&M cost	1.5 - 2.4M	€
Yearly wind power cost	1 666 020 - 3 332 041	€
Yearly buy-in costs	739 971.80	€
Yearly ancillary benefits	13 731.74 - 23 473.59	€

Table 5.2: Production and economic results for the first day of each month, obtained from the OpenModelica model

Parameter	Jan	Feb	Mar	Apr	May	Jun	Jul	Aug	Sep	Oct	Nov	Dec	Average
H _{2out} [m ³]	54492.3	42928.7	60156.2	47466.6	54451.9	32377.0	53235.2	31947.3	32172.2	53633.8	37353.8	48916.6	45761.0
O _{2out} [m ³]	27236.5	21456.7	30067.5	23724.9	27216.3	16182.8	26608.2	15968.0	16080.4	26807.4	18670.3	24449.6	22872.4
E _{tot} [kWh]	215060	164141	239264	184378	214652	119195	209663	117467	118370	210846	140409	190531	176998
E _{wp} [kWh]	139225	150633	239264	33464	130989	18223	132154	3655	8563	205579	130863	176723	114111
E _{grid} [kWh]	75835	13508	0	150914	83663	100972	77509	113812	109807	5267	9546	13808	62887
C _h [€]	533.00	593.54	0.00	3097.50	507.00	4331.77	1171.60	6555.22	6174.61	251.36	450.56	661.72	2027.32
E _H [MWh]	8.2021	9.1342	0.0000	3.5666	5.8848	2.2388	9.2981	0.9134	1.2165	5.3801	8.6378	11.1146	5.4656
E _L [MWh]	6.8956	8.3477	0.6956	3.8611	4.83037	3.0442	7.4764	0.5501	1.2762	9.1217	7.1713	10.7847	5.3380

6

Conclusions

The energy transition has lifted off in recent years and a lot of focus is given on the research of renewable energy technologies and smart grids. The focus of this thesis has been the integration of a large-scale electrolyser within an electrical, industrial grid. The research objective of this thesis was thus the

"modeling, scheduling and control of a hydrogen producing electrolyser in an industrial microgrid"

and this objective has been carried out during this research. The objective was divided in four sub-objectives to achieve the main research objective. These sub-objectives are 1) modeling an electrolyser, 2) modeling an industrial grid, 3) applying a smart control strategy for control, optimization and scheduling, and 4) an economic analysis for hydrogen production. These sub-objectives were subjected to several requirements that were fulfilled.

A Proton-Exchange Membrane electrolyser has been designed and build in OpenModelica. The modular approach used allows custom sizing of the model, in which a single PEM cell was designed that operates at a range in between 0 and 3 Watt, and can be extended in cell stacks to large-scale sizes ranging to Megawatts. For the experimental setup used in this thesis, a size of 10 Megawatts was chosen. The PEM cells are temperature dependent and operate better at higher temperatures, showing a positive linear growth in hydrogen/oxygen production from 275K up to 373K. A fixed temperature of 353K was chosen for the experimental setup. The cell efficiency typically ranges from 72% to 81% within operating boundaries regarding injected power and temperature. A custom controllable load has been built in OpenModelica as well, which controls the amount of electrical power the electrolyser receives. This load integrates the electrolyser with the industrial grid.

A 15-bus 20kV industrial microgrid has been build in OpenModelica as well, a grid that represents the Maasvlakte area of the Port of Rotterdam. A benchmark network specifically designed for the integration of renewable energy technologies is being used. Several industrial loads are connected to the grid, and the grid itself has an exchange with the transmission grid which has been modeled as a 4th order generator with infinite power consumption and absorption capabilities. Two wind parks are integrated with the industrial grid, one rated at 20 MW and the other at 18 MW. At last the electrolyser is connected to the same bus as the last mentioned wind park.

A control algorithm for the power demand of the electrolyser has been developed and integrated into the OpenModelica model. The algorithm decides the base load level of the electrolyser based upon the expected wind power to be produced and the economic feasibility of buying extra electricity from the intraday market. The dynamic load level is controlled by the algorithm as well, and is based upon the fluctuations in wind power generation. The result is an improvement in scheduling of power demand and supply to the external grid, and a method to cope with energy imbalances due to intermittent energy production.

At last an economic analysis of the hydrogen production has been performed. The cost price was determined by a number of cost factors, including the investment, operation and maintenance of the electrolyser, the cost price of electricity from wind power and the external grid, and avoiding production penalties. The hydrogen

cost price is determined to be in the range of €50.99-90.65/MWh, which is significant higher than current natural gas prices. The main cost factors are the electricity consumption and the initial investment, which both need to get cheaper in the future to let hydrogen gas become cost-competitive with natural gas.

6.1. Novelties

This thesis project has developed some novelties and contributions in the research field of intelligent electrical power grids. These novelties and contributions are outlined in this section.

1. A simulation setup of an industrial grid in OpenModelica has been contributed. The industrial grid is accompanied with wind power and large-scale hydrogen production, and can be expanded with future renewable technologies.
2. An OpenModelica model of a large-scale PEM electrolyser has been developed that can be scaled to a desirable size ranging into Megawatts. The model can be integrated into future power systems to study the coupling of the electrical grid and the hydrogen pipeline network, and provide feasible hydrogen production.
3. Reliable power scheduling and stability has been realized with continuous demand side management. The controller responsible for the management is scalable for any wind park and electrolyser size and can be flexibly integrated into future power systems to help restore energy imbalance and enable power scheduling.
4. A method to calculate the hydrogen cost price has been developed, to give insight into the economic feasibility of hydrogen gas in regards to natural gas.

6.2. Recommendations & Future work

The work done in this thesis yields some initial promising results regarding the integration of renewable energy production, hydrogen production, and power scheduling and stability. Yet, much gaps in these topics need to be filled and further research is required. Some recommendations and possible future research topics are given in this section.

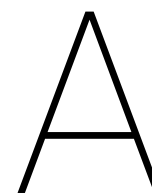
Large-scale hydrolysis is at its infancy and has barely been applied in practical cases. It is therefore hard to validate current theoretical large-scale electrolysers with real cases. Some large-scale appliances are being developed or have just been developed and can provide insight in their performance. Validating current models and improving them based on real cases will significantly advance the research field of large-scale electrolysers.

The industrial grid modeled in this thesis is based on a proven benchmark system to test the integration of renewable energy sources and technologies. However, it is important to gain knowledge in the energy ecosystem in which a renewable energy technology such as an electrolyser will be integrated to. It is recommended to build a distribution grid that matches an existing grid suitable for hydrogen production. A further extension on the chemical side, with an hydrogen pipeline and storage, is recommended to study the integration of an electrolyser as well.

A contribution has been made in ancillary services that an energy producer can provide with the flexible load demand of the electrolyser. The focus has been mostly on restoring energy imbalance and power scheduling, but more services are possible such as active Frequency Restoration Reserve (aFFR), reactive power and voltage control. With a growing share of distributed renewable energy sources, these services are becoming more important in power systems. A more in-depth analysis and research into possibilities of available services that the electrolyser can provide should be made.

This thesis was mostly done in OpenModelica to build the models and perform the simulations to obtain results. However, OpenModelica is not well suited for long-term simulations such as cases covering a whole day. Workarounds have been made for this thesis to be able to simulate for a longer time span, but it can still lead to results that do not correctly represent behaviour that would occur in real cases. Another issue is the lack of scripting support within OpenModelica. A Python module has been developed to work with the OM

API, but its implementation and use is cumbersome and lacking in usability. Other modeling and simulation programs might provide a better tool to simulate multi-domain setups with active control.



KNMI wind data

	1 Jan	1 Feb	1 Mar	1 Apr	1 May	1 Jun	1 Jul	1 Aug	1 Sep	1 Oct	1 Nov	1 Dec
Hour 1	14.0	10.0	13.0	3.0	19.0	2.0	8.0	2.0	2.0	7.0	7.0	7.0
Hour 2	13.0	9.0	13.0	2.0	20.0	3.0	8.0	2.0	2.0	6.0	8.0	7.0
Hour 3	13.0	9.0	13.0	3.0	20.0	2.0	8.0	2.0	2.0	12.0	8.0	6.0
Hour 4	11.0	9.0	13.0	4.0	18.0	2.0	8.0	2.0	2.0	12.0	9.0	7.0
Hour 5	10.0	8.0	15.0	5.0	16.0	2.0	8.0	2.0	2.0	12.0	8.0	7.0
Hour 6	9.0	7.0	16.0	5.0	14.0	3.0	8.0	3.0	3.0	14.0	9.0	7.0
Hour 7	9.0	8.0	15.0	8.0	12.0	2.0	9.0	3.0	3.0	13.0	8.0	8.0
Hour 8	10.0	7.0	15.0	9.0	10.0	4.0	10.0	3.0	3.0	13.0	9.0	7.0
Hour 9	10.0	5.0	16.0	7.0	9.0	5.0	10.0	3.0	1.0	15.0	9.0	8.0
Hour 10	11.0	7.0	17.0	5.0	9.0	5.0	10.0	4.0	1.0	14.0	8.0	9.0
Hour 11	11.0	9.0	16.0	8.0	9.0	5.0	11.0	4.0	2.0	13.0	9.0	10.0
Hour 12	9.0	9.0	16.0	7.0	8.0	4.0	9.0	4.0	3.0	13.0	10.0	10.0
Hour 13	9.0	11.0	16.0	6.0	8.0	4.0	9.0	4.0	3.0	12.0	8.0	10.0
Hour 14	8.0	10.0	16.0	6.0	9.0	4.0	9.0	3.0	3.0	13.0	8.0	11.0
Hour 15	6.0	10.0	17.0	5.0	8.0	6.0	9.0	4.0	4.0	13.0	8.0	12.0
Hour 16	5.0	8.0	16.0	4.0	6.0	6.0	9.0	3.0	5.0	12.0	8.0	12.0
Hour 17	4.0	7.0	15.0	4.0	5.0	5.0	8.0	3.0	5.0	12.0	8.0	12.0
Hour 18	3.0	8.0	15.0	4.0	5.0	4.0	8.0	3.0	4.0	13.0	8.0	11.0
Hour 19	5.0	9.0	14.0	3.0	5.0	4.0	8.0	3.0	5.0	11.0	8.0	11.0
Hour 20	6.0	9.0	14.0	1.0	5.0	2.0	6.0	3.0	5.0	11.0	8.0	11.0
Hour 21	6.0	10.0	15.0	1.0	5.0	4.0	5.0	3.0	4.0	10.0	7.0	11.0
Hour 22	7.0	11.0	15.0	2.0	6.0	5.0	5.0	2.0	4.0	8.0	7.0	11.0
Hour 23	6.0	6.0	15.0	3.0	6.0	5.0	6.0	2.0	4.0	7.0	6.0	10.0
Hour 24	8.0	13.0	14.0	3.0	6.0	6.0	7.0	2.0	4.0	8.0	13.0	10.0



EPEX intraday market prices

	1 Jan	1 Feb	1 Mar	1 Apr	1 May	1 Jun	1 Jul	1 Aug	1 Sep	1 Oct	1 Nov	1 Dec
Hour 1	0.34	27.86	26.57	38.56	8.91	40.11	11.84	45.36	58.74	51.07	45.40	49.99
Hour 2	-2.57	26.52	27.58	35.78	2.82	37.00	12.77	46.69	56.89	48.81	45.55	48.83
Hour 3	-20.10	27.78	31.96	31.43	0.45	37.15	9.42	45.01	55.30	46.09	44.94	47.00
Hour 4	-21.45	25.49	30.15	29.05	-1.05	33.25	9.91	44.86	51.73	43.36	43.77	45.10
Hour 5	-38.17	25.67	30.71	26.49	-3.38	32.47	9.39	44.89	50.61	42.08	42.97	46.18
Hour 6	-43.60	30.27	33.05	23.52	-2.45	33.80	9.20	45.63	55.95	45.36	43.95	47.34
Hour 7	-49.68	42.99	36.25	18.47	-2.12	40.79	9.87	51.15	53.79	65.03	43.08	48.15
Hour 8	-57.46	49.46	41.23	18.53	-0.99	49.25	15.07	59.6	55.61	70.69	44.27	49.23
Hour 9	-50.68	49.04	38.87	22.64	-0.32	50.84	18.20	58.19	58.11	75.16	42.54	61.97
Hour 10	-37.54	47.24	35.97	27.31	2.44	47.37	11.67	57.30	62.03	69.37	42.67	66.29
Hour 11	-16.42	45.77	27.02	30.71	2.11	48.14	-0.32	63.7	62.16	57.29	46.63	62.75
Hour 12	-2.25	42.2	24.3	30.75	5.87	48.42	-0.84	63.08	58.61	53.74	52.22	58.87
Hour 13	0.70	41.61	15.28	29.81	-0.69	46.38	4.71	61.24	53.49	47.5	52.67	57.31
Hour 14	3.76	41.37	15.43	25.21	-5.98	42.65	-3.99	59.24	51.15	45.38	52.25	53.10
Hour 15	6.01	43.00	17.02	17.70	-22.33	39.82	-7.70	59.06	52.91	45.80	51.53	55.4
Hour 16	4.85	45.07	19.01	15.55	-21.07	39.05	-4.32	59.61	54.33	44.44	50.99	59.37
Hour 17	13.74	46.93	28.37	13.08	-4.62	38.86	3.37	60.08	53.79	44.25	50.72	62.31
Hour 18	26.09	50.41	40.73	-2.12	4.10	43.56	15.25	66.77	55.31	49.34	61.30	65.73
Hour 19	28.57	50.59	46.44	11.77	16.09	46.38	36.04	66.10	63.43	54.29	64.63	61.27
Hour 20	26.33	42.07	43.84	18.84	28.43	48.74	46.83	67.65	63.34	57.30	56.70	52.45
Hour 21	25.00	34.92	40.80	20.28	33.62	48.20	47.40	69.42	68.66	56.65	48.57	44.86
Hour 22	27.51	32.89	36.46	23.38	36.59	49.00	47.55	67.01	64.32	50.73	43.88	42.64
Hour 23	26.21	34.88	33.61	25.07	36.75	49.57	46.84	65.86	52.41	45.49	40.92	41.67
Hour 24	15.46	29.82	34.06	25.96	33.13	44.19	35.04	56.59	46.58	39.03	37.74	36.76

C

Other results

February Case

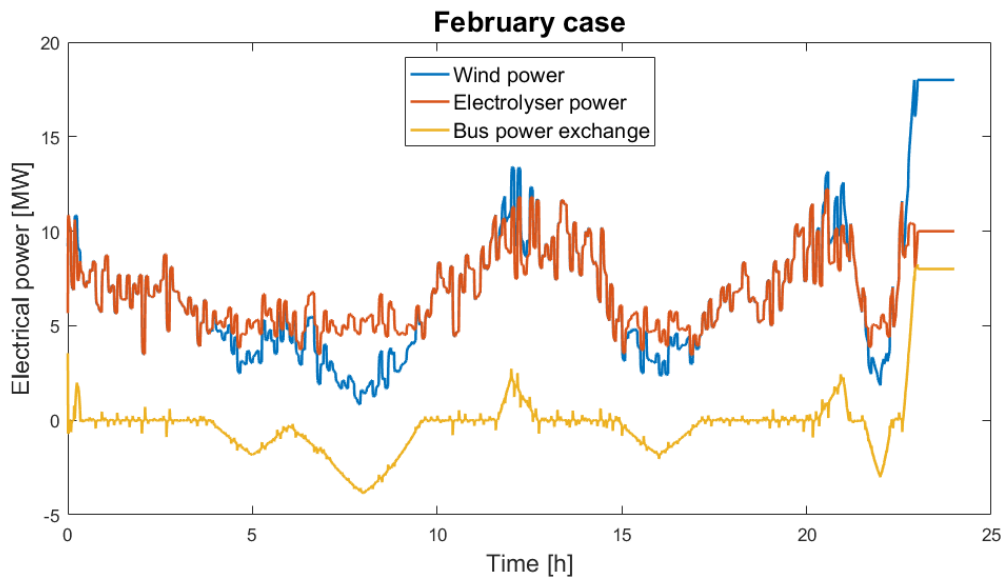


Figure C.1: Power curves of the wind turbines, electrolyser and exchange with the industrial grid for the February case

March Case

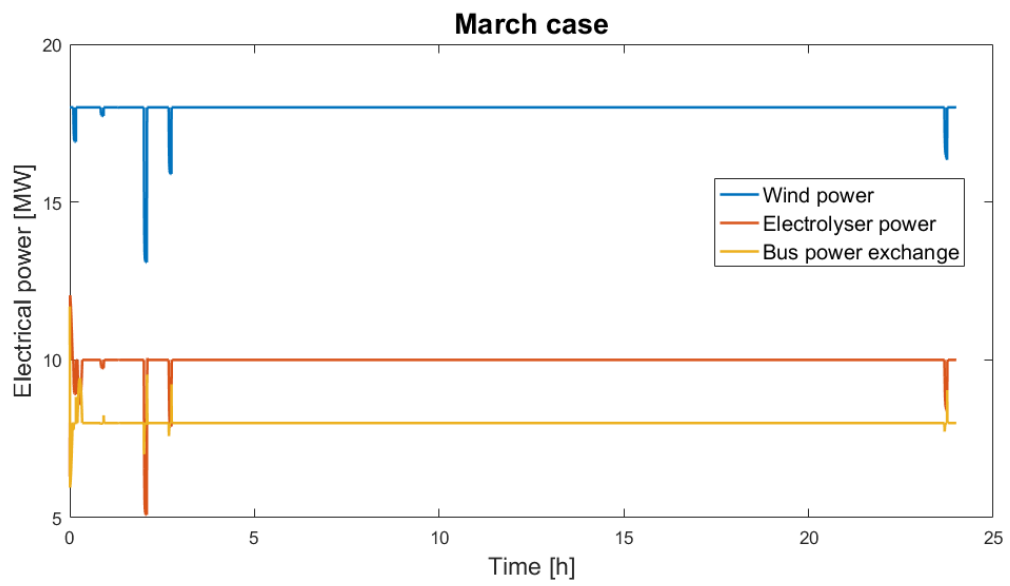


Figure C.2: Power curves of the wind turbines, electrolyser and exchange with the industrial grid for the March case

May Case

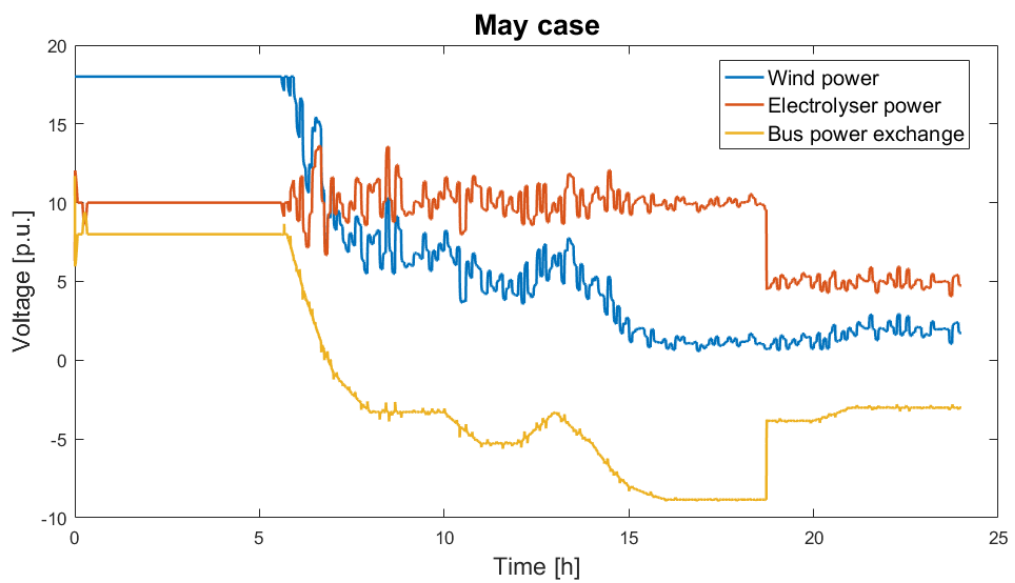


Figure C.3: Power curves of the wind turbines, electrolyser and exchange with the industrial grid for the May case

June Case

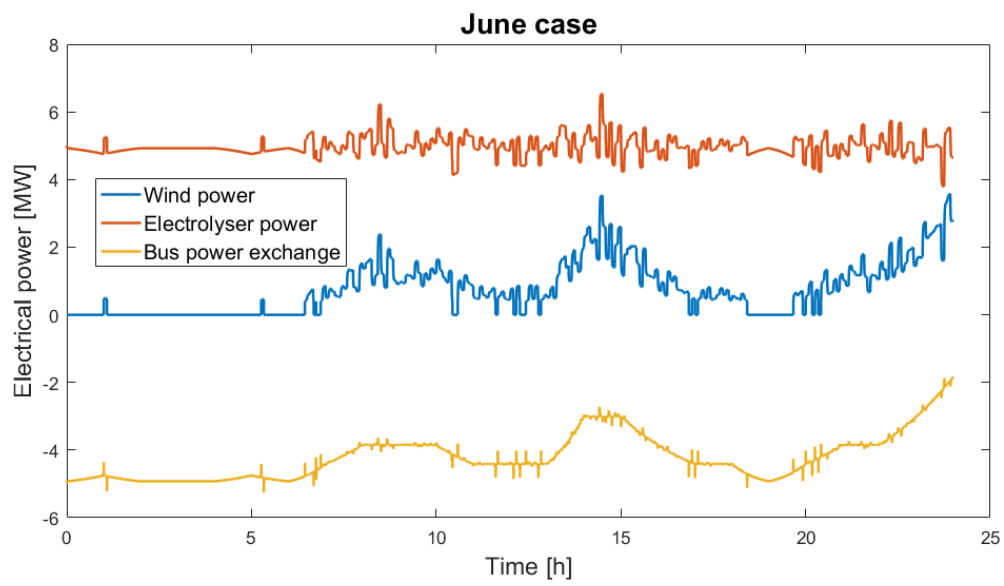


Figure C.4: Power curves of the wind turbines, electrolyser and exchange with the industrial grid for the June case

Augustus Case

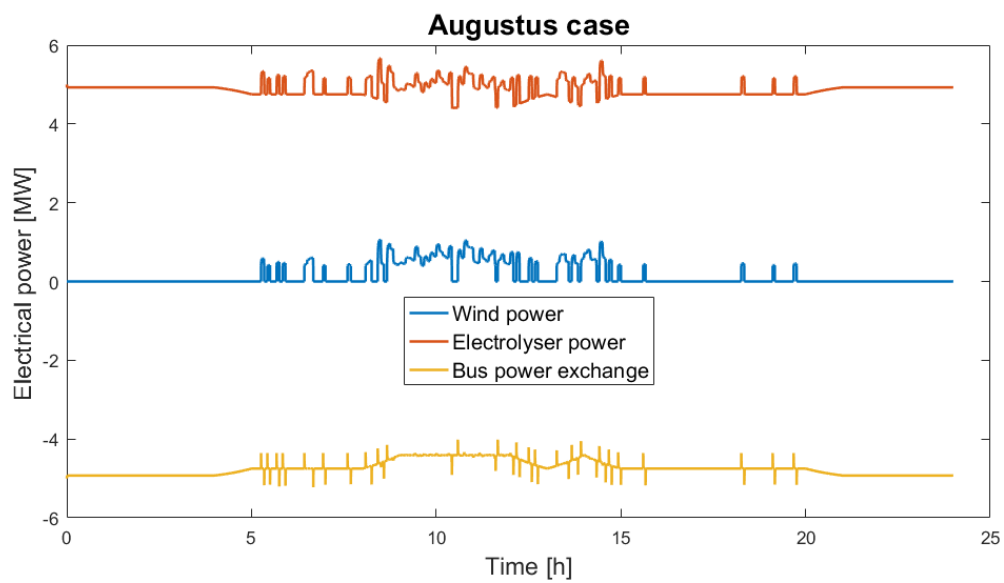


Figure C.5: Power curves of the wind turbines, electrolyser and exchange with the industrial grid for the Augustus case

September Case

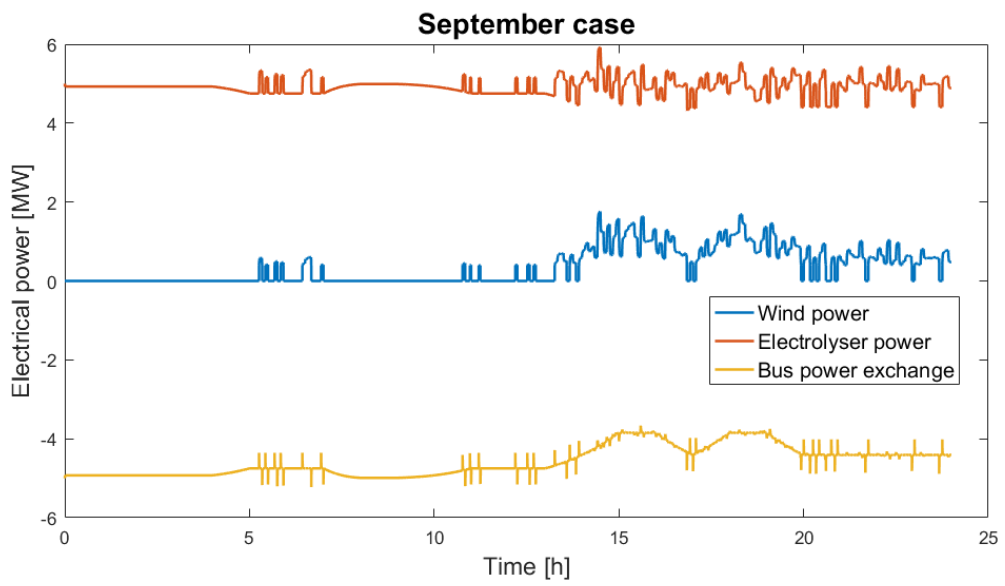


Figure C.6: Power curves of the wind turbines, electrolyser and exchange with the industrial grid for the September case

November Case

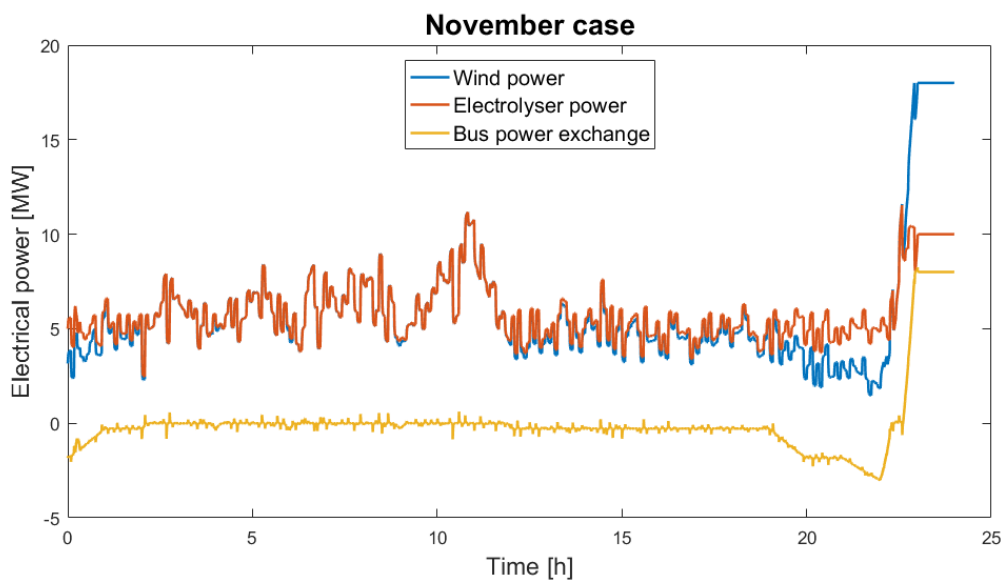


Figure C.7: Power curves of the wind turbines, electrolyser and exchange with the industrial grid for the November case

December Case

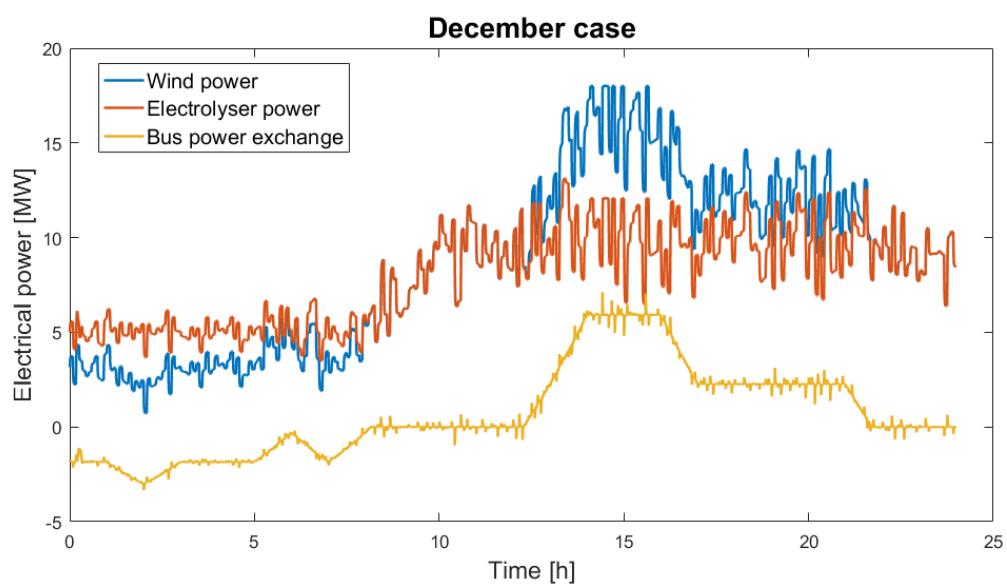
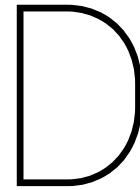


Figure C.8: Power curves of the wind turbines, electrolyser and exchange with the industrial grid for the December case



OpenModelica code: Controller

```
model E_Controller

  parameter Real baseLoad=5 "Base load of electrolyser in MW";
  parameter Real maxLoad=10 "Maximum load of electrolyser in MW";
  parameter Real nominalWindPower=18 "Maximum wind power in MW";
  parameter Real v_max=12.5 "Rated windspeed";
  parameter Real v_min=3.5 "Cut-in windspeed";
  parameter Real C_max=30 "Maximum buy-in price of electricity in €/MWh";

protected

  Modelica.Blocks.Interfaces.RealInput v "Forecast Windspeed" annotation(
    Placement(visible = true,
      transformation(origin = {-100, 26}, extent = {{-10, -10}, {10, 10}},
        rotation = 0),
      iconTransformation(origin = {-100, 26}, extent = {{-10, -10}, {10, 10}},
        rotation = 0)));

  Modelica.Blocks.Interfaces.RealInput P "Actual Wind power" annotation(
    Placement(visible = true,
      transformation(origin = {-100, -26}, extent = {{-10, -10}, {10, 10}},
        rotation = 0),
      iconTransformation(origin = {-100, -26}, extent = {{-10, -10}, {10, 10}},
        rotation = 0)));

  Modelica.Blocks.Interfaces.RealInput E_c "Emergency control" annotation(
    Placement(visible = true,
      transformation(origin = {-100, -94}, extent = {{-10, -10}, {10, 10}},
        rotation = 0),
      iconTransformation(origin = {-100, -94}, extent = {{-10, -10}, {10, 10}},
        rotation = 0)));

  Modelica.Blocks.Interfaces.RealInput C "Intraday Electricity Price" annotation(
    Placement(visible = true,
      transformation(origin = {0, -100}, extent = {{-10, -10}, {10, 10}},
        rotation = 90),
      iconTransformation(origin = {0, -100}, extent = {{-10, -10}, {10, 10}},
        rotation = 90)));
```

```

Modelica.Blocks.Interfaces.RealOutput y1 "Baseload factor" annotation(
  Placement(visible = true,
    transformation(origin = {110, 26}, extent = {{-10, -10}, {10, 10}},
      rotation = 0),
    iconTransformation(origin = {110, 26}, extent = {{-10, -10}, {10, 10}},
      rotation = 0)));

Modelica.Blocks.Interfaces.RealOutput y2 "Variable factor" annotation(
  Placement(visible = true,
    transformation(origin = {110, -26}, extent = {{-10, -10}, {10, 10}},
      rotation = 0),
    iconTransformation(origin = {110, -26}, extent = {{-10, -10}, {10, 10}},
      rotation = 0)));

Modelica.Blocks.Interfaces.RealOutput y3 "Underproduction wind power" annotation(
  Placement(visible = true,
    transformation(origin = {50, -110}, extent = {{-10, -10}, {10, 10}},
      rotation = -90),
    iconTransformation(origin = {50, -110}, extent = {{-10, -10}, {10, 10}},
      rotation = -90)));

Modelica.Blocks.Interfaces.RealOutput y4 "Overproduction wind power" annotation(
  Placement(visible = true,
    transformation(origin = {90, -110}, extent = {{-10, -10}, {10, 10}},
      rotation = -90),
    iconTransformation(origin = {90, -110}, extent = {{-10, -10}, {10, 10}},
      rotation = -90)));

parameter Real P_w = (1/v_max^3)*nominalWindPower "Forecast wind power";

```

equation

```

if (E_c == 0) then
  y1 = 0;
elseif ((v^3)*P_w > maxLoad) or (C < C_max) then
  y1 = 1;
elseif ((v^3)*P_w < baseLoad) then
  y1 = 0;
else
  y1 = (((v^3)*P_w)-baseLoad)*(1/(maxLoad-baseLoad));
end if;

if (E_c == 0) then
  y2 = 0;
elseif (v>v_max) then
  y2 = -(nominalWindPower-P)*(1/(maxLoad-baseLoad));
elseif ((v^3)*P_w-P > 0) then
  y2 = -((v^3)*P_w-P)*(1/(maxLoad-baseLoad));
elseif ((v^3)*P_w-P < 0) then
  y2 = -((v^3)*P_w-P)*(1/(maxLoad-baseLoad));
else
  y2 = 0;
end if;

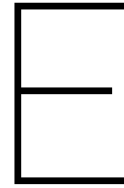
if ((v^3)*P_w > P) and (v < v_max) and (v > v_min) then

```

```
    y3 = ((v^3)*P_w)-P;
elseif ((v^3)*P_w > P) and (v > v_max) then
    y3 = ((v_max^3)*P_w)-P;
else
    y3 = 0;
end if;

if ((v^3)*P_w < P) then
    y4 = P-((v^3)*P_w);
else
    y4 = 0;
end if;

end E_Controller;
```

OpenModelica code: Electrolyser

```
model Electrolyser_Subsystem "PEM Electrolyser"

import Modelica.Constants.pi;

Modelica.Blocks.Math.Product product1 annotation(
  Placement(visible = true,
    transformation(origin = {-84, -24}, extent = {{-10, -10}, {10, 10}},
      rotation = 0)));

Modelica.Blocks.Math.Gain gain1(k = -1.5421e-3) annotation(
  Placement(visible = true,
    transformation(origin = {-92, -58}, extent = {{-10, -10}, {10, 10}},
      rotation = 0)));

Modelica.Blocks.Math.Log log1 annotation(
  Placement(visible = true,
    transformation(origin = {-82, 6}, extent = {{-10, -10}, {10, 10}},
      rotation = 0)));

Modelica.Blocks.Math.Product product2 annotation(
  Placement(visible = true,
    transformation(origin = {-46, 0}, extent = {{-10, -10}, {10, 10}},
      rotation = 0)));

Modelica.Blocks.Math.Gain gain2(k = 9.523e-5) annotation(
  Placement(visible = true,
    transformation(origin = {-8, 0}, extent = {{-10, -10}, {10, 10}},
      rotation = 0)));

Modelica.Blocks.Math.Gain gain3(k = 9.84e-8) annotation(
  Placement(visible = true,
    transformation(origin = {-44, -24}, extent = {{-10, -10}, {10, 10}},
      rotation = 0)));

Modelica.Blocks.Sources.Constant const(k = 1.5184) annotation(
  Placement(visible = true,
    transformation(origin = {-94, -90}, extent = {{-10, -10}, {10, 10}},
      rotation = 0)));

Modelica.Blocks.Math.Sum E_rev(nin = 4) annotation(
```

```
Placement(visible = true,
transformation(origin = {16, -46}, extent = {{-10, -10}, {10, 10}},
rotation = 0)));

Modelica.Blocks.Math.Division Input_current annotation(
Placement(visible = true,
transformation(origin = {-80, 66}, extent = {{-10, -10}, {10, 10}},
rotation = 0)));

Modelica.Blocks.Math.Product CellCurrent annotation(
Placement(visible = true,
transformation(origin = {-2, 64}, extent = {{-10, -10}, {10, 10}},
rotation = 0)));

Modelica.Blocks.Continuous.FirstOrder firstOrder2(T = 0.5) annotation(
Placement(visible = true,
transformation(origin = {44, 64}, extent = {{-10, -10}, {10, 10}},
rotation = 0)));

Modelica.Blocks.Discrete.ZeroOrderHold zeroOrderHold1 annotation(
Placement(visible = true,
transformation(origin = {82, 16}, extent = {{-10, -10}, {10, 10}},
rotation = -90)));

Modelica.Blocks.Math.Sum CellVoltage(nin = 3) annotation(
Placement(visible = true,
transformation(origin = {32, 20}, extent = {{-10, -10}, {10, 10}},
rotation = 90)));

Modelica.Blocks.Math.Add E_Ohm_constant annotation(
Placement(visible = true,
transformation(origin = {62, -76}, extent = {{-10, -10}, {10, 10}},
rotation = 180)));

Modelica.Blocks.Sources.Constant const2(k = 0.2798) annotation(
Placement(visible = true,
transformation(origin = {110, -90}, extent = {{-10, -10}, {10, 10}},
rotation = 180)));

Modelica.Blocks.Math.Division CellEfficiency annotation(
Placement(visible = true,
transformation(origin = {-34, 46}, extent = {{-10, -10}, {10, 10}},
rotation = 0)));

Modelica.Blocks.Math.Division division1 annotation(
Placement(visible = true,
transformation(origin = {104, 78}, extent = {{-10, -10}, {10, 10}},
rotation = 0)));

Modelica.Blocks.Sources.Constant FaradayConstant(k = 96485) annotation(
Placement(visible = true,
transformation(origin = {14, 114}, extent = {{-10, -10}, {10, 10}},
rotation = 0)));

Modelica.Blocks.Math.Add add3 annotation(
Placement(visible = true,
```

```
transformation(origin = {70, 116}, extent = {{-10, -10}, {10, 10}},
rotation = 0)));

Modelica.Blocks.Math.Product product4 annotation(
  Placement(visible = true,
  transformation(origin = {150, 70}, extent = {{-10, -10}, {10, 10}},
  rotation = 0)));

Modelica.Blocks.Sources.Constant HydrogenMass(k = 2.016e-3) annotation(
  Placement(visible = true,
  transformation(origin = {114, 36}, extent = {{-10, -10}, {10, 10}},
  rotation = 0)));

Modelica.Blocks.Sources.Constant HydrogenDensity(k = 0.06953) annotation(
  Placement(visible = true,
  transformation(origin = {156, 14}, extent = {{-10, -10}, {10, 10}},
  rotation = 0)));

Modelica.Blocks.Math.Division division2 annotation(
  Placement(visible = true,
  transformation(origin = {190, 44}, extent = {{-10, -10}, {10, 10}},
  rotation = 0)));

Modelica.Blocks.Continuous.Integrator TotalHydrogen annotation(
  Placement(visible = true,
  transformation(origin = {228, 52}, extent = {{-10, -10}, {10, 10}},
  rotation = 0)));

Modelica.Blocks.Interaction.Show.RealValue CellTotHydrogen annotation(
  Placement(visible = true,
  transformation(origin = {264, 70}, extent = {{-10, -10}, {10, 10}},
  rotation = 0)));

Modelica.Blocks.Nonlinear.Limiter CellPower(limitsAtInit = true,
uMax = 9999999, uMin = 0) annotation(
  Placement(visible = true,
  transformation(origin = {-120, 72}, extent = {{-10, -10}, {10, 10}},
  rotation = 0)));

Modelica.Blocks.Sources.Constant NCells(k = 500000) annotation(
  Placement(visible = true,
  transformation(origin = {-24, 196}, extent = {{-10, -10}, {10, 10}},
  rotation = -90)));

Modelica.Blocks.Math.Product product5 annotation(
  Placement(visible = true,
  transformation(origin = {258, 114}, extent = {{-10, -10}, {10, 10}},
  rotation = 0)));

Modelica.Blocks.Math.Division Power_division annotation(
  Placement(visible = true,
  transformation(origin = {-192, 72}, extent = {{-10, -10}, {10, 10}},
  rotation = 0)));

Modelica.Blocks.Interaction.Show.RealValue NCellsTotHydrogen annotation(
  Placement(visible = true,
```

```

    transformation(origin = {288, 114}, extent = {{-10, -10}, {10, 10}},
    rotation = 0)));

Modelica.Blocks.Math.Product product6 annotation(
  Placement(visible = true,
  transformation(origin = {122, 164}, extent = {{-10, -10}, {10, 10}},
  rotation = 0)));

Modelica.Blocks.Sources.Constant OxygenMass(k = 31.9988e-3) annotation(
  Placement(visible = true,
  transformation(origin = {80, 158}, extent = {{-10, -10}, {10, 10}},
  rotation = 0)));

Modelica.Blocks.Sources.Constant OxygenDensity(k = 1.104) annotation(
  Placement(visible = true,
  transformation(origin = {156, 154}, extent = {{-10, -10}, {10, 10}},
  rotation = 0)));

Modelica.Blocks.Math.Division division3 annotation(
  Placement(visible = true,
  transformation(origin = {184, 170}, extent = {{-10, -10}, {10, 10}},
  rotation = 0)));

Modelica.Blocks.Continuous.Integrator TotalOxygen annotation(
  Placement(visible = true,
  transformation(origin = {216, 180}, extent = {{-10, -10}, {10, 10}},
  rotation = 0)));

Modelica.Blocks.Interaction.Show.RealValue CellTotOxygen annotation(
  Placement(visible = true,
  transformation(origin = {248, 190}, extent = {{-10, -10}, {10, 10}},
  rotation = 0)));

Modelica.Blocks.Math.Product product7 annotation(
  Placement(visible = true,
  transformation(origin = {250, 158}, extent = {{-10, -10}, {10, 10}},
  rotation = 0)));

Modelica.Blocks.Interaction.Show.RealValue NCellsTotOxygen annotation(
  Placement(visible = true,
  transformation(origin = {282, 158}, extent = {{-10, -10}, {10, 10}},
  rotation = 0)));

Modelica.Blocks.Math.Gain E_Ohm(k = 0.09) annotation(
  Placement(visible = true,
  transformation(origin = {72, -22}, extent = {{-10, -10}, {10, 10}},
  rotation = -90)));

Modelica.Blocks.Math.Gain E_Act(k = 0.0514) annotation(
  Placement(visible = true,
  transformation(origin = {110, -22}, extent = {{-10, -10}, {10, 10}},
  rotation = -90)));

Modelica.Blocks.Math.Gain gain4(k = 0.5) annotation(
  Placement(visible = true,
  transformation(origin = {122, 116}, extent = {{-10, -10}, {10, 10}},

```

```
rotation = 90)));
```

```
Modelica.Blocks.Sources.Constant E_power(k = 1000000) annotation(
  Placement(visible = true,
    transformation(origin = {-278, 156}, extent = {{-10, -10}, {10, 10}},
      rotation = 0)));
```

```
Modelica.Blocks.Math.Product product3 annotation(
  Placement(visible = true,
    transformation(origin = {-244, 94}, extent = {{-10, -10}, {10, 10}},
      rotation = 0)));
```

```
Modelica.Blocks.Interfaces.RealInput u2 "Power" annotation(
  Placement(visible = true,
    transformation(origin = {-316, 62}, extent = {{-20, -20}, {20, 20}},
      rotation = 0),
    iconTransformation(origin = {-80, -44}, extent = {{-20, -20}, {20, 20}},
      rotation = 0)));
```

```
Modelica.Blocks.Interfaces.RealOutput y2 "Hydrogen" annotation(
  Placement(visible = true,
    transformation(origin = {310, 88}, extent = {{-16, -16}, {16, 16}},
      rotation = 0),
    iconTransformation(origin = {120, -42}, extent = {{-20, -20}, {20, 20}},
      rotation = 0)));
```

```
Modelica.Blocks.Interfaces.RealOutput y1 "Oxygen" annotation(
  Placement(visible = true,
    transformation(origin = {309, 141}, extent = {{-17, -17}, {17, 17}},
      rotation = 0),
    iconTransformation(origin = {121, 41}, extent = {{-21, -21}, {21, 21}},
      rotation = 0)));
```

```
Modelica.Blocks.Math.Product RatedPower annotation(
  Placement(visible = true,
    transformation(origin = {-30, 148}, extent = {{-10, -10}, {10, 10}},
      rotation = -90)));
```

```
Modelica.Blocks.Interfaces.RealInput u1 "RatedPower" annotation(
  Placement(visible = true,
    transformation(origin = {-314, 188}, extent = {{-20, -20}, {20, 20}},
      rotation = 0),
    iconTransformation(origin = {-80, 40}, extent = {{-20, -20}, {20, 20}},
      rotation = 0)));
```

```
Modelica.Blocks.Sources.Constant Temp annotation(
  Placement(visible = true,
    transformation(origin = {-166, -24}, extent = {{-10, -10}, {10, 10}},
      rotation = 0)));
```

equation

```
connect(Temp.y, gain1.u) annotation(
  Line(points = {{-154, -24}, {-106, -24}, {-106, -58}, {-104, -58}},
    color = {0, 0, 127}));
```

```

connect(Temp.y, product2.u2) annotation(
  Line(points = {{-154, -24}, {-120, -24}, {-120, -6}, {-58, -6}, {-58, -6}},
    color = {0, 0, 127}));

connect(Temp.y, log1.u) annotation(
  Line(points = {{-154, -24}, {-120, -24}, {-120, 6}, {-94, 6}, {-94, 6}},
    color = {0, 0, 127}));

connect(Temp.y, product1.u2) annotation(
  Line(points = {{-154, -24}, {-98, -24}, {-98, -30}, {-96, -30}},
    color = {0, 0, 127}));

connect(Temp.y, product1.u1) annotation(
  Line(points = {{-154, -24}, {-98, -24}, {-98, -18}, {-96, -18}},
    color = {0, 0, 127}));

connect(product7.y, y1) annotation(
  Line(points = {{262, 158}, {264, 158}, {264, 142}, {309, 142}, {309, 141}},
    color = {0, 0, 127}));

connect(product5.y, y2) annotation(
  Line(points = {{270, 114}, {270, 88}, {310, 88}},
    color = {0, 0, 127}));

connect(u1, RatedPower.u2) annotation(
  Line(points = {{-314, 188}, {-38, 188}, {-38, 160}, {-36, 160}},
    color = {0, 0, 127}));

connect(RatedPower.y, product5.u1) annotation(
  Line(points = {{-30, 137}, {246, 137}, {246, 120}},
    color = {0, 0, 127}));

connect(RatedPower.y, product7.u2) annotation(
  Line(points = {{-30, 137}, {236, 137}, {236, 152}, {238, 152}},
    color = {0, 0, 127}));

connect(RatedPower.y, Power_division.u2) annotation(
  Line(points = {{-30, 137}, {-218, 137}, {-218, 66}, {-204, 66}},
    color = {0, 0, 127}));

connect(RatedPower.u1, NCells.y) annotation(
  Line(points = {{-24, 160}, {-24, 186}},
    color = {0, 0, 127}));

connect(CellVoltage.y, Input_current.u2) annotation(
  Line(points = {{32, 32}, {-94, 32}, {-94, 60}, {-92, 60}},
    color = {0, 0, 127}));

connect(CellVoltage.y, CellEfficiency.u2) annotation(
  Line(points = {{32, 32}, {-46, 32}, {-46, 40}, {-46, 40}},
    color = {0, 0, 127}));

connect(u2, product3.u2) annotation(
  Line(points = {{-316, 62}, {-256, 62}, {-256, 88}, {-256, 88}},
    color = {0, 0, 127}));

```

```
connect(Power_division.y, CellPower.u) annotation(
  Line(points = {{-181, 72}, {-132, 72}},
    color = {0, 0, 127}));

connect(product3.y, Power_division.u1) annotation(
  Line(points = {{-232, 94}, {-204, 94}, {-204, 78}},
    color = {0, 0, 127}));

connect(E_power.y, product3.u1) annotation(
  Line(points = {{-266, 156}, {-256, 156}, {-256, 100}, {-256, 100}},
    color = {0, 0, 127}));

connect(CellEfficiency.y, CellCurrent.u2) annotation(
  Line(points = {{-23, 46}, {-15, 46}, {-15, 58}, {-16, 58}, {-16, 58}, {-15, 58}},
    color = {0, 0, 127}));

connect(CellCurrent.y, firstOrder2.u) annotation(
  Line(points = {{10, 64}, {32, 64}, {32, 64}, {32, 64}},
    color = {0, 0, 127}));

connect(Input_current.y, CellCurrent.u1) annotation(
  Line(points = {{-69, 66}, {-49, 66}, {-49, 66}, {-27, 66}, {-27, 70}, {-15, 70}},
    color = {0, 0, 127}));

connect(gain4.y, product6.u1) annotation(
  Line(points = {{122, 128}, {98, 128}, {98, 170}, {110, 170}, {110, 170}},
    color = {0, 0, 127}));

connect(division1.y, gain4.u) annotation(
  Line(points = {{116, 78}, {122, 78}, {122, 104}, {122, 104}},
    color = {0, 0, 127}));

connect(E_Act.y, E_Ohm_constant.u2) annotation(
  Line(points = {{110, -34}, {110, -34}, {110, -70}, {74, -70}, {74, -70}},
    color = {0, 0, 127}));

connect(zeroOrderHold1.y, E_Act.u) annotation(
  Line(points = {{82, 6}, {110, 6}, {110, -10}, {110, -10}},
    color = {0, 0, 127}));

connect(E_Ohm.y, CellVoltage.u[2]) annotation(
  Line(points = {{72, -34}, {32, -34}, {32, 8}, {32, 8}},
    color = {0, 0, 127}));

connect(zeroOrderHold1.y, E_Ohm.u) annotation(
  Line(points = {{82, 6}, {72, 6}, {72, -10}, {72, -10}},
    color = {0, 0, 127}));

connect(NCellsTotOxygen.numberPort, product7.y) annotation(
  Line(points = {{262, 158}, {270, 158}, {270, 158}, {270, 158}},
    color = {0, 0, 127}));

connect(product7.u1, TotalOxygen.y) annotation(
  Line(points = {{238, 164}, {228, 164}, {228, 180}, {228, 180}},
    color = {0, 0, 127}));
```

```

connect(TotalOxygen.y, CellTotOxygen.numberPort) annotation(
  Line(points = {{227, 180}, {235, 180}, {235, 190}, {235, 190}},
    color = {0, 0, 127}));

connect(division3.y, TotalOxygen.u) annotation(
  Line(points = {{196, 170}, {202, 170}, {202, 180}, {204, 180}},
    color = {0, 0, 127}));

connect(OxygenDensity.y, division3.u2) annotation(
  Line(points = {{168, 154}, {170, 154}, {170, 164}, {172, 164}},
    color = {0, 0, 127}));

connect(product6.y, division3.u1) annotation(
  Line(points = {{134, 164}, {172, 164}, {172, 176}, {172, 176}},
    color = {0, 0, 127}));

connect(OxygenMass.y, product6.u2) annotation(
  Line(points = {{91, 158}, {110, 158}},
    color = {0, 0, 127}));

connect(TotalHydrogen.u, division2.y) annotation(
  Line(points = {{216, 52}, {213.5, 52}, {213.5, 44}, {201, 44}},
    color = {0, 0, 127}));

connect(TotalHydrogen.y, CellTotHydrogen.numberPort) annotation(
  Line(points = {{239, 52}, {251.5, 52}, {251.5, 70}, {252, 70}},
    color = {0, 0, 127}));

connect(product5.u2, TotalHydrogen.y) annotation(
  Line(points = {{246, 108}, {239, 108}, {239, 52}},
    color = {0, 0, 127}));

connect(NCellsTotHydrogen.numberPort, product5.y) annotation(
  Line(points = {{276.5, 114}, {269, 114}},
    color = {0, 0, 127}));

connect(HydrogenDensity.y, division2.u2) annotation(
  Line(points = {{168, 14}, {176, 14}, {176, 38}, {178, 38}},
    color = {0, 0, 127}));

connect(product4.y, division2.u1) annotation(
  Line(points = {{162, 70}, {178, 70}, {178, 50}, {178, 50}},
    color = {0, 0, 127}));

connect(HydrogenMass.y, product4.u2) annotation(
  Line(points = {{126, 36}, {138, 36}, {138, 64}, {138, 64}},
    color = {0, 0, 127}));

connect(product4.u1, division1.y) annotation(
  Line(points = {{138, 76}, {116, 76}, {116, 78}, {116, 78}},
    color = {0, 0, 127}));

connect(CellPower.y, Input_current.u1) annotation(
  Line(points = {{-109, 72}, {-91, 72}, {-91, 72}, {-93, 72}},
    color = {0, 0, 127}));

```



```
connect(FaradayConstant.y, add3.u2) annotation(  
  Line(points = {{26, 114}, {56, 114}, {56, 110}, {58, 110}},  
    color = {0, 0, 127}));  
  
connect(FaradayConstant.y, add3.u1) annotation(  
  Line(points = {{26, 114}, {56, 114}, {56, 122}, {58, 122}},  
    color = {0, 0, 127}));  
  
connect(add3.y, division1.u2) annotation(  
  Line(points = {{82, 116}, {90, 116}, {90, 72}, {92, 72}},  
    color = {0, 0, 127}));  
  
connect(division1.u1, firstOrder2.y) annotation(  
  Line(points = {{92, 84}, {56, 84}, {56, 64}},  
    color = {0, 0, 127}));  
  
connect(E_rev.y, CellEfficiency.u1) annotation(  
  Line(points = {{28, -46}, {-48, -46}, {-48, 52}, {-46, 52}},  
    color = {0, 0, 127}));  
  
connect(const2.y, E_Ohm_constant.u1) annotation(  
  Line(points = {{100, -90}, {76, -90}, {76, -82}, {74, -82}},  
    color = {0, 0, 127}));  
  
connect(E_Ohm_constant.y, CellVoltage.u[3]) annotation(  
  Line(points = {{52, -76}, {32, -76}, {32, 8}, {32, 8}},  
    color = {0, 0, 127}));  
  
connect(E_rev.y, CellVoltage.u[1]) annotation(  
  Line(points = {{28, -46}, {32, -46}, {32, 8}, {32, 8}},  
    color = {0, 0, 127}));  
  
connect(zeroOrderHold1.u, firstOrder2.y) annotation(  
  Line(points = {{82, 28}, {82, 64}, {56, 64}},  
    color = {0, 0, 127}));  
  
connect(const.y, E_rev.u[1]) annotation(  
  Line(points = {{-83, -90}, {5, -90}, {5, -46}, {3, -46}},  
    color = {0, 0, 127}));  
  
connect(gain1.y, E_rev.u[2]) annotation(  
  Line(points = {{-81, -58}, {3, -58}, {3, -46}, {3, -46}},  
    color = {0, 0, 127}));  
  
connect(gain2.y, E_rev.u[4]) annotation(  
  Line(points = {{3, 0}, {5, 0}, {5, -46}, {3, -46}},  
    color = {0, 0, 127}));  
  
connect(gain3.y, E_rev.u[3]) annotation(  
  Line(points = {{-32, -24}, {4, -24}, {4, -46}, {4, -46}},  
    color = {0, 0, 127}));  
  
connect(product1.y, gain3.u) annotation(  
  Line(points = {{-72, -24}, {-58, -24}, {-58, -24}, {-56, -24}},  
    color = {0, 0, 127}));
```

```

connect(gain2.u, product2.y) annotation(
  Line(points = {{-20, 0}, {-34, 0}, {-34, 0}, {-34, 0}},
    color = {0, 0, 127}));

connect(product2.u1, log1.y) annotation(
  Line(points = {{-58, 6}, {-72, 6}, {-72, 6}, {-71, 6}, {-71, 6}, {-70, 6}},
    color = {0, 0, 127}));

annotation(
  uses(Modelica(version = "3.2.2"), OpenIPSL(version = "1.0.0")),
  Diagram(coordinateSystem(extent = {{-300, -300}, {300, 300}})),
  Icon(coordinateSystem(extent = {{-300, -300}, {300, 300}})),
  version = "",
  __OpenModelica_commandLineOptions = "",
  Documentation(info = "<html><head></head><body>A simplified model of a single cell
Proton-exchange membrane(PEM) electrolyser. The cell is designed for an input power of
0-5W, but a maximum of 2W per cell is recommended to obtain better efficiencies. The
cell is operating at atmospheric pressure (1 atm) and a temperature of 80 Celsius
(353.15 K). The cell will output both hydrogen (H2) gas as well as oxygen (O2) gas.
both at 80 Celsius.<div><br></div><div>The model can be 'expanded' with multiple cells
by setting the number of cells in the 'NCells' constant block. Note that in this case
the behaviour and output of a single cell will be simply multiplied by the number of
cells. This is done due simulation time constraints and complexity of the
model.</div><div><br></div><div>The efficiency of the cell is determined by the ratio
of the required reversible cell voltage to make electrolysis happen, and the total
voltage with losses included. Voltage losses occur due to activation overpotential and
ohmic resistances within the cell. The reversible voltage, activation voltage and ohmic
voltage are modelled according to [1] and [2].</div><div><br></div><div>The input
current (after losses) into the electrolysis process determines the amount of hydrogen
and oxygen produced. Two electrons circulate through the external circuit for the
production of one mole of hydrogen gas. Multiplying the amount of mole produced with
the hydrogen mass and dividing by hydrogen density results in an output of H2 in m3/s.
The same procedure is used to determine the m3/s output of O2, with a special note that
for every H2 only 1/2O2 is produced according to:</div><div><br></div><div>H2O -> H2
+ 1/2O2</div><div><br></div><div>Since the cell is operating at 80 Celsius temperature,
the hydrogen and oxygen density is different from standard values, since density is
temperature dependend. The density is taken from density tables of
WolframAlpha.</div><div><br></div><div><br></div><div><br></div><div>The input voltage also determines
the efficiency of the cell: ideally the voltage is 1 pu, a lower voltage actually
increases the efficiency (as long as it is above E_rev) while a high voltage decreases
the efficiency.</div><div><br></div><div>[1] <b>R. Garcia-Valverde, N. Espinosa, A.
Urbina,</b>&nbsp;<i>Simple PEM water electrolyser model and experimental
validation</i></div><div>[2] <b>Francisco da Costa Lopes, Edson H.
Watanabe,</b>&nbsp;<i>Experimental and theoretical development of a PEM electrolyzer
model applied to energy storage systems</i></div></body></html>"));

end Electrolyser_Subsystem;

```

Bibliography

- [1] R. Heinberg and D. Fridley. *Our Renewable Future*. Island Press, 2016.
- [2] Earth System Research Laboratory (ESRL). Trends in atmospheric carbon dioxide, 2018.
- [3] M.K. Hubbert. *Energy Resources*. National Academy of Sciences, 1962.
- [4] International Renewable Energy Agency. *Renewable Power Generation Costs in 2017*, 2018.
- [5] International Energy Agency. Iea sankey diagram - netherlands (2014), 2017.
- [6] Havenbedrijf Rotterdam. Pathways to a sustainable port, 2008.
- [7] M.A.M.M. van der Meijden. Electrical power systems of the future - lecture 1, 2018.
- [8] F.M. Mulder. Implications of diurnal and seasonal variations in renewable energy generation for large scale energy storage. *Journal of Renewable and Sustainable Energy*, 6(3):033105, 2014.
- [9] A. Ozarslan. Large-scale hydrogen energy storage in salt caverns. *International Journal of Hydrogen Energy*, 37(19):14265–14277, 2012.
- [10] Gasunie. Infrastructuur in beeld, 2018.
- [11] K.K. Pant and R.B. Gupta. *Hydrogen Fuel: Production, Transport, and Storage*. Taylor & Francis Group, LLC, 2009.
- [12] J. Mergel D. Stolten M. Carmo, D.L. Fritz. A comprehensive review on pem water electrolysis. *Hydrogen Energy*, 38(12):4901–4934, 2013.
- [13] J. Oviedo E. Amores, J. Rodriguez and A. de Lucas-Consuegra. Development of an operation strategy for hydrogen production using solar pv energy based on fluid dynamic aspects. *Open Engineering*, 7(1):141–152, 2017.
- [14] National Renewable Energy Laboratory (NREL). Ten years of analyzing the duck chart, 2006.
- [15] Fraunhofer ISE. Stromproduktion in deutschland in woche 32 2018, 2018.
- [16] K. Apunn S. Amelang. The causes and effects of negative power prices, 2018.
- [17] P. Baran. *On Distributed Communications*. Rand Corporation, 1964.
- [18] T. Agarwal. Overview of smart grid technology and its operation and application, 2017.
- [19] C. Yan S. Wang, X. Xue. Building power demand response towards smart grid. *HVAC&R Research*, 2014.
- [20] Pandapower. About pandapower v1.6.0, 2018.
- [21] E.H. Watanabe F.C. Lopes. Experimental and theoretical development of a pem electrolyzer model applied to energy storage systems. In *2009 Brazilian Power Electronics Conference*, pages 775–782, 2009.
- [22] American Institute of Physics. The discovery of global warming, 2018.
- [23] S. Arrhenius. On the influence of carbonic acid in the air upon the temperature of the ground. *The London, Edinburgh and Dublin Philosophical Magazine and Journal of Science*, 1896.
- [24] G.S. Callendar. The artificial production of carbon dioxide and its influence on temperature. *Quarterly Journal of the Royal Meteorological Society*, 1938.

- [25] A.E. Bainbridge C.A. Ekdahl Jr. P.R. Guenther L.S. Waterman C.D. Keeling, R.B. Bacastow and J.E.S. Chin. Atmospheric carbon dioxide variations at mauna loa observatory, hawaii. *Tellus*, 1976.
- [26] R. Revelle and H.S. Suess. Carbon dioxide exchange between atmosphere and ocean and the question of an increase of atmospheric co₂ during the past decades. *Tellus*, 1956.
- [27] W. S. Broecker. Climatic change: Are we on the brink of a pronounced global warming? *Science*, 1975.
- [28] Intergovernmental Panel on Climate Change. History, 2018.
- [29] United Nations Framework Convention on Climate Change (UNFCCC). Kyoto protocol introduction, 2018.
- [30] R.K. Pachauri and L.A. Meyer. Climate change 2014: Synthesis report. contribution of working groups i, ii and iii to the fifth assessment report of the intergovernmental panel on climate change. Technical report, Intergovernmental Panel on Climate Change (IPCC), 2014.
- [31] S. Shafiee and E. Topal. When will fossil fuel reserves be diminished? *Energy Policy*, 2009.
- [32] D.R. Simbeck J.P. Dorian, H.T. Franssen. Global challenges in energy. *Energy Policy*, 34(15):1984–1991, 2006.
- [33] U.S. Energy Information Administration. *Annual Energy Outlook 2018*, 2018.
- [34] REN21. Renewables 2018 - global status report. Technical report, Renewable Energy Policy Network for the 21st Century, 2018.
- [35] World Energy Council. Gas in the netherlands, 2018.
- [36] The Brookings Institution. The end of dutch natural gas production as we know it, 2016.
- [37] Nederlandse Aardolie Maatschappij (NAM). Gaswinning in het groningen-gasveld, 2018.
- [38] Rijksoverheid. Kabinet: einde aan gaswinning in groningen, 2018.
- [39] Rijksoverheid. Energieagenda 2016. Technical report, Rijksoverheid, 2016.
- [40] N.B. Vargaftik. *Handbook of physical properties of liquids and gases - pure substances and mixtures. Second edition*. Springer-Verlag Berlin Heidelberg, 1 1975.
- [41] J.A. Donovan D.E. Rawl M. Louthan, G.R. Caskey. Hydrogen embrittlement of metlas. *Materials Science and Engineering*, 10:357–368, 1972.
- [42] Thomas Rostrup-Nielsen J.R. Rostrup-Nielsen. Large-scale hydrogen production, 2001.
- [43] P. Hammingh K. Schoots, M. Hekkenberg. Nationale energieverkenning 2017. Technical report, Energieonderzoek Centrum Nederland (ECN), 2017.
- [44] Volvo Car Corporation. Volvo cars to go all electric, 2017.
- [45] Reuters. Volkswagen accelerates push into electric cars with \$40 billion spending plan, 2017.
- [46] BMW Group. Bmw group announces next step in electrification strategy, 2017.
- [47] Adam Baidawi (New York Times). Australia powers up the world's biggest battery — courtesy of elon musk, 2017.
- [48] Amsterdam Power Exchange. Epex spot power nl day ahead, 2018.
- [49] J.M. Tarascon B. Dunn, H. Kamath. Electrical energy storage for the grid: a battery of choices. *Science*, 334(6058):928–935, 2011.
- [50] M. Alam S. Rehman, L.M. Al-Hadrami. Pumped hydro energy storage system: A technological review. *Renewable and Sustainable Energy Review*, 44:586–598, April 2015.

- [51] A. van Wijk. The green hydrogen economy in the northern netherlands. Technical report, Noordelijke InnovationBoard, 2017.
- [52] S.M. Amin and B.F. Wollenberg. Toward a smart grid: power delivery for the 21st century. *IEEE Power and Energy Magazine*, 3:34–41, Sept-Oct 2005.
- [53] G. Xue X. Fang, S. Misra and D. Yang. Smart grid — the new and improved power grid: A survey. *IEEE Communications Surveys & Tutorials*, 14:944–980, Oct 2012.
- [54] R. Roche B. Li and A. Miraoui. Sizing of a stand-alone microgrid considering electric power, cooling/heating and hydrogen. In *IEEE Manchester PowerTech*, pages 1–6, 2017.
- [55] R. Bo W. Liu G. Zhou W. Chen Z. Wu W. Gu, Z. Wu. Modeling, planning and optimal energy management of combined cooling, heating and power microgrid: A review. *International Journal of Electrical Power & Energy Systems*, 54:26–37, 2014.
- [56] R.K. Menon R. Ramachandran. An overview of industrial uses of hydrogen. *International Journal of Hydrogen Energy*, 23(7):593–598, 1998.
- [57] H. Alharbi. Optimal planning and scheduling of battery energy storage systems for isolated microgrids. Master's thesis, University of Waterloo, 2015.
- [58] H.B. Gooi S.X. Chen and M.Q. Wang. Sizing of energy storage for microgrids. *IEEE Transactions on Smart Grid*, 3(1):142–151, 2012.
- [59] M. Zimmermann A. Züttel M. Biemann, U.F.Vogt. Seasonal energy storage system based on hydrogen for self sufficient living. *Journal of Power Sources*, 196(8):4054–4060, 2011.
- [60] R. Etz E. Lázár, D. Petreuş and T. Pătărău. Optimal scheduling of an islanded microgrid based on minimum cost. In *2016 39th International Spring Seminar on Electronics Technology (ISSE)*, pages 290–295, 2016.
- [61] R. Schober V. W. S. Wong P. Samadi, A. H. Mohsenian-Rad and J. Jatskevich. In *Optimal Real-Time Pricing Algorithm Based on Utility Maximization for Smart Grid*, pages 415–420, 2010.
- [62] S. Ropenus C. Jørgensen. Production price of hydrogen from grid connected electrolysis in a power market with high wind penetration. *International Journal of Hydrogen Energy*, 33(20):5335–5344, 2008.
- [63] H. Zhu E. Dall'Anese and G.B. Giannakis. Distributed optimal power flow for smart microgrids. *IEEE Transactions on Smart Grid*, 4(3):1464–1475, 2013.
- [64] J. M. Guerrero Y. Levron and Y. Beck. Optimal power flow in microgrids with energy storage. *IEEE Transactions on Power Systems*, 28(3):3226–3234, 2013.
- [65] G.W. Ault S. Gill, I. Kockar. Dynamic optimal power flow for active distribution networks. *IEEE Transactions on Power Systems*, 29(1):121–131, 2013.
- [66] A. Midilli, M. Ay, I. Dincer, and M.A. Rosen. On hydrogen and hydrogen energy strategies: I: current status and needs. *Renewable and Sustainable Energy Reviews*, 9(3):255 – 271, 2005.
- [67] O. Antonia M.W. Melaina and M. Penev. Blending hydrogen into natural gas pipeline networks: A review of key issues. Technical report, National Renewable Energy Laboratory, 2013.
- [68] A. Milbrandt M.K. Mann, R.M. Margolis. An analysis of hydrogen production from renewable electricity sources. *Solar Energy*, 81:773–780, 2007.
- [69] K. Cha T. Lim T. Hur J. Lee, M. Yoo. Life cycle cost analysis to examine the economical feasibility of hydrogen as an alternative fuel. *International Journal of Hydrogen Energy*, 34:4243–4255, 2009.
- [70] A.T. Holten M. Korpas. Operation planning of hydrogen storage connected to wind power operating in a power market. *IEEE Transactions on Energy Conversion*, 21:742–749, 2006.
- [71] J. Rokadia C. Mishra, S.P. Singh. Optimal power flow in the presence of wind power using modified cuckoo search. *IET Generation, Transmission & Distribution*, 9:615–626, 2014.

- [72] S. Russwurm. Kick-off for world's largest electrolysis system in mainz, 2015.
- [73] R. Markillie. 10mw refinery hydrogen project with shell, 2017.
- [74] European Commission. Topic : Demonstration of a large-scale (min. 20mw) electrolyser for converting renewable energy to hydrogen, 2018.
- [75] D. Zhang K. Zeng. Recent progress in alkaline water electrolysis for hydrogen production and applications. *Progress in Energy and Combustion Science*, 36(3):307–326, 2010.
- [76] F. Barbir. Pem electrolysis for production of hydrogen from renewable energy sources. *Solar Energy*, 78(5):661–669, 2005.
- [77] M. Cali F. Marangio, M. Santarelli. Theoretical model and experiment analysis of a high pressure pem water electrolyzer for hydrogen production. *Hydrogen Energy*, 34(3):1143–1158, 2009.
- [78] A. Dicks J. Larminie. *Fuel Cell Systems Explained*. John Wiley & Sons Ltd, 2003.
- [79] TenneT TSO B.V. Verzoek extra biedingen reservevermogen overige doeleinden in opregelrichting, 2018.
- [80] Nederlandse Omroep Stichting (NOS). Grilligheid zon en wind bedreigt stabiliteit elektriciteitsnet, 2018.
- [81] M. Glowacki. Balance responsible parties (brps), 2019.
- [82] S. Deilami M.A.S. Masoum M.E.H. Golshan S.Y. Derakhshandeh, A.S. Masoum. Coordination of generation scheduling with pevs charging in industrial microgrids. *IEEE Transactions on Power Systems*, 28(3):3451–3461, 2013.
- [83] P. Paigi R.H. Lasseter. Microgrid: A conceptual solution. In *IEEE Power Electronics Specialists Conference*, 2004.
- [84] M.L. Abundo M.L. Tuballa. A review of the development of smart grid technologies. *Renewable and Sustainable Energy Reviews*, 59:710–725, 2016.
- [85] A. Leon-Garcia A.H. Mohsenian-Rad. Optimal residential load control with price prediction in real-time electricity pricing environments. *IEEE Transactions on Smart Grid*, 1(2):120–133, 2010.
- [86] P. Siano. Demand response and smart grids. *Renewable and Sustainable Energy Reviews*, 30:461–478, 2014.
- [87] J.P.S. Catalao N.G. Paterakis, O. Erdinc. An overview of demand response: key-elements and international experience. *Renewable and Sustainable Energy Reviews*, 69:871–891, 2017.
- [88] Modelica Association. *Modelica - A Unified Object-Oriented Language for Systems Modeling*, 2017.
- [89] ALSETLab. Openipsl: Open-instance power system library, 2019.
- [90] F. Schäfer J. Menke J. Dollichon F. Meier S. Meinecke M. Braun L. Thurner, A. Scheidler. pandapower — an open-source python tool for convenient modeling, analysis, and optimization of electric power systems. *IEEE Transactions on Power Systems*, 33(6):6510–6521, Nov 2018.
- [91] Koninklijk Nederlands Meteorologisch Instituut. Uurgegevens van het weer in nederland, 2019.
- [92] EPEX Spot SE. Market data: Intraday continuous, 2019.
- [93] European Commission. A fully-integrated internal energy market, 2019.
- [94] S. Bourne (ITM Power). Scaling pem electrolysis to 100mw, 2017.
- [95] Fraunhofer ISE. Levelized cost of electricity renewable energy technologies, 2018.
- [96] CIGRE. *Benchmark Systems for Network Integration of Renewable and Distributed Energy Resources*, 2014.
- [97] A. Urbina R. Garcia-Valverde, N. Espinosa. Simple pem water electrolyser model and experimental validation. *International Journal of Hydrogen Energy*, 37:1927–1938, 2011.
- [98] BP. *BP Statistical Review of World Energy 2017*, 2017.